`

STEROL BINDING TO NIEMANN-PICK TYPE C1 DISEASE PROTEIN (NPC1)-
IMPLICATIONS FOR ITS FUNCTION IN CHOLESTEROL TRANSPORT

APPROVED BY COMMITTEE

Michael S. Brown, M.D. (Mentor) _____

Joseph L. Goldstein, M.D. (Mentor) _____

Sandra Hofmann, M.D., Ph.D. (Chair) _____

Melanie Cobb, Ph.D. _____

Michael Roth, Ph.D. _____

Guosheng Liang, Ph.D. _____

DEDICATION

This is dedicated to my precious mom, Zalfa Talhouk.

Your words of great encouragement inspire me everyday of my life. You are much more than a ‘mom’ to me; you are my best friend and confidante.

STEROL BINDING TO NIEMANN-PICK TYPE C1 DISEASE PROTEIN (NPC1)- IMPLICATIONS FOR ITS FUNCTION IN CHOLESTEROL TRANSPORT

by

LINA FOUAD ABI MOSLEH

DISSERTATION

Presented to the Faculty of the Graduate School of Biomedical Sciences

The University of Texas Southwestern Medical Center at Dallas

In Partial Fulfillment of the Requirements

For the Degree of

DOCTOR OF PHILOSOPHY

The University of Texas Southwestern Medical Center at Dallas

Dallas, Texas

April, 2009

STEROL BINDING TO NIEMANN-PICK TYPE C1 DISEASE PROTEIN (NPC1)-
IMPLICATIONS FOR ITS FUNCTION IN CHOLESTEROL TRANSPORT

Publication No. _____

Lina Fouad Abi Mosleh, Ph.D.

The University of Texas Southwestern Medical Center at Dallas, 2009

Supervising Professors: Michael S. Brown, M.D. and Joseph L. Goldstein, M.D.

Through studies of inborn errors of metabolism, scientists have uncovered many pathways involved in the transport of cholesterol within cells. Despite intense scientific interest, the mechanism by which cholesterol is transported between membrane compartments in animal cells remains obscure. Studies on Niemann-Pick type C disease (NPC) defined the requirement of at least two proteins involved in the transport of lipoprotein-derived cholesterol from lysosomes. Both proteins are located in the lysosomes and mutations in either NPC1, a membrane bound protein, or NPC2, a soluble protein, causes the accumulation of large amounts of cholesterol throughout the body. We encountered

NPC1 in the course of isolating a cholesterol-homeostasis membrane protein that binds oxygenated metabolites of cholesterol, oxysterols. We then showed that NPC1's sterol binding domain was localized to its N-terminal luminal soluble domain (NTD) and that this domain bound cholesterol as well.

We first attempted to understand the functional significance of NPC1 binding to oxysterols. We were able to demonstrate that NPC1 is not required for the regulatory actions of oxysterols since the oxysterol-mediated inhibition of the proteolytic processing of the sterol regulatory element-binding protein (SREBP) and activation of acyl-CoA:cholesterol acyltransferase (ACAT) was not defective in NPC1 mutant fibroblasts.

Many studies emphasized the importance of NPC1 in the transport of LDL-derived cholesterol out of the lysosomes. However, there is contradictory evidence for the role of NPC1 in transporting plasma membrane cholesterol and endogenously synthesized cholesterol to the compartment of the endoplasmic reticulum (ER) that contains ACAT. Experiments presented in this study characterize NPC1 dependent and independent transport of cholesterol in cells. We definitively show that NPC1 is only required for the transport of cholesterol from the LDL particle that has entered the cell through receptor-mediated endocytosis.

After defining that NPC1's role is only in the transport of cholesterol out of the lysosome, we began to study the mechanism involved in this transport. Inside the lysosome reside the two proteins, NPC1 and NPC2, that when mutated cause the NPC disease. Both NPC1 and NPC2 bind cholesterol with ~ 100nM affinity, but they bind to opposite ends of the cholesterol molecule. Recently an *in vitro* assay using purified proteins was developed to

measure transfer of [^{3}H]cholesterol between the NPC1(NTD), NPC2 and phosphatidylcholine liposomes. NPC1(NTD) donates or accepts cholesterol from liposomes very slowly, whereas NPC2 acts quickly. NPC2 stimulates the bidirectional transfer of cholesterol between NPC1(NTD) and liposomes. This evidence suggested that NPC2 could stimulate NPC1's rates of dissociation or association of cholesterol. This was the first evidence suggesting a direct interaction between both proteins. Using mutational analysis, we identified two functional subdomains of NPC1(NTD) – one for sterol binding and the other for NPC2-mediated transfer. NPC1 with point mutations in either one of the subdomains cannot accept cholesterol from NPC2 and therefore cannot restore cholesterol exit from lysosomes in NPC1-deficient cells. These studies explain the dual requirement of these proteins in the export of cholesterol from lysosomes, defining how mutations in either protein produce similar clinical phenotypes.

Based on these biochemical and tissue culture studies, in addition to the availability of the crystal structure of both proteins bound to sterols, we propose a working model: after lysosomal hydrolysis of LDL-cholesteryl esters, cholesterol binds to NPC2, which transfers it to NPC1(NTD), reversing its orientation and allowing insertion of its isooctyl side chain into the outer-limiting lysosomal membranes.

ACKNOWLEDGEMENTS

I would like to thank both of my mentors, Dr. Michael Brown and Dr. Joseph Goldstein for their patience, support and excellent guidance. The knowledge that I have acquired from working under their supervision is priceless.

I was also lucky to have distinguished scientists on my thesis committee. I appreciate their great suggestions and insight into my project.

I would like to acknowledge all the former and current members of the Brown and Goldstein lab for providing a truly cooperative and collaborative environment. Specifically, Rodney Infante, YK Ho, Arun Radhakrishnan, Li-ping Sun, Yukio Ikeda, and Michael Wang. Also, none of this work would have been possible without the great technical assistance from the tissue culture staff which includes Lisa Beatty, Ije Onweneme, Shomanike Head, and Angela Carrol. Special thanks to the technical staff of the Department of Molecular Genetics, especially, Dorothy Goddard, Richard Gibson, and Debbie Morgan. I also wish to thank Linda Donelly and Meryl Davis for their cooperation in the use of lab facilities.

To all my friends from AUB and the great bunch of wonderful people whom I met in Dallas, thank you for your emotional support. I know that I'll have a friend in each and every one of you for life.

Finally, I am in debt to my wonderful parents. I wish you could see deep in my heart for its hard to find just the right words. Thank you for supporting me in every decision that I made and doing more than your best to help me achieve my aims every step of the way. I

know that it was hard on you having me move halfway across the world, but I have no doubt that it was worth it. I strive to make you both proud. My younger brother, Nidal, not a day has passed where I didn't think about you. I just hope that my experience has instilled in you the importance of pursuing your dreams no matter how hard it may be.

TABLE OF CONTENTS

PRIOR PUBLICATIONS

El-Sabban ME, **Abi-Mosleh LF**, Ralhouk RS. Developmental regulation of gap junctions and their role in mammary epithelial cell differentiation. J Mammary Gland Biol Neplasia. 2003 Oct;8(4):463-73. Review.

Infante RE, **Abi-Mosleh L**, Radhakrishnan A, Dale JD, Brown MS, Goldstein JL. Purified NPC1 protein. I. Binding of cholesterol and oxysterols to a 1278-amino acid membrane protein. J Biol Chem. 2008 Jan 11;283(2):1052-63. Epub 2007 Nov 6.

Infante RE, Radhakrishnan A, **Abi-Mosleh L**, Kinch LN, Wang ML, Grishin NV, Goldstein JL, Brown MS. Purified NPC1 protein: II. Localization of sterol binding to a 240-amino acid soluble luminal loop. J Biol Chem. 2008 Jan 11;283(2):1064-75. Epub 2007 Nov 6.

Talhouk RS, Mroue R, Mokalled M, **Abi-Mosleh L**, Nehme R, Ismail A, Khalil A, Zaatari M, El-Sabban ME. Heterocellular interaction enhances recruitment of alpha and beta-catenins and ZO-2 into functional gap-junction complexes and induces gap junction-dependent differentiation of mammary epithelial cells. Exp Cell Res. 2008 Nov 1;314(18):3275-91.

Kwon HJ , **Abi-Mosleh L** ,Wang ML, Deisenhofer J, Goldstein JL, Brown MS, Goldstein JL, Infante RE. Structure of the N-terminal domain of NPC1 suggests transfer mechanism for exit of LDL-Cholesterol from lysosomes. Cell 2009 (*in press*).

LIST OF FIGURES

INTRODUCTION

CHAPTER 1

CHAPTER 2

CHAPTER 3

CONCLUSION AND PERSPECTIVE

LIST OF ABBREVIATIONS

ACAT, acyl-CoA:cholesterol acyl-transferase

ALLN, N-acetyl-Leu-Leu-norleucinal

ASM, acid sphingomyelinase

BSA, bovine serum albumin

CHAPS, 3-[(3-cholamidopropyl)dimethylammonio]-1-propane-sulfonic acid

CHO, Chinese hamster ovary

CMC, critical micellar concentration

CMV, cytomegalovirus

DMEM, Dulbecco's modified Eagle's medium

EndoH, endogylcosidase H

ER, endoplasmic reticulum

FCS, fetal calf serum

HMG CoA, 3-hydroxy-3-methylglutaryl coenzyme A

HSV, herpes simplex virus

PBS, phosphate-buffered saline

LDL, low density lipoprotein

LPDS, lipoprotein-deficient serum

MCD, methyl-β-cyclodextrin

Ni-NTA, nickel-nitrilotriacetic acid

NP-40, nonidet P-40

NPC, Niemann-Pick Type C

NPC1, Niemann-Pick Type C1 disease protein

NPC1(NTD), N-terminal soluble domain of NPC1 protein (amino acids 25-264)

NPC2, Niemann-Pick Type C2 disease protein

NTD, N-terminal domain

PC, Egg Yolk L-α-phosphatidylcholine

r-[25HC oleate]LDL, reconstituted 25-hydroxycholesteryl oleate LDL

SCAP, SREBP cleavage-activating protein

SREBP, sterol regulatory element-binding protein

hTERT, catalytic subunit of human telomerase

Texas Red dye, Texas Red 1,2,-dihexadecanoyl-sn-glycero-3-phosphoethanolamine

TK, thymidine kinase

β-VLDL, β-migrating very low density lipoprotein

25-HC, 25-hydroxycholesterol

INTRODUCTION

CHOLESTEROL TRANSPORT AND HOMEOSTASIS IN CELLS

Cholesterol plays crucial roles in maintaining cell viability and function. It is the primary component of the plasma membrane of cells and is used for the synthesis of bile acids, steroid hormones and vitamin D [1, 2]. Mammalian cells acquire cholesterol from both *de novo* synthesis in the endoplasmic reticulum (ER) and exogenously mainly from low-density lipoprotein (LDL), via the LDL receptor pathway [3]. In normal cells, both newly synthesized and exogenously derived cholesterol redistribute in cell membranes. The cholesterol concentration of cellular membranes is highly variable, but the majority of cellular cholesterol resides in the plasma membrane. Much of our knowledge of intracellular cholesterol trafficking comes from studies on key proteins that have been discovered by identifying gene defects that underlie human disorders of cholesterol trafficking [4]. Familial hypercholesterolemia, a prototype of this group of diseases [3], sheds light on the receptor mediated pathway for the internalization of low-density lipoprotein-cholesterol into cells, homeostatic regulation of LDL receptors and the rate limiting enzyme of *de novo* cholesterol synthesis, 3- hydroxy-3-methylglutaryl-coenzyme A (HMG CoA) reductase. Wolman's syndrome elucidated the role of lysosomes and cholesterol ester hydrolase in processing the cholesterol ester core of LDL [5]. Studies on Niemann-Pick type C, a disease of cholesterol metabolism [5], showed that the transport of LDL-derived cholesterol from lysosomes is protein mediated [6]. The recently acquired knowledge of genes encoding for proteins that modulate cholesterol's cellular functions provide valuable experimental tools in order to

uncover mechanisms that control cholesterol levels in the different compartments within the cell.

The ER of mammalian cells contains a feedback system that senses the level of membrane cholesterol and modulates the transcription of genes that mediate cholesterol synthesis and uptake. When the membrane cholesterol levels decrease, this system responds by increasing cholesterol synthesis and uptake of LDL-derived cholesterol. When the membrane cholesterol accumulates in excess, the system downregulates these processes. The key players in this regulatory system are a family of membrane bound transcription factors called sterol regulatory element binding proteins (SREBPs) [7]. SREBP is synthesized as an inactive precursor bound to the ER membrane and must be proteolytically cleaved by Golgi-localized proteases in order to become activated. Two others proteins that act as sensing mechanisms in order to keep the cellular cholesterol concentration within limits are HMG-CoA reductase, the rate limiting enzyme for cholesterol synthesis [8, 9] and SREBP cleavage activating protein (Scap), a polytopic membrane protein that binds SREBPs [10]. HMG CoA reductase is rapidly degraded under high sterol conditions in order to decreases the endogenous synthesis of cholesterol [10]. Also under high sterol conditions, the Scap/SREBP complex binds to a resident ER protein, designated Insig. This binding prevents the translocation of the Scap/SREBP complex to the Golgi apparatus. As a result, the Scap/SREBP complex remains in the ER, transcription of the target genes declines, and cholesterol synthesis and uptake falls.

In addition to downregulating cholesterol synthesis and uptake, cells respond to high cholesterol levels by activating the esterification enzyme acyl-CoA:cholesterol

acyltransferase (ACAT) which catalyzes the formation of cholesterol esters from cholesterol and long chain fatty acyl-coenzyme A. ACAT-mediated esterification of cholesterol limits its solubility in cell membrane lipids and thus promotes the accumulation of cholesterol ester in fat droplets within the cytoplasm; this process is important because it prevents the toxic accumulation of free cholesterol in various cell membrane fractions and allows the cells to use cholesterol esters within lipid droplets as a source of free cholesterol when the cholesterol levels decrease [11].

All of the homeostatic mechanisms that control the cholesterol content of cells are located in the ER, thus maintenance of cellular cholesterol homeostasis necessitates the transport of cholesterol between subcellular membranes. It has long been known that the concentration of cholesterol in ER membranes is much lower than the concentration of cholesterol in plasma membranes when expressed as the molar ratio of cholesterol to phospholipids [12-14]. Due to its hydrophobicity, spontaneous exchange of cholesterol from one membrane to another across the aqueous cytoplasm is slow. A major challenge is to understand how cholesterol transports from the plasma membrane to the ER where it can execute its regulatory functions. Methods used to monitor cholesterol trafficking consist of pulse experiments in order to label the cholesterol pools in cell membranes. There are two commonly used methods to label membrane cholesterol in cells, the first is by incubating the cells with [^{3}H]cholesterol and the second by incubating the cells with [^{3}H]acetate which will be used as a precursor to synthesize and therefore label cholesterol. In order to monitor the fate of labeled cholesterol, chase experiments are performed. If the labeled cholesterol could traffic to the ER, it will activate ACAT enzyme which would result in an increase in the

amount of [^{3}H]cholesterol ester formation and if the labeled cholesterol could traffic to the plasma membrane, then it should be available for extraction by cyclodextrin, a water-soluble molecule which binds cholesterol with a high affinity [15].

As mentioned earlier, our knowledge of cholesterol transport is linked to advances in identifying proteins involved in trafficking. Recent studies on the inherited cholesterol storage disease, Niemann-Pick type C (NPC), identified the gene that encodes the NPC1 protein [16]. The transport defect in NPC specifically involves cellular trafficking of LDL-derived cholesterol. Since the NPC1 gene was cloned in 1997 [16], the involvement of NPC1 protein in lipid trafficking in cells has been under intense investigation [17].

NIEMANN-PICK TYPE C DISEASE

Niemann-Pick Type C Disease (NPC) disease is an autosomal recessive lipid storage disease with variable clinical manifestations that include hepatosplenomegaly, supranuclear ophthalmoplegia, progressive ataxia, dystonia and dementia. Age of onset of the disease varies from perinatal-adolescent to adult. Patients die before age 20 [18]. Biochemically, the disease is characterized by unique error in trafficking of low-density lipoprotein (LDL)-derived cholesterol that is associated with lysosomal accumulation of excess cholesterol [19]. As a result, unesterified cholesterol, sphingomyelin, phospholipids and glycolipids accumulate in the lysosomes of affected organs [19].

The majority of the patients with this disease have a defect in a gene that encodes a protein designated NPC1 [20]. *NPC1* gene was identified by positional cloning and maps to chromosome 18q11–12 [16]. It encodes an approximately 4.9-kb messenger RNA that is

predicted to produce a 1278- amino acid protein with 13 putative membrane-spanning helices separated by a variety of loops. The protein has a cleaved NH_2-terminal signal sequence that targets the protein for insertion into membranes. Three of these loops are quite large (~240 amino acids) and project into the lumen of endosomes or lysosomes and a cytoplasmic COOH-terminal segment that includes a dileucine sequence that targets the protein to lysosomes [21]. The sequence of five of the transmembrane helices (helices 3 to 7) resembles a sequence that has been observed in other polytopic membrane proteins, including Scap, the protein that transports SREBPs from ER to Golgi; HMG CoA reductase, the rate controlling enzyme in cholesterol synthesis; and Patched, a regulatory protein in the Hedgehog pathway, but its functional role is not equally understood yet [16, 22-24].

More than 170 mutations have been described in patients with NPC1 disease [25] that include nonsense and missense mutations as well as insertions, deletions and duplications. These mutations are spread throughout the gene and do not suggest a single, functionally significant protein domain; however, distinguishing between functional mutants that do not transport cholesterol and folding mutants that do not exit the ER remains unsolved.

In cultured fibroblasts, the phenotype of the disease is quite simple, a block in the egress of cholesterol from lysosomes results in an inability to downregulate two key components of cholesterol homeostasis, HMG CoA reductase and the LDL receptor [26], due to defective regulation of the transcription factor SREBP.

The importance of NPC1 in the transport of LDL-derived cholesterol out of the lysosomes is well established. However, there is contradictory evidence for the role of NPC1 in transporting plasma membrane cholesterol and endogenously synthesized cholesterol to

the ER. Studies done by Reid et al. (2003) [27] showed that shortly after its synthesis, the majority of cholesterol is transported to the plasma membrane. Pulse-chase experiments suggest that this transport is independent of NPC1 because when cells were labeled with [^{3}H]acetate, the newly synthesized [^{3}H]cholesterol was available for extraction by cyclodextrin. However, the post-plasma membrane fate of cholesterol was dependent on NPC1, since cholesterol was not available for esterification by ACAT [27, 28]. This effect was cell type specific, while macrophages and glial cells were affected by the NPC1 mutation, the differences seen in embryonic fibroblasts were less [27].

Approximately 5-10% of patients with NPC disease have a mutation in *NPC2* gene that encodes a 131 amino acid protein. NPC2 is a soluble glycosylated protein located in the lumen of the late endosomes/lysosomes and can be secreted into the medium of cultured cells [29]. NPC1 and NPC2 are likely to work in the same pathway, since homozygous mutations in either one of the proteins results in the same NPC phenotype [30]. Since NPC1 and NPC2 proteins are involved in the egress of LDL-derived cholesterol from lysosomes, it is not surprising that both proteins bind cholesterol with similar affinity [31-33]. However, there are major differences in the sterol binding pocket of the two proteins. While NPC1 buries the 3β-hydroxyl group and the tetracyclic ring and leaves the isooctyl side chain partially exposed, NPC2 binds in the opposite orientation with the isooctyl side chain buried deep in the binding pocket and the 3β-hydroxyl group exposed [30-32, 34, 35]. This data confirms that the NPC proteins bind to opposite ends of the cholesterol molecule.

The exact roles of NPC1 and NPC2 in the endosomal lipid transport process are not clear at present. Recent studies by Infante *et al.* (2008), localizes the cholesterol binding site

to the soluble luminal N-terminal domain (NTD) of NPC1 (amino acids 25–264) [34, 36]. Using purified protein of NPC1(NTD) and NPC2, they established an *in vitro* assay to measure transfer of [^{3}H]cholesterol between these two proteins and phosphatidylcholine liposomes. Whereas NPC2 rapidly donates or accepts cholesterol from liposomes, NPC1(NTD) acts much more slowly. Bidirectional transfer of cholesterol between NPC1(NTD) and liposomes is accelerated >100-fold in the presence of NPC2. A naturally occurring human mutant of NPC2 (P120S) fails to bind cholesterol [37] and fails to stimulate cholesterol transfer from NPC1(NTD) to liposomes. NPC2 may be essential to deliver or remove cholesterol from NPC1, an interaction that links both proteins to the cholesterol egress process from lysosomes. These findings may explain how mutations in either protein can produce a similar clinical phenotype. Within cells, cholesterol egress from lysosomes is unidirectional, i.e., from LDL to lysosomal membranes to ER. To establish this unidirectional flux, NPC1 and NPC2 could act in one of two possible orders, as illustrated in Figure 1. In both models, NPC2 performs a shuttling function with respect to NPC1. In Model B, acid lipase interacts with the membranous domain of NPC1 and releases cholesterol directly to the NTD of NPC1, which then transfers it to NPC2. Given the relative simplicity of NPC2's structure, insertion of cholesterol into the lysosomal membrane, from which it travels to the ER, would likely require NPC2 to interact with a lysosomal cholesterol transporter, as yet unidentified. In Model A, acid lipase liberates cholesterol which is then bound by NPC2 and delivered to the NTD of NPC1. NPC1 then inserts the cholesterol into lysosomal membranes, from which it is transferred to the ER. In this case, membrane

insertion is likely mediated by the complex membranous domain of NPC1. The current *in vitro* data do not permit an experimental distinction between these two models.

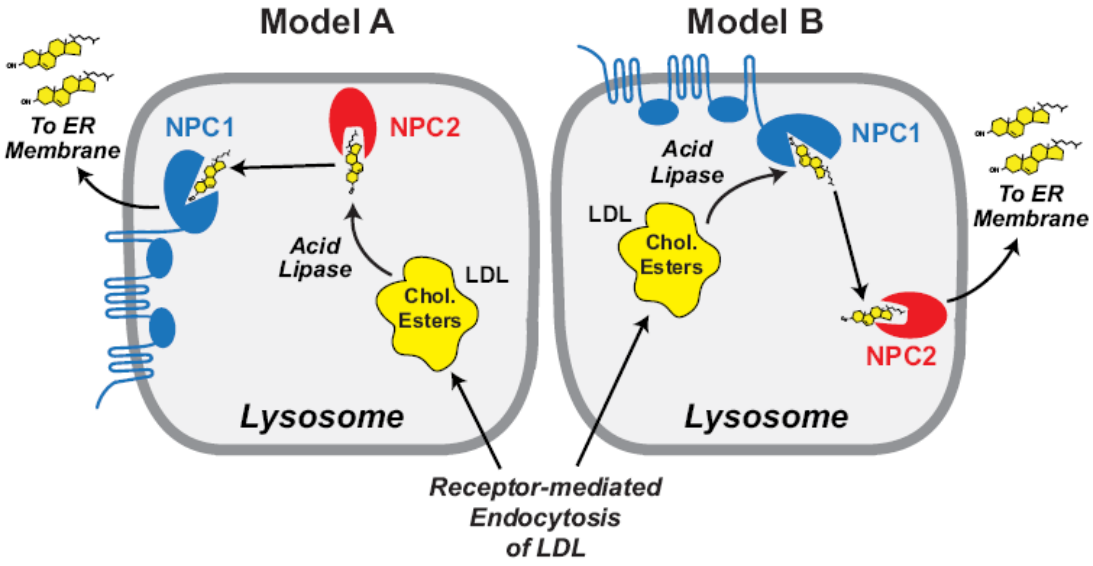

Figure 1: Alternative models for the transfer of cholesterol from LDL to lysosomal membranes. The interpretations of Model A and Model B are discussed in the introduction. Adapted from Infante et al. (2008) [36].

The mechanism by which NPC1 and NPC2 facilitate lipoprotein-derived cholesterol transport out of the lysosome into membranes still remains a mystery. Direct binding between these two proteins has never been shown probably because of the transient interaction between the two proteins in order to transfer cholesterol. The latest studies by Infante *et al.*, (2008) provide a useful tool in order to test for such weak interaction [36]. Although NPC1 and NPC2 have been cloned for over 10 years, we are only beginning to understand how these proteins are involved in the trafficking of LDL-derived cholesterol in cells.

CHAPTER ONE

FUNCTIONAL SIGNIFICANCE OF STEROL BINDING TO NIEMANN-PICK TYPE C1 DISEASE PROTEIN

SUMMARY

The Niemann-Pick C1 protein (NPC1) is required for the transport of lipoprotein-derived cholesterol from lysosomes to endoplasmic reticulum (ER). Recombinant version of the 1278-amino acid, polytopic membrane protein has been purified, and was shown to bind oxysterols with a hydroxyl group on the 24, 25, or 27 positions as well as cholesterol when the detergent concentration was reduced below the critical micellar concentration (CMC), however the mechanism of action of sterol binding is unknown. Here we show that NPC1 is not required for the known regulatory actions of oxysterols. Thus, in NPC1-deficient fibroblasts 25-HC blocked the processing of sterol regulatory element-binding proteins (SREBP) and activated acyl-CoA:cholesterol acyltransferase (ACAT) in a normal fashion. We also localize the binding site to the N-terminus of NPC1, a 240-amino acid luminal domain with 18 cysteines. NPC1(NTD) bound [^{3}H]cholesterol and [^{3}H]25-hydroxycholesterol (25-HC) with one sterol binding site per two NPC1(NTD) proteins. When Glutamine-79 in NPC-1(NTD) was mutated to Aalanine, it abolished the binding of [^{3}H]25-HC, but not [^{3}H]cholesterol. Having a mutation that selectively disrupts oxysterol binding to NPC1 allowed us to test the importance of oxysterol binding to NPC1. The Q79A

mutant restored cholesterol transport to NPC1-deficient CHO cells similar to wild-type. Thus, oxysterol binding to NPC1(NTD) is not essential for NPC1 function in fibroblasts, but it may function in other cells where NPC1 deficiency produces more complicated lipid abnormalities.

INTRODUCTION

.

This chapter describes the functional significance of sterol binding to NPC1. We encountered NPC1 unexpectedly in a search for a membrane-bound protein that binds oxysterols such as 25-hydroxycholesterol (25-HC) [31]. 25-HC belongs to a class of sterols called oxysterols because they contain an additional hydroxyl group on the isooctyl side chain. We were searching for such a protein because 25-HC and related oxysterols mimic the regulatory actions of cholesterol in the ER of animal cells. Thus, 25-HC blocks the ER-to-Golgi transport of sterol regulatory element-binding proteins (SREBPs), which are transcriptional activators for synthesis of cholesterol and other lipids [38]; it accelerates the degradation of HMA CoA reductase [39]; and it activates ACAT [40].

We purified recombinant human NPC1 and confirmed that it binds [^{3}H]25-HC [31]. We also found that the recombinant protein binds [^{3}H]cholesterol, but only when the detergent is reduced to submicellar concentrations [31]. When delivered to cells in ethanol, these oxysterols mimic the ER regulatory actions of cholesterol, i.e., they block SREBP cleavage and they activate ACAT [31, 41]. However whether oxysterols traverse lysosomes is unknown and there is no evidence that they require the actions of NPC1 in order to reach the ER. We were therefore surprised to find that a purified membrane-bound, oxysterol-binding protein turned out to be NPC1.

In the current studies we localize the sterol binding site in human NPC1 to its N-terminal domain, NPC1(NTD). We tested for the ability of several clinical mutations corresponding to substitutions in NPC1(NTD) observed in patients with NPC1 disease to

regulate SREBP-2 processing in response to sterols. We then show that a novel mutation with a single amino acid substitution of Glutamine at position 79 to Alanine selectively abolished the binding to [^{3}H]25-HC. Having a mutant that selectively eliminated oxysterol binding allowed us to test for the significance of oxysterol binding to NPC function. We tested for the ability of sterols to regulate SREBP-2 cleavage and activate ACAT in a CHO mutant cell line that does not have a functional NPC1 protein and overexpresses the Q79A mutant. This work provides a beginning for the eventual analysis of the mechanism by which NPC1 transports cholesterol from lysosomes to ER.

EXPERIMENTAL PROCEDURES

Materials– We obtained [26,27-^{3}H]25-hydroxycholesterol (75-80 Ci/mmol), [1,2,6,7-^{3}H]cholesterol (60 Ci/mmol), and [1-^{14}C]oleic acid (54.6 mCi/mmol) from American Radiolabeled Chemicals; CHAPS from Anatrace, Inc.; and bovine serum albumin (BSA) from Pierce (Cat. No. 23210); anti-Flag M2-Agarose affinity beads and 6-methylcholesterol from Sigma; all other sterols from Steraloids; FuGENE 6 and Nonidet P-40 (NP-40) from Roche Applied Sciences; and Hybond C nitrocellulose filters and all chromatography products (unless otherwise mentioned) from GE Healthcare Biosciences. Rabbit β-migrating very low density lipoproteins (β-VLDL) ($d < 1.006$) [42] and human and newborn calf lipoprotein-deficient serum (LPDS, $d > 1.215$ g/ml) [22] were prepared by ultracentrifugation as described in the indicated reference. Solutions of compactin and sodium mevalonate were prepared as previously described [43].

Buffers – Buffer A contains 50 mM Tris-chloride at pH 7.4, 150 mM NaCl, and 0.004% (w/v) NP-40. Buffer B contains 50 mM Tris-chloride at pH 7.4, 100 mM KCl, and 1% NP-40. Buffer C contains 50 mM Tris-chloride at pH 7.4 and 150 mM NaCl. Buffer D contains 50 mM Tris-chloride at pH 7.4, 50 mM KCl, 10% (v/v) glycerol, 5 mM dithiothreitol, 1 mM sodium EDTA, and protease inhibitor mixture (1 μg/ml pepstatin A, 2 μg/ml aprotinin, 10 μg/ml leupeptin, 200 μM phenylmethylsulfonyl fluoride, and 25 μg/ml of *N*-acetyl-leucinal-leucinal nonleucinal).

Plasmid Constructions– pCMV-NPC1-His_8-Flag encodes wild-type human NPC1 followed sequentially by eight-histidines and a Flag tag under control of the cytomegalovirus (CMV) promoter. This plasmid was constructed from pCMV-NPC1 (Origene Technologies) by site-directed mutagenesis (QuickChange II XL kit, Stratagene). pCMV-NPC1(1-307;1254-1278)-His_8-Flag was constructed from pCMV-NPC1-His_8-Flag by site-directed mutagenesis (QuickChange II XL kit, Stratagene) using the 5'-oligonucleotide, 5'-CTCCGAGTACACTCCCATCGATAGCGTAAATAAAGCCAAAAGTTGTGCC-3' and the 3'oligonucleotide, 5' GGCACAACTTTTGGCTTTATTTACGCTATCGATGGGAGT GTAGTCGGA-3'. pCMV-NPC1(1-264)-His_8-Flag was constructed from pCMV-NPC1(1-307;1254-1278)-His_8-Flag by site-directed mutagenesis using the 5'oligonucleotide, 5'-CCTGCTCCCTGGACGATCCTTGGCCATCACCATCACCATCACCATCACGACTA-3' and the 3'oligonucleotide, 5'-TTATAGTCGTGATGGTGATGGTGATGGTGATGGCCAA GGATCGTCCAGGGAGCAGG-3'. When this plasmid is expressed in CHO-K1 cells, the resulting protein (after signal peptide cleavage) consists of the N-terminal domain (NTD) of NPC1 (amino acids 25-264). This protein is hereafter referred to as NPC1(NTD).

Under control of the Herpes Simplex virus thymidine kinase promoter, pTK-NPC1-His8-FLAG3 encodes WT human NPC1 followed sequentially by 8 histidines and 3 FLAG tags. The sequence encoding NPC1-His_8-FLAG was derived from digestion of pCMV-NPC1-His_8-FLAG with Not1, Xba1, and Xho1. This sequence was gel-purified and ligated into a pTK vector obtained from digestion of pTK-HSV-BP2 with Not1 and Xba1. Two additional FLAG tags were added to the C-terminus of this construct through two rounds of site-directed mutagenesis. The coding region of each plasmid was sequenced to ensure

integrity of the construct. Mutations in NPC1 were produced by site-directed mutagenesis of pCMV-NPC1(1-264)-His_8-Flag, pCMV-NPC1-His_8-Flag and pTK-NPC1-His_8-$Flag_3$ plasmids.

pTK-HSV-BP-2 encodes wild-type *Herpes simplex* virus (HSV)-tagged human SREBP-2 under control of the thymidine kinase promoter [22].

SREBP-2 Processing in Cultured Cells – Skin fibroblasts from a normal subject and a patient with NPC1 disease (obtained from American Type Culture Collection, ATTC No. GM3123) were immortalized with the catalytic subunit of telomerase (hTERT) by retroviral infection of the cells with the Babepuro-hTERT vector as previously described [44, 45]. The resulting immortalized cell lines are designated h-TERT-Control and h-TERT-NPC1(P237S/I1061T). The cells were grown in monolayer at 37°C in 5% CO_2 and maintained in medium B (Dulbecco's modified Eagle's medium containing 100 units/ml penicillin and 100 μg/ml streptomycin sulfate) supplemented with 10% FCS. On day 0, h-TERT-Control and h-TERT-NPC1(P237S/I1061T) fibroblasts were set up in medium B containing 10% FCS at $6x10^4$ and $7x10^4$ cells/60-mm dish, respectively. On day 2, cells were washed once with phosphate-buffered saline and switched to medium B containing 5% human LPDS. On day 4, cells were switched to medium C (medium B containing 50 μM compactin, 50 μM sodium mevalonate) supplemented with 10% human LPDS and various concentrations of 25-HC or β-VLDL. After incubation for 5 h, cells were treated with 25 μg/ml ALLN for 1 h and then harvested. Six dishes for each condition were pooled for

preparation of nuclear extract and membrane fractions, which were analyzed by immunoblotting for SREBP (described below).

Primary fibroblast cultures from a wild type BALB/c mouse and a mutant BALB/c *npc*^{nih} mouse [46] were established from explants of skin taken at 7 to 8 weeks of age [47]. Cells were cultured and set up for experiments as described above for the human fibroblasts except that the density for plating was 4 x 10^4 cells/60-mm dish. The wild type and mutant mice were obtained from Drs. Stephen Turley and John Dietschy (UT Southwestern Medical Center, Dallas, TX).

Mutant CHO 4-4-19 cells, defective in NPC1 [48], were obtained from Laura Liscum (Tufts University School of Medicine, Boston, MA). The defective NPC1 in 4-4-19 cells results from an amino acid substitution (Gly660Arg). Mutant CHO 4-4-19 cells were transfected as described later. On day 3, the medium was switched to medium A (1:1 mixture of Ham's F12 medium and Dulbecco's modified Eagle's medium, 100 units/ml penicillin and 100 μg/ml streptomycin sulfate) containing 5% newborn calf LPDS, 5 μM compactin, and 50 μM sodium mevalonate. On day 4, the cells received fresh medium A supplemented with 5% newborn calf LPDS, 50 μM compactin, 50 μM sodium mevalonate and various concentrations of β-VLDL or 25-HC. After incubation at 37°C for 5 h, cells were treated with 25 μg/ml of *N*-acetyl-leucinal-leucinal-norleucinal for 1 h and then harvested. Duplicate dishes were pooled for preparation of nuclear extract and 100,000*g* membrane fractions, which were then analyzed by immunoblotting for SREBP-2 (described below).

Preparation of Reconstituted LDL — LDL was extracted with heptane and reconstituted with 25-HC oleate (r-[25-HC oleate]LDL) as described previously [49]. 25-HC oleate was synthesized from *cis*-9-octadecenoic acid (Grace Davison Discovery Sciences) and 25-HC in the laboratory of Dr. Jef DeBrabander (UT Southwestern Medical Center). The product was isolated on a silica gel column, and its purity verified by thin-layer chromatography.

Immunoblot Analysis – Nuclear extract and membrane fractions from cultured cells were subjected to 8% or 12% SDS-PAGE, after which the proteins were transferred to nitrocellulose filters. The immunoblots were performed at room temperature using the following primary antibodies: 1 μg/ml of a rabbit polyclonal antibody against human NPC1 (Novus); 5 μg/ml of a mouse monoclonal anti-Flag (IgG fraction; Sigma); 8 μg/ml of a rabbit polyclonal antibody (IgG-R139) directed against hamster Scap [50]; 0.2 μg/ml of IgG-HSV-Tag, a monoclonal antibody directed against the glycoprotein D epitope of *Herpes simplex* virus (Novagen, Inc); and 10 μg/ml of a rabbit polyclonal antibody (IgG-1819) directed against amino acids 1-100 of human SREBP-2. The latter antibody was raised by injecting rabbits with a His_8-tagged recombinant version of the antigen. Bound antibodies were visualized by chemiluminescence (SuperSignal Substrate; Pierce) using a 1:5000 dilution of anti-mouse IgG (Jackson Immunoresearch Laboratories, Inc.) or a 1:2000 dilution of anti-rabbit IgG conjugated to horseradish peroxidase (Amersham Biosciences). The filters were exposed to Kodak X-Omat Blue XB-1 film at room temperature.

ACAT Assay – The rate of incorporation of [^{14}C]oleate into cholesteryl [^{14}C]oleate and [^{14}C]triglycerides by intact cell monolayers was measured as described previously [51].

Transfection of NPC1 Constructs in CHO Cells – CHO-K1 cells were grown and transfected in medium A containing 5% (v/v) fetal calf serum (FCS). Each dish was transfected with one of the following plasmids: 5 μg of pCMV-NPC1-His_8-Flag, 5 μg of pCMV-NPC1(1-307;1254-1278)-His_8-Flag, or 5 μg of pCMV-NPC1(1-264)-His_8-Flag (wild-type or the indicated mutant versions) using FuGENE 6 reagent as described [52]. After 16 h, the transfected cells were used for purification of NPC1 proteins as described below.

Mutant CHO 4-4-19 cells, defective in NPC1 (defective in NPC1) [48], were set up on day 0 in medium A containing 5% FCS at $2x10^5$ cells/60-mm dish. On day 2, each dish was transfected in OPTI-MEM (Gibco) with the indicated plasmid, using Lipofectamine 2000 according to the manufacturer's directions. After 5 h, the medium was switched to medium A containing 5% newborn calf LPDS. After 16 h, the cells were used for assays of ACAT and SREBP-2 processing.

Purification of Full Length NPC1 and Internally Deleted NPC1(1-307;1254-1278) from Transfected CHO Cells – Recombinant NPC1 proteins were overexpressed in CHO-K1 cells as described above. After incubation at 37°C for 16 h, the cells were harvested, washed, and resuspended in ice-cold buffer A containing 25 μg/ml ALLN. Cells were homogenized with a 15-ml or 40-ml Dounce homogenizer, and then subjected to 100,000*g* centrifugation for 30 min at 4°C. The membrane pellet was resuspended by Dounce homogenization in buffer C containing the protease inhibitor mixture and 25 μg/ml ALLN (4 dishes of cells per 1 ml of buffer), incubated overnight at 4°C to solubilize membrane proteins, and centrifuged at 100,000*g* for 30 min. The resulting 100,000*g* supernatant (containing detergent-solubilized

membranes) was dialyzed against buffer G for 6-12 h at 4°C, after which imidazole was added at a final concentration of 20 mM. This material was then loaded onto a 1-ml His Trap HP nickel column pre-equilibrated with buffer G. The column was washed sequentially with 10 column volumes of buffer G, 10 column volumes of buffer G plus 25 mM imidazole, and 20 column volumes of buffer G plus 50 mM imidazole. Bound protein was eluted in 1.5-ml fractions with buffer G plus 200 mM imidazole. The eluted fractions containing anti-Flag (NPC1) immunoblot reactivity were then loaded onto a column containing 1-ml Anti-Flag M2-Agarose beads (Sigma), which had been pre-equilibrated with buffer G. The column was washed with either 10 column volumes of buffer G (1% NP-40) or 25 column volumes of buffer H (0.1% Fos-Choline 13). Bound protein was eluted with 0.1 mg/ml of Flag peptide in 9 column volumes of either buffer G or buffer H. The pooled proteins were subjected to SDS/PAGE followed by Coomassie staining to determine purity.

Purification of Secreted Forms of NPC1(NTD) from Medium of Transfected CHO Cells – Recombinant NPC1 protein were overexpressed in CHO-K1 cells as described above. On day 3, the medium was switched to medium A containing 1% (v/v) Cellgro® ITS (Fisher Scientific). After 24 h, the medium was collected and fresh medium A containing 1% Cellgro® ITS was added. This was done for 3 consecutive days for each group of transfected cells. After each collection, the medium was subjected to centrifugation at 2,500 rpm for 5 min at 4°C and then filtered through an Express PLUS 0.22-μm filter apparatus (Millipore). Medium was stored at 4°C covered in aluminum foil. Gravity columns were each filled with a 20-ml slurry of Ni-NTA agarose beads, after which each column was pre-

equilibrated with 4 column volumes of buffer C. Filtered medium (1 L per column) was then passed overnight at 4°C through each Ni-NTA agarose column ~1 ml/min. Each column was washed sequentially with 50 ml of buffer C containing 20 mM and 40 mM imidazole. Bound protein was eluted with 50 ml of buffer C containing 200 mM imidazole. The eluted fraction containing NPC1(25-264)-His_8-Flag was concentrated to 0.5 ml by using a spin concentrator with an Amicon Ultracel 30K or 10K Filter Device (Millipore), respectively. The concentrated material was then subjected to gel filtration chromatography on a 24-ml Superdex-200 column that was pre-equilibrated with buffer C. The fractions containing the peak A_{280} activity and eluting between 12.5 and 15 ml (for NPC1(25-264)-His_8-Flag) were pooled, and their protein content was quantified by either the BCA kit (Pierce) or the Lowry method (44). The pooled proteins were subjected to SDS/PAGE followed by Coomassie staining to determine purity.

Ni-NTA Agarose Assay for ^{3}H-Sterol Binding – For the standard assay of wild-type and mutant versions of NPC1, each reaction contained, in a final volume of 80 μl of buffer A, either [^{3}H]25-HC (165-180 dpm/fmol) or [^{3}H]cholesterol (132 dpm/fmol) delivered in ethanol (final ^{3}H-sterol concentration, 10-400 nM), 1 μg of BSA as indicated, and varying amounts of NPC1 protein. After incubation for 4 h or 16 h at 4°C, the mixture was loaded onto a column packed with 0.3 ml of Ni-NTA Agarose beads (Qiagen) that had been pre-equilibrated with the appropriate assay buffer. Each column was washed for ~ 15 min with 5-6 ml of buffer B. The protein-bound ^{3}H-sterol was eluted with 250 mM imidazole in buffer B and quantified by scintillation counting as previously described [53]. For competition experiments with unlabeled sterols, the standard assays were carried out in the

presence of the indicated unlabeled sterol (0-3 μM) delivered in ethanol (final ethanol concentration, 1-4%). In each experiment, all tubes received the same amount of ethanol.

RESULTS

NPC1 is Not Required for Oxysterol-mediated Inhibition of SREBP-2 Processing– Oxysterols such as 25-HC are potent inhibitors of SREBP-2 processing in mammalian cells [38]. To test whether NPC1 is required for this processing event, we analyzed the proteolytic processing of SREBP-2 in mutant fibroblasts that lack functional NPC1. The first set of experiments was performed with telomerase-immortalized human fibroblasts from an individual with NPC1 disease (GM3123). Previous studies have shown that NPC1 is required for the export of lipoprotein-derived cholesterol from the lysosome to the ER where the cholesterol activates ACAT, thereby causing an increase in the incorporation of radiolabeled fatty acids into cholesteryl esters [54, 55]. However, NPC1 is not required for the stimulation of cholesterol esterification by 25-HC [54]. To deliver lipoprotein cholesterol to cells, we used cholesterol-rich rabbit β-VLDL, which binds with high affinity to human LDL receptors [56] and reaches lysosomes through receptor-mediated endocytosis. We tested the ability of increasing concentrations of β-VLDL to stimulate the incorporation of [^{14}C]oleate into cellular cholesteryl [^{14}C]oleate. As shown in Figure 1-1*A* (*left panel*), β-VLDL markedly increased the amount of cholesteryl [^{14}C]oleate formed in h-TERT-control fibroblasts, but not in h-TERT-NPC1(P237S/I1061T) fibroblasts. On the other hand, 25-HC increased cholesteryl [^{14}C]oleate formation in both h-TERT-control and h-TERT-NPC1(P237S/I1061T) cells (*right panel*).

If NPC1 is required for the oxysterol-mediated inhibition of the proteolytic processing of SREBPs, then the telomerase-immortalized NPC1 fibroblasts should show a decreased nuclear accumulation of the cleaved form of SREBP. Figure 1-1*B* shows an immunoblot analysis of SREBP-2 processing in h-TERT-control and h-TERT-NPC1(P237S/I1061T) fibroblasts. As a positive control for NPC1 function, we added β-VLDL, which inhibited cleavage in h-TERT-control cells (lanes *2-4*), but not in h-TERT-NPC1(P237S/I1061T) cells that fail to transport lipoprotein-derived cholesterol to the ER (lanes *9-11*). In contrast, 25-HC blocked the generation of nuclear SREBP-2 at 0.3-1 μg/ml both in h-TERT-control (lanes *5- 7*) and h-TERT-NPC1(P237S/I1061T) (lanes *12-14*) cells.

To verify the above result in another cell culture system, we carried out similar studies of SREBP-2 processing in fibroblasts from a mouse homozygous for a nonfunctional *NPC1* gene [46]. Figure 1-1*C* shows that the mouse NPC1$^{nih/nih}$ cells responded similarly to the control cells in terms of inhibition of SREBP-2 processing by 25-HC (lanes *2-4*, *9-11*), but not in terms of their response to β-VLDL (lanes *5-7*, *12-14*).

Egress of LDL-derived Cholesterol but not LDL-derived 25-HC from Lysosomes is Dependent on NPC1 — When delivered to cells in ethanol, oxysterols mimic the ER regulatory actions of cholesterol, i.e., they block SREBP cleavage and they activate ACAT [31, 41]. However, there is no evidence that oxysterols traverse lysosomes. A method was developed in the lab for extracting the free and esterified cholesterol from the LDL particle with heptane and reconstituting the hydrophobic core of the lipoprotein with exogenous 25-hydroxycholesteryl oleate [49]. The resulting particle, designated r-[25-HC oleate]LDL, bound to LDL receptors on human fibroblasts, was taken up by receptor mediated

endocytosis and was hydrolyzed in lysosomes in a manner similar to that of native LDL and suppressed the activity of 3-hydroxy- 3-methylglutaryl-coenzyme A (HMG CoA) reductase, the rate-limiting enzyme in cholesterol biosynthesis [49]. We wanted to test if the transport of LDL-derived 25-HC from lysosomes is dependent on NPC1, to that end we looked at the effect of r-[25-HC oleate]LDL treatment on SREBP-2 processing (Figure 1-2*A*) and HMG CoA reductase degradation (Figure 1-2*B*) in NPC1 cells. Monolayers from immortalized h-TERT-control and h-TERT-NPC1(P237S/I1061T) human skin fibroblasts were treated with 25-HC in ethanol, the native LDL particle, or the indicated concentration of r-[25-HC oleate]LDL (Figure 1-2*A and B*). 25-HC in ethanol could suppress the proteolytic cleavage of SREBP-2 (Figure 1-*2A, lane* 2) as well as induce the degradation HMG CoA reductase (Figure 1-2*B, lanes 4 and 9*) in both h-TERT-control and h-TERT-NPC1(P237S/I1061T) cells, whereas LDL could only suppress the proteolytic processing of SREBP-2 (Figure 1-2A, *lane 3*) and induce the degradation of HMG CoA reductase (Figure 1-2*B, lanes 5 and 10*) in h-TERT-control, but not in h-TERT-NPC1(P237S/I1061T) cells. r-[25-HC oleate]LDL could suppress the cleavage of SREBP-2 in both h-TERT-control and h-TERT-NPC1(P237S/I1061T) cells at 5-10 μg protein/ml (Figure 1-5*A, lanes 4-8*), suggesting that the transport of LDL-derived 25-HC from the lysosomes to the ER is independent of NPC1. Moreover, r-[25-HC oleate]LDL could induce the degradation of HMGCoA reductase in h-TERT-control and h-TERT-NPC1(P237S/I1061T) cells (Figure 1-5*B, lanes 2, 3, 7 and 8*). These results prove that the transport of 25-HC in cells is independent of NPC1 function, because when 25-HC was delivered to lysosomes of cells through receptor-mediated

endocytosis, it could still bypass the NPC1 mutation and transport 25-HC to the ER where it could execute its regulatory functions.

Localization of Oxysterol Binding Site in NPC1 – Figure 1-3*A* shows a diagram of the postulated domain structure of human NPC1, a 1278-amino acid protein. The protein is believed to contain 13 putative transmembrane helices [21] that divide the protein into the following structural domains: 1) a cleaved signal sequence (amino acids 1-24) (11); 2) a soluble, luminal N-terminal domain (amino acids 25-264); 3) large luminal loop-2 (amino acids 371-615); 4) a putative sterol-sensing domain (transmembrane helices 3-7, amino acids 616-791) (45,47); 5) large luminal loop-3 (amino acids 855-1098); and 6) a lysosomal targeting signal (LLNF) at the COOH-terminus (amino acids 1275-1278) [57].

To localize the region in NPC1 that binds 25-HC, we created plasmids encoding the first 307, 644, 809, or 1178 amino acids of the protein fused to a fragment comprising the COOH-terminal 24 amino acids, which contains the lysosomal targeting signal. The epitope-tagged proteins were purified as described for the full length protein under "Experimental Procedures". All of these internally deleted proteins bound [^{3}H]25-HC with saturation kinetics that were similar to that of the full-length protein (data not shown). The smallest of these deleted proteins contain 332 NPC1-derived amino acids and is designated NPC1-His_8-Flag(Δ1-307;1254-1278) (see bottom panel of Figure 1-3*A*). Figure 1-3*B* shows the migration of this internally deleted protein on SDS-PAGE as determined by immunoblotting (*lane 2*). Migration of the full-length protein is also shown (*lane 1*). Both proteins exhibited broad bands, presumably owing to extensive *N*-linked glycosylation. The internally deleted and full-length protein bound similar amounts of [^{3}H]25-HC (Figure 1-3*C*). Unlabeled 25-

HC and 27-hydroxycholesterol (27-HC) competed effectively for the binding of [^{3}H]25-HC. Unlabeled cholesterol and 19-hydroxycholesterol (19-HC) did not compete (Figure 1-3*D*). The binding specificity of the internally deleted NPC1 with respect to oxysterols is thus similar to that of the full-length molecule.

Secretion and Purification of NPC1(NTD) - In order to further define the oxysterol-binding site within the membrane-anchored, internally deleted NPC1(1-307;1254-1278), we made a further truncation from the COOH-terminus to remove the single transmembrane domain and the lysosomal targeting sequence. This protein, designated NPC1(25-264)-His_8-Flag, contains 240 amino acids after the signal sequence has been cleaved, as shown in Figure 1-4*A*. Figure 1-4*B* shows a comparison of the amino acid sequence of human NPC1(NTD) with a consensus sequence that was derived from the sequences of 12 vertebrate species, including 10 mammals. Of the 240 amino acids in this domain, 124 are invariant (Figure 1-4*B*, *black boxes*). Eighteen of the invariant residues are cysteines (Figure 1-4*B*, *yellow boxes*).

When expressed in CHO cells by transfection, full-length NPC1-His_8-Flag and NPC1(1-307;1254-1278)-His_8-Flag were found exclusively in a 10^5g pellet of cell membranes (Figure 1-4*C*, *lanes 6* and *9*). In contrast, the vast bulk of NPC1(25-264)-His-Flag was secreted into the medium (*lane 10*). Note that the relative amount of the medium fraction applied to the gel was only one-fifth the amount of the cell supernatant and pellet fractions.

Mutational Analysis of NPC1(NTD) – We subjected NPC1(25-264)-His_8-Flag to mutational analysis in order to pinpoint amino acids crucial for sterol binding. We focused

on five residues (Q79, N103, Q117, F120, and Y157) that are conserved in 12 vertebrate NPC1 orthologs and that exhibit >75% identity among homologs of NPC1 found in 76 eukaryotic species (data not shown). These residues were also chosen for their hydrogen-bonding potential (Q79, N103, and Q117) or for their ability to form ring-stacking interactions (F120 and Y157). Each of these residues was mutated to alanine (see Figure 1-4*C*, *red boxes*). The two hydrophobic residues, F120 and Y157, were also mutated to methionine. In addition to these novel mutations, we reproduced six "clinical" mutations corresponding to substitutions in NPC1(NTD) observed in patients with NPC1 disease (Q92R, T137M, P166S, N222S, D242H, and G248V; see Figure 2-2*C*, *blue boxes*) [25]. Plasmids encoding each mutant version of NPC1(NTD) were expressed in CHO cells, and the recombinant proteins were purified from the medium. The medium of transfected cells was subjected to Ni-chromatography followed by gel filtration chromatography in the absence of detergents (see "Experimental Procedures"). When stored at 4°C in buffer C (without detergent) at concentrations between 0.3-2.0 mg/ml, the protein retained full binding activity and continued to appear monodisperse on gel filtration. To measure the binding of ^{3}H-labeled sterols to purified wild-type and mutant NPC1(25-264)-His_8-Flag, we used an assay in which the protein was trapped on a nickel agarose column, and bound ^{3}H-sterols were quantified by scintillation counting [31, 58]. The binding reactions were conducted in a low concentration of NP-40 (0.004%), which is slightly higher than the critical micellar concentration (CMC). Wild-type and all mutant proteins were secreted, and they all showed a normal behavior on gel filtration and SDS-PAGE.

The binding of [^{3}H]25-HC to purified NPC1(25-264)-His$_8$-Flag was saturable with an apparent Kd of 10 nM (Figure 1-5*A*). At saturation, we estimated that 1 molecule of [^{3}H]25-HC bound to two NPC1(25-264)-His$_8$-Flag proteins. We then tested the ability of NPC1(NTD) to bind [^{3}H]cholesterol. As shown in Figure 1-5*B*, this protein fragment bound [^{3}H]cholesterol with an apparent K_d of 130 nM. At saturation, we estimated that 1 molecule of [^{3}H]cholesterol bound to two NPC1(25-264)-His$_8$-Flag proteins, a similar binding stoichiometry to that of [^{3}H]25-HC. Of the 14 mutant proteins, only two of the novel mutants, Q79A and Q117A, showed an abnormality in sterol binding. The most striking abnormality was observed with the Q79A mutant, which showed no detectable binding of [^{3}H]25-HC (Figure 1-5*A*) and a 40% decrease in maximal binding of [^{3}H]cholesterol (Figure 1-5*B*). Similar results were obtained in 4 additional experiments involving 3 different preparations of purified NPC1(NTD). Circular dichroism spectra of the Q79A protein was identical to that of the wild-type protein, indicating no major structural changes (data not shown). Mutant Q117A also showed a 40% decrease in binding of [^{3}H]cholesterol (Figure 1-5*B*), but only a slight decrease in [^{3}H]25-HC binding (Figure 1-5A). Figures 1-5*C* and 1-5*D* show the binding data for two of the clinical mutants, Q92R and T137M, both of which showed normal binding for both [^{3}H]25-HC and [^{3}H]cholesterol. To determine whether the point mutation Q79A that disrupts 25-HC binding in NPC1(NTD) also affects the binding properties of the full-length NPC1 molecule, we expressed and purified the Q79A mutant version of full-length NPC1-His$_8$-Flag in 0.004% NP-40 as described for the wild-type full length protein under "Experimental Procedures". [^{3}H]25-HC did not bind to the Q79A

mutant protein. The Q79A mutant protein also bound very little [^{3}H]cholesterol as compared with the wild-type version (data not shown).

Full-Length Mutant NPC1(Q79A) Restores NPC1 Function to CHO 4-4-19 Cells when Expressed Under the Control of a Strong CMV Promoter– The availability of a point mutation in the full-length NPC1 protein that abolishes its 25-HC binding activity provided the opportunity to determine whether oxysterol binding to wild-type NPC1 influences the transport of lipoprotein-derived cholesterol from endosomes/lysosomes to the ER. To test this hypothesis, we transfected wild-type and mutant versions of NPC1-His_8-Flag into CHO 4-4-19 cells, a mutant line of CHO cells with a deficiency of NPC1 function. In these cells, LDL and β-VLDL have a reduced ability to stimulate ACAT activity as measured by cholesteryl [^{14}C]oleate formation in intact cells [48] On the other hand, 25-HC activates ACAT normally in these cells [48]. Figure 1-6*A* shows an immunoblot of membrane extracts from CHO 4-4-19 cells that were transfected with cDNAs encoding wild-type and Q79A mutant versions of NPC1-His_8-Flag. As a result of this transient transfection, these cells expressed high levels of both versions of NPC1 as compared to the mock-transfected cells (Figure 1-6*A*). When the transfected CHO 4-4-19 cells were incubated with β-VLDL, a cholesterol-rich lipoprotein that binds to LDL receptors with high affinity and delivers cholesterol to lysosomes [56], the cholesterol from β-VLDL reached the ER and markedly stimulated cholesteryl [^{14}C]oleate formation in the cells expressing either the wild-type or the Q79A mutant version of NPC1, but not in the cells transfected with a control mock plasmid (Figure 1-6*B*).

In wild-type cells, when cholesterol derived from β-VLDL reaches the ER, it prevents the exit of SREBP-2, thereby blocking its proteolytic processing [41]. In mock-transfected CHO 4-4-19 cells, high concentrations of β-VLDL (30 μg protein/ml) did not block SREBP-2 processing (Figure 1-6*C, lane 2*). In contrast, when the CHO 4-4-19 cells were transfected with cDNAs encoding either wild-type NPC1 or its Q79A mutant version, β-VLDL blocked SREBP-2 processing at concentrations as low as 1 μg protein/ml (Figure 1-6*D*, *lanes 4, 11*). All three transfected CHO 4-4-19 cells (mock, NPC1 wild-type, and NPC1 Q79A mutant) responded to 25-HC (Figure 1-6*C*, *lane 3*; Figure 1-6*D*, *lanes 8* and *15*).

Novel Mutations in Conserved Residues and Clinical Mutations in Patients with NPC1 Restores NPC1 Function to CHO 4-4-19 Cells when Expressed Under the Control of a Weak Thymidine Kinase Promoter – It should be noted that the latter studies (Figure 1-6) involved marked overexpression of the Q79A mutant using a strong CMV promoter and thus could be obscuring a sterol-dependent regulatory role for the luminal loop-1. For that reason, we cloned NPC1 into a plasmid that is driven by a weaker thymidine kinase promoter (TK). We transfected wild-type and mutant versions of NPC1-His_8-Flag, both novel (Figure 1-7*A*) and clinical (Figure 1-7*B and C*) mutations into CHO 4-4-19 cells using the NPC1 construct driven by the TK promoter (Figure 1-7*A*, *B* and *C*) and tested for the ability of these mutants to block SREBP-2 processing in response to β-VLDL. Unlike mock transfected cells, CHO 4-4-19 cells expressing the novel mutations in NPC1, Q79A and Q117A could block SREBP-2 processing when treated with β-VLDL at a concentration similar to that of wild-type (compare Figure 1-*7A, lanes3* to Figure 1-7*A, lanes7, 12 and 17*). All four transfected

CHO 4-4-19 cells (mock, NPC1 wild-type, and NPC1 Q79A or Q79A mutants) responded to 25-HC (Figure 1-7*A, lanes 4,9,14, and 19*). Three of the clinical mutants tested could not rescue SREBP-2 processing when their cDNA was transfected into CHO 4-4-19 cells. Two of these mutations were in a cysteine residue (C63R and C113R). The expression level of the cysteine mutants was less than that of the wild-type, suggesting that the protein is getting degraded, and the band corresponding to NPC1 shows less of the N-linked glycosylated form of the protein suggesting that these mutants do not exit the ER because cysteine mutations affect the stability of the protein which results in its degradation (Figure 1-7*B, lanes 6, 7, 10 and 11*). The third clinical mutation tested, Q92R did not seem to rescue SREBP-2 processing (Figure 1-7 *A, lane 9*). We re-transfected this mutant into CHO 4-4-19 cells and treated with various concentrations of β-VLDL (Figure 1-7*C*). Even at a concentration of 10μg/ml of β-VLDL, (Figure 1-7*C, lane 13*) this mutant could not suppress the proteolytic cleavage of SREBP-2, whereas, the wild-type protein could rescue SREBP-2 processing at a concentration of 3 μg/ml β-VLDL (Figure 1-7*C, lane 7*). Similar to mock and wild-type transfected cells, CHO 4-4-19 cells transfected with Q92R cDNA responded to 25-HC treatment (Figure 1-7*C, lanes 4, 9 and 14*). Since Q92R mutant showed normal binding for [^{3}H]cholesterol we hypothesize that this mutation might disrupt the interaction of NPC1 with another protein involved in the transfer of cholesterol. Two other clinical mutants tested, P166S and T137M, could rescue SREBP-2 processing similar to wild-type NPC1 when transfected into CHO 4-4-19 cells treated with 10μg/ml β-VLDL (Figure 1-7*B*).

FIGURE 1-1: NPC1 does not regulate oxysterol-mediated inhibition of SREBP-2 processing in cultured cells.

A, cholesterol esterification assay in telomerase-immortalized NPC1 human fibroblasts. On day 0, h-TERT-Control (▲) and h-TERT-NPC1(P237S/I106IT) (●) fibroblasts were set up in medium B containing 10% FCS and grown as described under "Experimental Procedures." On day 4, after incubation for 2 days in LPDS, each dish received sterol-depleting medium C supplemented with 10% human LPDS the indicated concentration of β-VLDL (*left*) or 25-HC (*right*). After incubation for 5 h at 37°C, each monolayer was pulse-labeled for 2 h with 0.2 mM [^{14}C]oleate (7681 dpm/pmol). The cells were then harvested for measurement of their cholesteryl [^{14}C]oleate and [^{14}C]triglyceride content as described under "Experimental Procedures." Each value is the average of triplicate incubations. The cellular content of [^{3}H]triglycerides (data not shown in figure) was similar for control and NPC1 cells incubated with 10 μg protein/ml β-VLDL (25 and 21 nmol/h per mg, respectively) or 5 μg/ml 25-HC (39 and 29 nmol/h per mg, respectively). *B*, immunoblot analysis of SREBP-2 cleavage in NPC1 human fibroblasts. h-TERT-Control (*left*) and h-TERT NPC1(P237S/I106IT) (*right*) fibroblasts were set up for experiments as described under "Experimental Procedures." On day 4, after incubation for 2 days in LPDS, the cells were incubated with medium C supplemented with 10% human LPDS the indicated concentration of β-VLDL or 25-HC. After 6 h at 37°C, the cells were harvested. The nuclear extract and 100,000*g* membrane fractions were subjected to immunoblot analysis of SREBP-2. *C*, immunoblot analysis of SREBP-2 cleavage in NPC1 mouse fibroblasts. On day 4, after incubation for 1 day in 5% newborn calf LPDS, the cells were incubated with medium C supplemented with 5%

newborn calf LPDS and the indicated concentration of 25-HC or β-VLDL. After 5 h at 37°C, the cells were harvested, and processed as in *B*. All filters were exposed to X-ray film for 1-20 s.

FIGURE 1-1

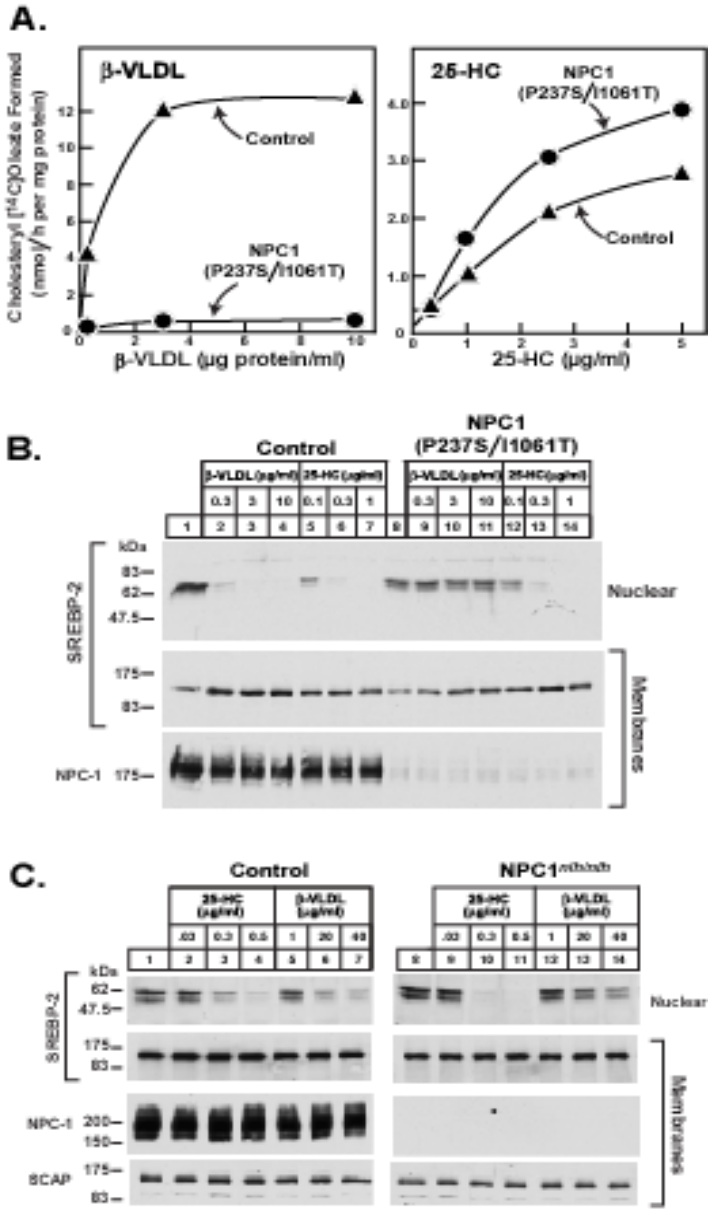

FIGURE 1-2: Egress from lysosomes of LDL-derived cholesterol, but not LDL-derived 25-HC is dependent on NPC1 as assessed by SREBP-2 processing and HMGCoA reductase degradation.

A and B, Immunoblot analysis of SREBP-2 cleavage and HMGCoA reductase. On day 0, h-TERT-control and h-TERT NPC1(P237S/I106IT) human fibroblasts were set up in medium B containing 10% FCS and grown as described under "Experimental Procedures." On day 4, after incubation for 2 days in LPDS, each dish received sterol-depleting medium C supplemented with 10% human LPDS and the indicated compound. After 5 h, cells received a direct addition of 25 μg/ml of N-acetyl-leucinal-leucinal norleucinal. After 1 h at 37°C, triplicate dishes were harvested and pooled for preparation of nuclear extract and 100,000*g* membrane fractions, which were analyzed by immunoblotting for the indicated protein as described under "Experimental Procedures". All filters were exposed to X-ray film for 1-30s.

FIGURE 1-2

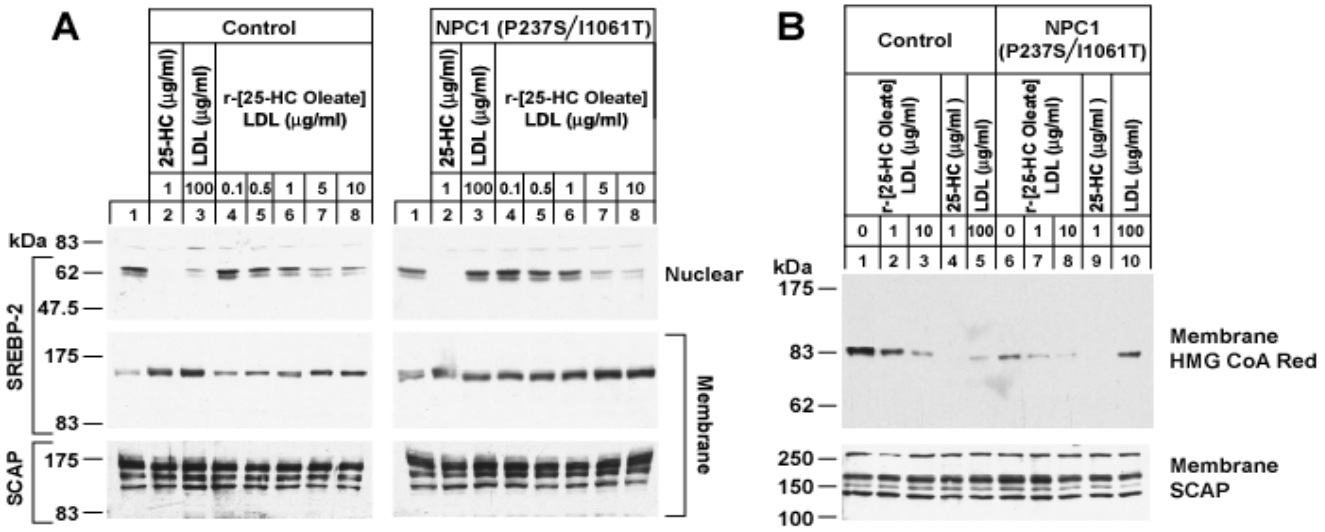

FIGURE 1-3: **Identification of oxysterol-binding site in recombinant human NPC1.**

A, predicted topology of full-length (*top panel*) and internally deleted NPC1 (*bottom panel*). The domain structure of NPC1 is discussed in Results. *B*, immunoblot analysis of equimolar amounts of full-length (*lane* 1) and NPC1-His_8-Flag (1-307;1254-1278) (*lane* 2). *C*, saturation curves for [^{3}H]25-HC binding to full-length and NPC1-His_8-Flag (1-307;1254-1278). Binding assays were carried out as described under "Experimental Procedures". Each reaction, in a final volume of 120 μl of buffer B (1% NP-40), contained 200 ng of purified human full-length NPC1 (*circles*) or 60 ng of purified internally deleted NPC1 (*triangles*) and 0-300 nM [^{3}H]25-HC (solubilized in 1% NP-40) in the absence (*closed symbols*) or presence (*open symbols*) of 8 mM unlabeled 25-HC (solubilized in 1% NP-40). After incubation for 3 h at 4C°, bound [^{3}H]25-HC was measured using the Ni-NTA agarose binding assay as described under "Experimental Procedures." Each data point represents total binding without subtraction of blank values. *D*, competitive binding of [^{3}H]25-HC to internally deleted NPC1. Each assay tube, in a total volume of 120 ml of buffer B (1% NP-40), contained 300 ng of NPC1-His_8-Flag (1-307;1254-1278), 100 nM [^{3}H]25-HC (solubilized in 1% NP-40), and varying concentrations of the indicated unlabeled sterol (solubilized in 1% NP-40). After incubation for 3 h at 4°C, bound [^{3}H]25-HC was measured as described in *C*. Each data point represents the amount of [^{3}H]25-HC bound relative to that in the control tube, which contained no unlabeled sterol. The "100% of control" value was 247 fmol/tube. 19-HC, 19-hydroxycholesterol; 27-HC, 27-hydroxycholesterol.

FIGURE 1-3

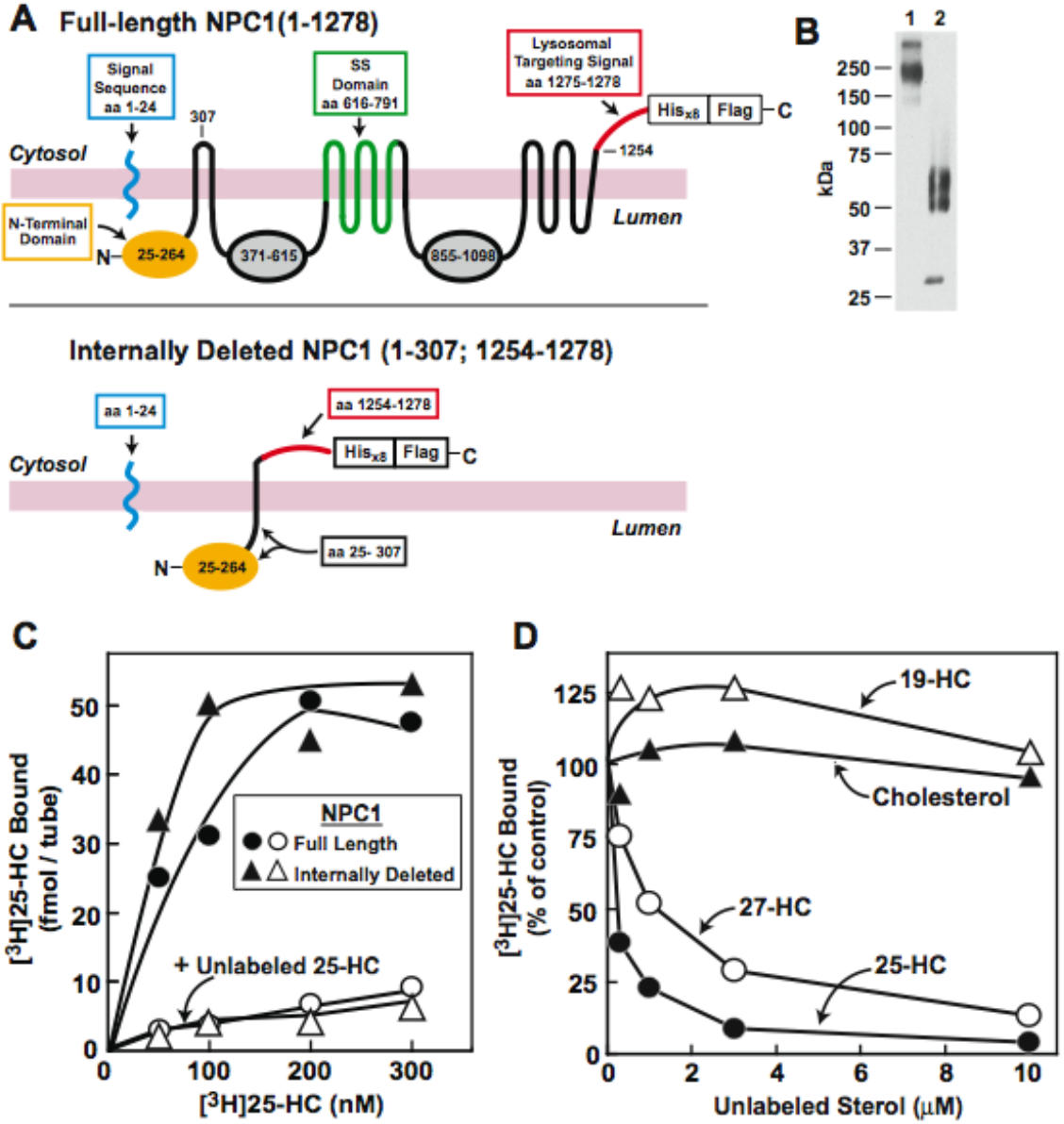

(This data reproduced with permission by Rodney Infante)

FIGURE 1-4: Secretion of NPC1(NTD).

A, diagrammatic illustration of NPC1(25-264)His_8-Flag, showing the cleaved signal sequence (amino acids 1-24) and the secreted soluble domain (amino acids 25-264). *B*, comparison of the amino acid sequence of human NPC1(22-264) with the consensus sequence of NPC1(NTD) from 12 vertebrate species. *Black boxes* denote residues invariant in all 12 vertebrate proteins. *White boxes* denote residues conserved in at least 50% of the aligned vertebrate sequences and are identical to the human sequence. *Yellow boxes* denote cysteine residues. *Red triangles* denote "novel mutations," i.e., alanine or methionine substitutions, created by site-directed mutagenesis. *Blue triangles* denote "clinical mutations," i.e., substitutions corresponding to naturally occurring mutations in patients with NPC1 disease. *Asterisks* (*) denote location of 5 potential *N*-linked glycosylation sites in the human sequence. *C*, immunoblot analysis of secreted NPC1(25-264). On day 0, CHO-K1 cells were set up and transfected with 5 μg pcDNA3.1 (mock), 5 μg pCMV-NPC1-His_8-Flag, 5 μg pCMV-NPC1(1-307;1254-1278)-His_8-Flag, or 5 μg pCMV-NPC1(1-264)-His_8-FLAG as described in "Experimental Procedures." After incubation for 48 h at 37°C, the medium was collected, and the cells were washed and homogenized through a 1-ml syringe with a 22-gauge needle in 0.6 ml of buffer D. The homogenate was centrifuged at 10^5g, after which the supernatant was collected and the pellet was solubilized in 10 mM Tris-chloride at pH 7.4, 100 mM NaCl, and 1% SDS and shaken at 37°C overnight. Fractions of medium (m), supernatant (s), and 10^5g pellet (p) were applied to the gel in a 1:5:5 ratio, respectively, and then subjected to 8% SDS/PAGE and immunoblot analysis using monoclonal anti-Flag antibody. The filter was exposed to X-ray film for 30 s.

FIGURE 1-4

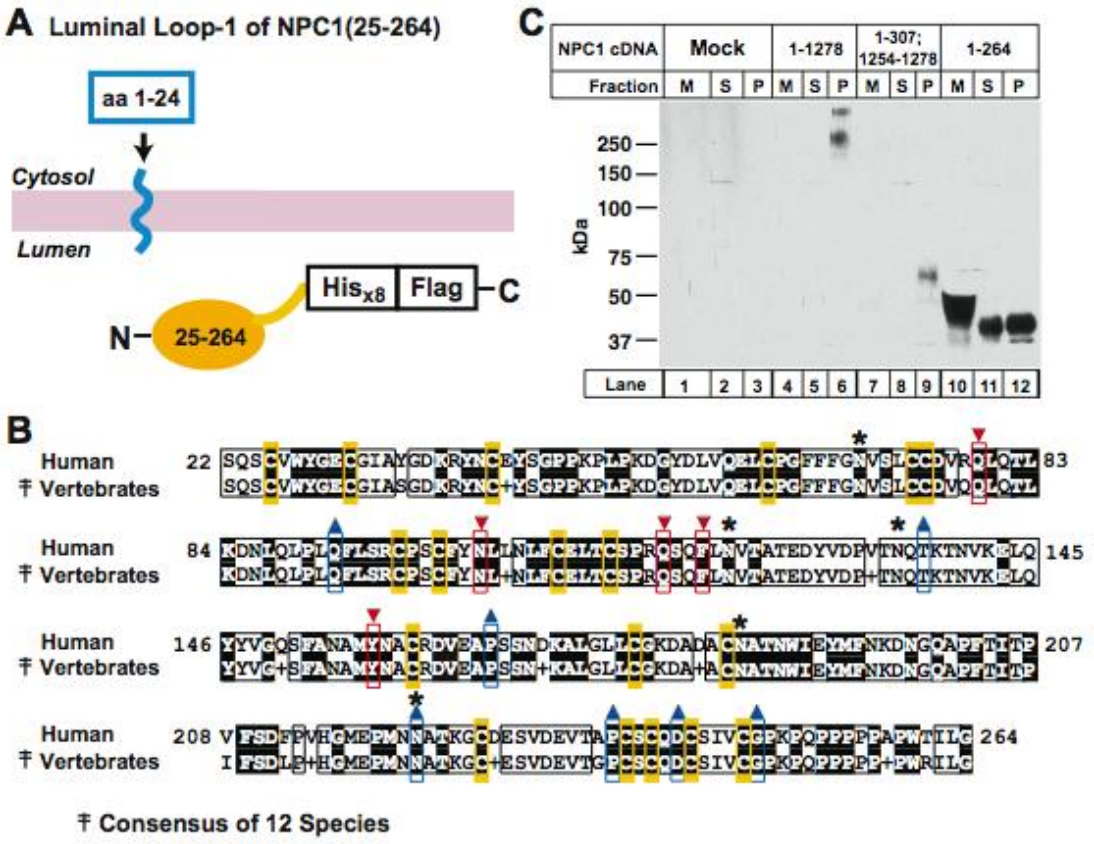

(This data reproduced with permission by Rodney Infante)

FIGURE 1-5: [^{3}H]25-HC and [^{3}H]cholesterol binding to versions of NPC1 corresponding to novel mutations in conserved residues and clinical mutations in patients with NPC1.

A-D, saturation curves for ^{3}H-sterol binding to wild-type and mutant NPC1 proteins. Each reaction, in a final volume of 80 μl of buffer A (0.004% NP-40), contained 100 ng of purified wild-type or the indicated mutant version of NPC1(25-264)-His_8-Flag, 1 μg of BSA, and 10-300 nM of either [^{3}H]25-HC (*A* and *C*) or [^{3}H]cholesterol (*B* and *D*), both delivered in ethanol. After incubation for 4 h at 4°C, bound [^{3}H]25-HC (*A*) or [^{3}H]cholesterol (*B*) was measured using the Ni-NTA agarose binding assay as described under "Experimental Procedures." Each data point is the average of duplicate assays and represents total binding without subtraction of blank values.

FIGURE 1-5

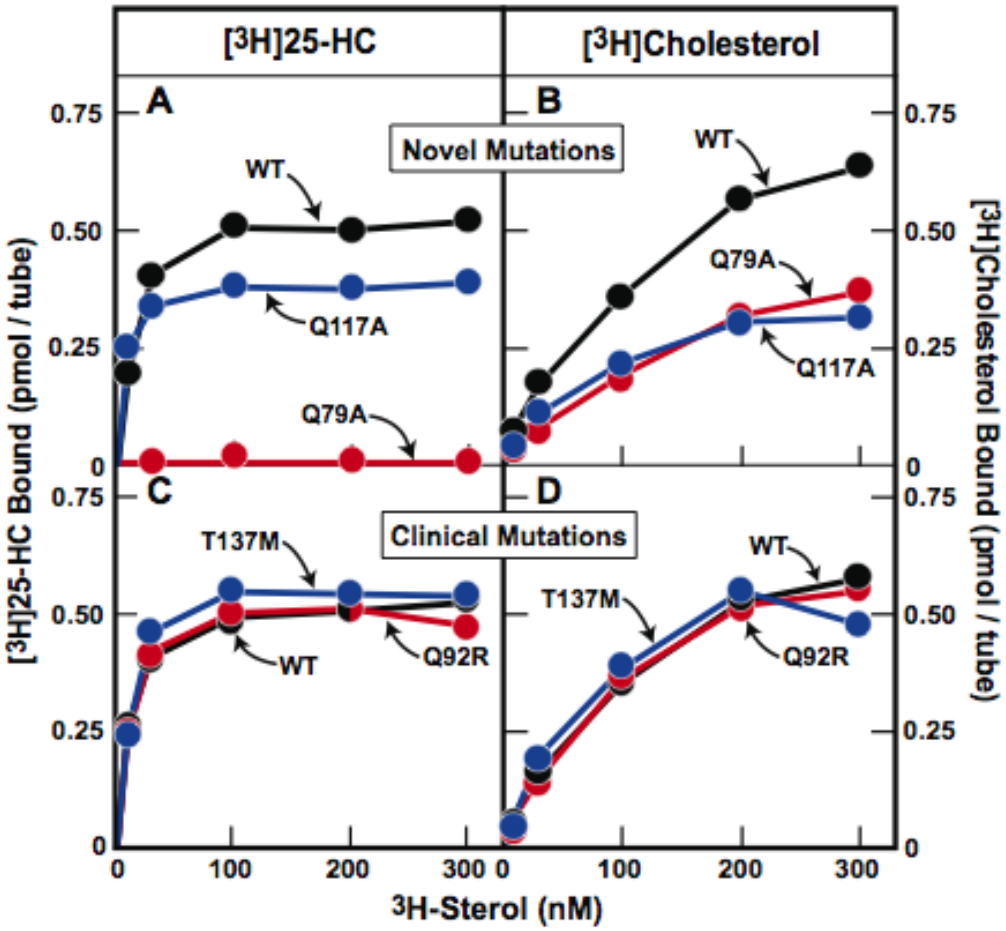

(This data reproduced with permission by Rodney Infante)

FIGURE 1-6: Regulatory actions of transfected wild-type and mutant Q79A versions of full-length NPC1 in mutant CHO 4-4-19 cells defective in NPC1.

On day 0, mutant CHO 4-4-19 cells were set up in medium A containing 5% FCS as described in "Experimental Procedures." *A*, immunoblot analysis of NPC1 proteins. On day 2, the cells were transfected with 2 μg pcDNA3.1 (mock, M) or 2 μg of wild-type or mutant Q79A version of pCMV-NPC1-His_8-Flag as described in "Experimental Procedures." On day 3, the cells were harvested, and whole cell extracts were prepared (1) and processed for immunoblot analysis of the indicated proteins. *B*, cholesterol esterification assay in mutant CHO cells. On day 2, the cells were transfected as described in *A*. On day 3, the medium was switched to medium A containing 5% newborn calf LPDS, 5 μM compactin, and 50 μM sodium mevalonate. On day 4, the medium was switched to medium A supplemented with 5% newborn calf LPDS, 50 μM compactin, and 50 μM sodium mevalonate with the indicated concentration of β-VLDL. After incubation for 5 h at 37°C, each monolayer was pulse-labeled for 2 h with 0.2 mM sodium [^{14}C]oleate (6446 dpm/pmol). The cells were then harvested for measurement of their content of cholesteryl [^{14}C]oleate and [^{14}C]triglycerides as described under "Experimental Procedures." Each value is the average of duplicate incubations. The cellular content of [^{14}C]triglycerides (data not shown in Figure) for mock, NPC1 wild-type, or NPC1(Q79A) transfected cells incubated with 10 μg protein/ml of β-VLDL were 209, 184, and 194 nmol/h per mg, respectively. *C*, immunoblot analysis of SREBP-2 in mutant CHO cells overexpressing SREBP-2. On day 2, the cells were transfected with 3 μg of pTK-HSV-BP2. *D*, immunoblot analysis of SREBP-2 cleavage in mutant CHO cells overexpressing full-length NPC1 (wild-type or Q79A). On day 2, the cells

were either mock transfected with pcDNA3.1 (M) or co-transfected with 3 µg pTK-HSV-BP-2 together with 2 µg of either wild-type or mutant Q79A version of pCMV-NPC1-Flag. *C* and *D*, on day 3, the medium was switched to medium A supplemented with 5% newborn calf LPDS, 5 µM compactin, and 50 µM sodium mevalonate. On day 4, the medium was switched to medium A supplemented with 5% newborn calf LPDS, 50 µM compactin, and 50 µM sodium mevalonate with the indicated concentration of β-VLDL or 1 µg/ml of 25-HC. After incubation for 6 h, the cells were harvested and processed for immunoblot analysis of the indicated proteins. *A* and *C*, all filters were exposed to X-ray film for 5-10 s except for the nuclear SREBP-2 filter, which was exposed for 20 s.

FIGURE 1-6

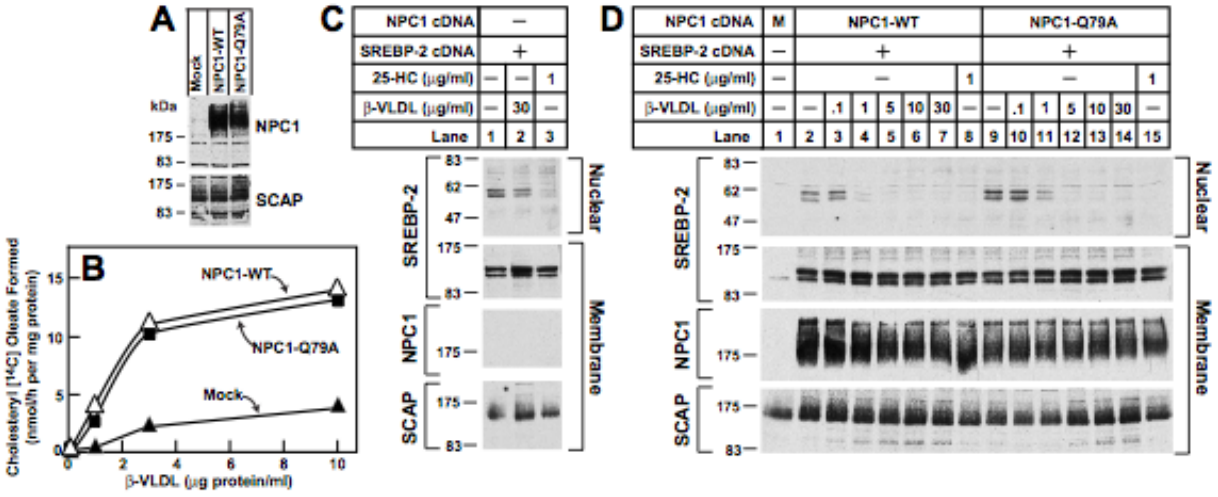

FIGURE 1-7: Regulatory actions of transfected wild-type, novel mutations in conserved residues and clinical mutations in patients with NPC1 under the control of a weak promoter.

On day 0, mutant CHO 4-4-19 cells were set up in medium A containing 5% FCS as described in "Experimental Procedures." *A*, *B* and C, immunoblot analysis of SREBP-2 in mutant CHO cells overexpressing SREBP-2 and full-length NPC1 whose expression is driven by a TK promoter (wild-type or mutant). On day 2, the cells were either mock transfected with pcDNA3.1 (Mock) or co-transfected with 3 μg pTK-HSV-BP-2 together with 2 μg of either wild-type or mutant versions (Q79A, Q117A, C63A, Q92R, C113R, P166S or T137M) of pTK-NPC1-$Flag_3$. On day 3, the medium was switched to medium A supplemented with 5% newborn calf LPDS, 5 μM compactin, and 50 μM sodium mevalonate. On day 4, the medium was switched to medium A supplemented with 5% newborn calf LPDS, 50 μM compactin, and 50 μM sodium mevalonate with the indicated concentration of β-VLDL or 1 μg/ml of 25-HC. After incubation for 6 h, the cells were harvested and processed for immunoblot analysis of the indicated proteins. All filters were exposed to X-ray film for 10-30 s.

FIGURE 1-7

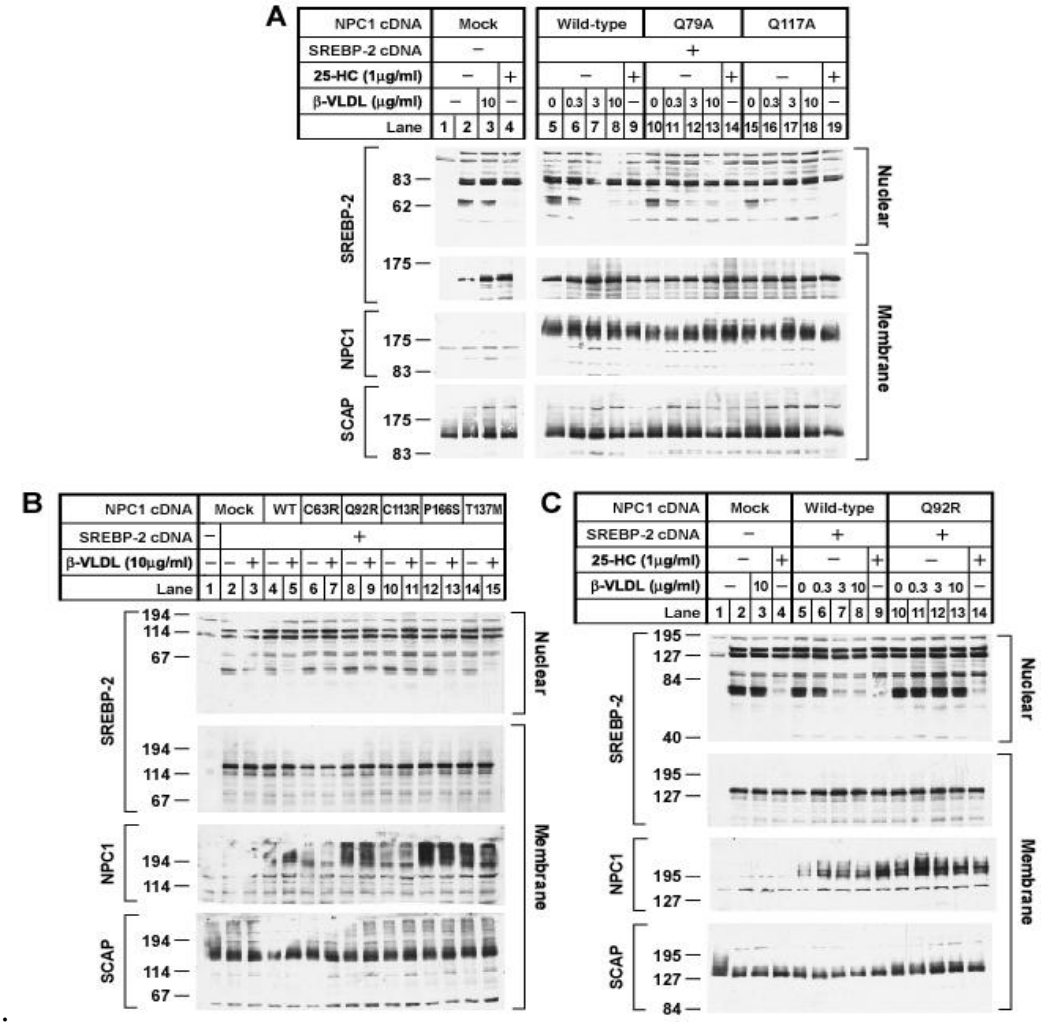
A
NPC1 cDNA
Mock
Wild-type
Q79A
Q117A
SREBP-2 cDNA
25-HC (1μg/ml)
β-VLDL (μg/ml)
Lane
SREBP-2
NPC1
SCAP
Nuclear
Membrane
B
NPC1 cDNA
Mock
WT
C63R
Q92R
C113R
P166S
T137M
SREBP-2 cDNA
β-VLDL (10μg/ml)
Lane
SREBP-2
NPC1
SCAP
Nuclear
Membrane
C
NPC1 cDNA
Mock
Wild-type
Q92R
SREBP-2 cDNA
25-HC (1μg/ml)
β-VLDL (μg/ml)
Lane
SREBP-2
NPC1
SCAP
Nuclear
Membrane

DISCUSSION

Our ultimate goal was to find a membrane protein that binds oxysterols and in turn regulates cholesterol synthesis and esterification. We were surprised to find that the oxysterol-binding protein was NPC1, a previously described protein with a known role in intracellular transport of cholesterol. There was no prior evidence to indicate that NPC1 binds oxysterols. We have been unable to find any evidence that NPC1 is required for this regulatory actions of 25-HC. When 25-HC is added to cultured cells that do not have a functional NPC1 protein in an ethanolic solution or reconstituted in an LDL particle, it could block the proteolytic processing of SREBP-2 and activate ACAT. While these studies were in progress, we demonstrated that the effect of 25-HC on SREBP processing is mediated by 25-HC binding to Insig proteins [53], which in turn prevents SREBPs from exiting from the ER [56]. Thus, we have no reason to postulate a direct role for NPC1 in regulating SREBP activity. The major challenge for the future is to define the functional role of the sterol binding site on luminal loop-1 of NPC1.Oxysterol binding to this site does not seem to be important for the known function of NPC1 in fibroblasts. Thus, in NPC1-deficient cells 25-HC blocks SREBP cleavage [16], accelerates the degradation of 3-hydroxy-3-methlglutyl CoA reductase [7] and activates ACAT in a normal manner [16, 59].

To confirm and characterize the oxysterol binding activity of NPC1, we prepared the human protein through recombinant DNA methodology and purified it through use of affinity tags [31]. The recombinant human NPC1 bound oxysterols with specificity and also bound cholesterol. Cholesterol binding was inhibited when the concentration of NP-40 exceeded

super micellar conditions. In the current studies, we found evidence that NPC1(NTD) is the sole sterol-binding site on NPC1, at least under the conditions of our *in vitro* assays. The importance of this 240-amino acid luminal, soluble protein is revealed by its strong sequence conservation in all vertebrate orthologs of NPC1 and in related proteins from eukaryotes as remote as yeast. A point mutation in NPC1(NTD) (Q79A) abolished binding of 25-HC to the full-length recombinant NPC1 [31]. The situation with regard to cholesterol binding is less clear. When produced in soluble NPC1(NTD), the Q79A mutation reduced binding of [^{3}H]cholesterol by about 40% [34], yet this mutation in full-length NPC1 abolished binding of [^{3}H]cholesterol completely. The important question of whether NPC1(NTD) is the sole cholesterol binding site on NPC1 will not be resolved until *in vitro* assays can be performed with NPC1 in a more normal environment, either *in situ* in isolated membranes or after reconstitution in liposomes.

Moreover, the Q79A mutant of NPC1, which does not bind oxysterols *in vitro*, nevertheless restored the ability of cholesterol-carrying β-VLDL to activate ACAT and block SREBP-2 processing in mutant CHO cells that lack NPC1 function. One major concern was that the initial studies involved marked overexpression of the Q79A mutant using a strong CMV promoter and thus could be obscuring a sterol-dependent regulatory role for the luminal loop-1. However, when those experiments were repeated with cells expressing wild-type and mutant NPC1 under control of a weak promoter, similar results were obtained suggesting that sterol binding at the Q79 position is not important for the known function of NPC1 in fibroblasts. Its worth mentioning that most of the non-cysteine clinical mutants of NPC1 could also rescue SREBP-2 processing in mutant CHO cells that lack NPC1 function.

CHAPTER TWO

NPC1 DEPENDENT AND INDEPENDENT CHOLESTEROL TRANSPORT IN CELLS

SUMMARY

Defects in Niemann-Pick, Type C-1 protein (NPC1) cause cholesterol, sphingolipids, phospholipids, and glycolipids to accumulate in lysosomes of liver, spleen, and brain. In cultured fibroblasts, NPC1 deficiency causes lysosomal retention of lipoprotein-derived cholesterol after uptake by receptor-mediated endocytosis. NPC1 fibroblasts are characterized by having a delayed homeostatic response toward the regulatory effects of low density lipoprotein (LDL)-derived cholesterol. In Chapter 1, we showed that NPC1 binds cholesterol. Here we evaluate the role of NPC1 in the transport of plasma membrane derived cholesterol and newly synthesized cholesterol to ER. We make use of two indirect and one direct method available for measuring this transport based on the known regulatory actions of cholesterol once it reaches the ER; 1) Suppression of the proteolytic processing of the Sterol Response Element Binding Protein-2 (SREBP-2); 2) Activation of acyl-CoA:cholesterol acyltransferase (ACAT); 3) Measuring the cholesterol content from purified ER membrane. We demonstrate that the transport of cholesterol from the plasma membrane to the ER is independent of NPC1 and that only the transport of LDL-derived cholesterol is dependent on NPC1.

INTRODUCTION

Despite intense scientific interest, the mechanism by which cholesterol is transported from one membrane compartment to another in animal cells remains obscure. One well characterized transport pathway begins in lysosomes where cholesterol is liberated from plasma lipoproteins that have entered the cell through receptor- mediated endocytosis to the plasma membrane to provide structural integrity [60] and endoplasmic reticulum (ER) [3] where it performs vital regulatory functions, and where excess cholesterol is stored by conversion to cholesteryl esters through the action of the ER enzyme acyl-CoA:cholesterol acyltransferase (ACAT). A clue to the mechanism of this movement comes from observations in cells from patients with Niemann-Pick Type C (NPC) disease [55], caused by a mutation in Niemann-Pick Type C1 (NPC1) protein. These cells accumulate a large amount of unesterified cholesterol in their lysosomes. In addition to exogenous uptake, cells acquire cholesterol by endogenous biosynthesis *de novo*. In cultured cells, biosynthesis of cholesterol takes place at the ER. Shortly after synthesis, most of the newly synthesized cholesterol is rapidly transported from the ER to the caveolae/lipid raft domain of the plasma membrane where most of the cell's cholesterol is located. Studies have shown that this process does not require NPC1 [27]. However, the fate of cholesterol after it reaches the plasma membrane and whether this process is dependent on NPC1 is still unclear. Understanding the involvement of NPC1 in the trafficking of plasma membrane cholesterol or endogenously synthesized cholesterol is important in understanding the etiology of NPC disease especially

in the central nervous system where the major source of cholesterol is provided by *de novo* synthesis.

In the current study, we show that the transport of cholesterol from the plasma membrane to ER is independent of NPC1 function. Using cultured macrophages and fibroblasts derived from wild-type BALB/c and mutant homozygous BALB/c *npc* $^{nih/nih}$ we followed the fate of plasma membrane derived cholesterol. To label the plasma membrane cholesterol we used either [^{3}H]cholesterol or [^{3}H]acetate, a precursor for cholesterol biosynthesis [27]; and to monitor the fate of labeled cholesterol, we performed chase experiments using 25-HC in an ethanolic solution. Both NPC1$^{nih/nih}$ mouse peritoneal macrophages and fibroblasts increased the percentage of cholesterol esters formed similar to control cells.

Looking at the activation of ACAT enzyme is an indirect way to assay for the transport of cholesterol to the ER. Another indirect method is by testing for proteolytic processing of SREBP-2. A new procedure was developed in the lab for the purification of ER membranes from cultured mammalian cells, which allows for the direct measurement of the ER cholesterol content by mass spectroscopy [13]. Using the two indirect methods and the direct cholesterol measurement we analyzed the transport of cholesterol from the plasma membrane of control and NPC1 human fibroblasts to the ER. Instead of supplying cholesterol to cells in ethanol or relying on its endogenous synthesis, cholesterol was delivered to cells complexed with methyl-β-cyclodextrin (MCD). Cholesterol can be solubilized by MCD in a form that allows it to partition into membranes [61]. The transport of cholesterol to ER in NPC1 human skin fibroblasts was not defective, as those cells could

increase the amount of cholesterol esters formed, suppress the proteolytic processing of SREBP-2, and increase the cholesterol content of the ER as measured by mass spectroscopy. Furthermore, we induced the mobilization of plasma membrane cholesterol to the ER by depleting the sphingomyelin pool after treating NPC1 human fibroblasts with neutral sphingomyelinase [62]. Consistent with the above data, both control and NPC1 human fibroblasts could prevent the cleavage of SREBP-2, activate ACAT, and increase the content of cholesterol in purified ER membranes when treated with neutral sphingomyelinase. The results confirmed that the movement plasma membrane cholesterol to the ER is independent of NPC1 and that only the transport of LDL-derived cholesterol is dependent on NPC1 function.

EXPERIMENTAL PROCEDURES

Materials – We obtained unlabeled cholesterol and 25-hydroxycholesterol (25-HC) from Steraloids, Inc.; methyl-β-cyclodextrin (MCD) from Cyclodextrin Technologies Development, Inc; thioglycollate from BD Biosciences; *Staphylococcus aureus* sphingomyelinase, iodixanol (Optiprep density gradient), and compound 58-035 from Sigma; [26,27-^{3}H]25-HC (75–80 Ci/mmol), [1,2,6,7-^{3}H]cholesterol (60 Ci/mmol), [^{3}H]acetate (150 mCi/mmol), and [1-^{14}C]oleic acid (54.6 mCi/mmol) from American Radiolabeled Chemicals; and Hybond C nitrocellulose filters from GE Healthcare Biosciences. Human low density lipoprotein (LDL, d=1.019-1.063 g/ml) [51], rabbit β-migrating very low density lipoproteins (β -VLDL, d < 1.006) [63], and human and newborn calf lipoprotein-deficient serum (LPDS, d < 1.215 g/ml) [51] were prepared by ultracentrifugation as described in the indicated reference. LDL was acetylated with repeated additions of acetic anhydride as previously described [64]. Complexes of cholesterol with MCD were prepared at a stock concentration of 2.5 mM [65]. Solutions of compactin and sodium mevalonate were prepared as previously described [66](Brown et al., 1978).

Culture Media – Medium A is Dulbecco's modified Eagle's medium containing 100 units/ml penicillin and 100 μg/ml streptomycin sulfate. Medium B is Dulbecco's modified Eagle's medium (high glucose, 4.5 g/l) containing 100 units/ml penicillin and 100 μg/ml streptomycin sulfate. Medium C is Medium B without sodium bicarbonate. Where

indicated, sterols (cholesterol or 25-HC) were added to the medium in an ethanolic solution in which the final ethanol concentration was <0.3%.

Cell Culture – Nontransformed skin fibroblasts from control subjects and from a patient with NPC1 disease (obtained from American Type Culture Collection, ATTC no. GM3123; compound heterozygote for mutations P237S and I1061T) were grown in monolayer at 37°C in 5% CO_2 and maintained in medium A with 10% (v/v) fetal calf serum (FCS). These fibroblasts strains are designated as control and NPC1(P237S/I1061T).

Control and NPC1(P237S/I1061T) fibroblasts were immortalized with the catalytic submit of human telomerase (hTERT) as previously described in Chapter 1. These transformed cells, designated as h-TERT-control and h-TERT-NPC1(P237S/I1061T), were grown in monolayer at 37°C in 5% CO_2 and maintained in medium A with 10% FCS.

Primary skin fibroblast cultures from a wild-type BALB/c mouse and a mutant BALB/c *npc*$^{nihi/nih}$ mouse were established as previously described in Chapter 1. The cells were grown in monolayer at 37°C in 5% CO_2 and maintained in medium B with 10% FCS.

Peritoneal macrophages were prepared from littermate wild-type BALB/c and mutant homozygous BALB/c *npc*$^{nih/nih}$ mice [46]. Heterozygotes for breeding were provided by Drs. Stephen Turley and John Dietschy (University of Texas Southwestern Medical Center, Dallas, TX). Macrophages were harvested from the peritoneum of mice 3 days after the intraperitoneal injection of 2.5 ml of a 3% (w/v) thioglycollate solution and then cultured as described previously [67]. The cells were resuspended in medium B supplemented with 10%

FCS at a final density of $2x10^6$ cells/35-mm dish and grown in monolayer at 37°C in 5% CO_2.

Radiolabeling of Cultured Cells – Monolayers of macrophages or fibroblasts were radiolabeled with either [^{3}H]cholesterol or [^{3}H]acetate, respectively, as described in the figure legends. The radiolabeled lipids were extracted from cells and separated by thin-layer chromatography, and the bands corresponding to [^{3}H]cholesterol and [^{3}H]cholesteryl ester were quantified by scintillation counting [66].

Acyl-CoA:cholesterol Acyltransferase (ACAT) Assay – The rate of incorporation of sodium [^{14}C]oleate-albumin into cholesteryl [^{14}C]oleate and [^{14}C]triglycerides by monolayers of fibroblasts was measured as described previously [51](Goldstein et al., 1983).

Analysis of SREBP-2 Processing in Cultured Cells – Monolayers of fibroblasts were tested for proteolytic processing of SREBP-2 as previously described in Chapter 1.

Isolation of Purified ER Membranes – Purified ER membranes were isolated from human fibroblasts by a fractionation scheme described for Chinese hamster ovary (CHO) cells by Radhakrishnan et al. (2008) [13].

Enzyme Assays – Enzyme assay for acid phosphatase (marker of lysosomes) was carried out using enzyme assay kit (Sigma) according to manufacturer's instructions. Glucose-6-phosphatase activity (marker of ER) was measured as described [68].

Protein Concentration – Protein content for immunoblot analysis was measured with a BCA kit Pierce. Other protein-content measurements were made by the method of Lowry *et al*. (1951) [69].

Immunoblot Analysis – Nuclear extract and membrane fractions from cultured cells were subjected to 8% SDS-PAGE, after which the proteins were transferred to nitrocellulose filters. The immunoblots were performed at room temperature using the following primary antibodies: 5 μg/ml of a rabbit polyclonal antibody (IgG-1819) directed against amino acids 1–100 of human SREBP-2 (Chapter 1); 1 μg/ml of a rabbit polyclonal antibody against human NPC1 (Novus); 8 μg/ml of a rabbit polyclonal antibody (IgG-R139) directed against hamster Scap [10]; 1 μg/ml of a rabbit polyclonal antibody directed against Sec61a (Millipore); 0.5 μg/ml of a mouse monoclonal antibody directed against transferrin receptor (Invitrogen); and 0.2 μg/ml of a mouse monoclonal antibody directed against Lamp1 (Biosciences). Bound antibodies were visualized by chemiluminescence (Super Signal Substrate, Pierce) using a 1:5000 dilution of anti-mouse IgG (Jackson ImmunoResearch Laboratories, Inc.) or a 1:2000 dilution of anti-rabbit IgG conjugated to horseradish peroxidase (Amersham Biosciences). The filters were exposed to Kodak X-Omat Blue XB-1 film at room temperature for 1-60 sec.

RESULTS

Role of NPC1 in Sterol-Mediated Cholesteryl Ester Formation and Inhibition of SREBP-2 Processing in Cultured Cells—Previous studies have shown that NPC1 is required for the export of lipoprotein-derived cholesterol from the lysosome to the ER where cholesterol activates acyl-CoA:cholesterol acyltransferase, thereby causing an increase in the incorporation of radiolabeled fatty acids into cholesteryl esters [18, 55]. However, NPC1 is not required for the stimulation of cholesterol esterification by 25-HC and is not required for the 25-HC mediated inhibition of the proteolytic processing of SREBPs (Chapter 1). We tested for the ability of cholesterol when complexed to MCD to stimulate the esterification of cholesterol (Figure 2-1*C*) or suppress SREBP-2 processing in NPC1 human skin fibroblasts (Figure 2-1*D and E*). Nontransformed control and human fibroblasts from an individual with NPC1 disease (GM3123), NPC1(P237S/I1061T) were treated with increasing concentrations of LDL, 25-HC or cholesterol complexed to MCD. We tested for the ability of the sterols to stimulate the incorporation of [^{14}C]oleate into cellular cholesteryl [^{14}C]oleate (Figure 2-1*A-C*) or suppress SREBP-2 (Figure 2-1*D-E*) in the cultured cells. As shown in Figure 2-1*A*, LDL markedly increased the amount of cholesteryl [^{14}C]oleate formed in control fibroblasts, but not in NPC1(P237S/I1061T) fibroblasts. On the other hand, both 25-HC (Figure 2-1*B*) and cholesterol/MCD complex (Figure 2-1*C*) increased cholesteryl [^{14}C]oleate formation in control and NPC1(P237S/I1061T) cells. If NPC1 is not required for the plasma membrane derived cholesterol-mediated inhibition of the proteolytic processing of SREBPs, then the

nontransformed NPC1(P237S/I1061T) fibroblasts should show a decreased nuclear accumulation of the cleaved form of SREBP when treated with cholesterol/MCD complex. Figure 1-4*D* and 1-4*E* show an immunoblot analysis of SREBP-2 processing in control and NPC1(P237S/I1061T) human skin fibroblasts. As previously described in Chapter 1, 25-HC blocked the generation of nuclear SREBP-2 at 0.3–1 μg/ml both in control and NPC1(P237S/I1061T) (*lanes2-4*) cells. As a positive control for NPC1 function, we added LDL, which inhibited cleavage in control cells, but not in NPC1(P237S/I1061T) cells that fail to transport lipoprotein-derived cholesterol to the ER (*lanes* 5-7). Consistent with the esterification data from figure 2-1*C*, cholesterol/MCD complex also blocked the generation of nuclear SREBP-2 at 6-12 μg/ml both in control and NPC1(P237S/I1061T) cells (*lanes 8-10*).

25-HC Stimulated Esterification of Cholesterol in Control and NPC1 Cells Prelabeled with [^{3}H]Cholesterol —Mouse peritoneal macrophages isolated from littermate wild-type BALB/c and mutant homozygous BALB/c *npc* $^{nih/nih}$ were preincubated with [^{3}H] cholesterol in order to label the macrophage cholesterol pools, and the formation of [^{3}H]cholesteryl ester in response to subsequent incubation with 25-HC for various times was assayed. As shown in Figure 2-2*A*, the increase in the percentage of [^{3}H]cholesteryl esters when the cells were treated with 25-HC was similar in both control cells and NPC1$^{nih/nih}$ with time. To show that we have succeeded in isolating pure macrophage cultures, control and NPC1$^{nih/nih}$ macrophages were incubated with the indicated concentration of acetyl-LDL which will be internalized by the scavenger receptors and enters through the same endocytic pathway as native LDL [67]. Cells were then pulsed with [^{14}C]oleate and the formation of

cholesteryl [^{14}C]oleate was assayed (Figure 2-2*B*). Under these conditions, acetyl-LDL markedly increased the amount of cholesteryl [^{14}C]oleate formed in control macrophages, but not in NPC1$^{nih/nih}$ macrophages. Macrophages are known to have a deficiency in uptaking LDL [67]. Therefore when control and NPC1$^{nih/nih}$ macrophages were treated with the indicated concentration of native LDL they showed a nonsignificant increase in the amount of cholesterol esters formed. These results suggest that the responses we obtained with the [^{3}H]cholesterol labeling are due to macrophage cells and not caused by another contaminating cell type. On the other hand, 25-HC (Figure 2-2*B*) increased cholesteryl [^{14}C]oleate formation in control and NPC1$^{nih/nih}$ macrophages.

25-HC Stimulated Esterification of Newly Synthesized Cholesterol in Control and NPC1 Cells Prelabeled with [^{3}H]Acetate —A similar experiment to that in Figure 2-3A was conducted, but instead of the long term labeling with [^{3}H]cholesterol, control and NPC$^{nih/nih}$ mouse fibroblasts were pulsed with [^{3}H]acetate to allow for the synthesis of [^{3}H]cholesterol. The cells were then treated with varying concentrations of 25-HC for different times and the incorporation of newly synthesized [^{3}H]cholesterol into [^{3}H]cholesteryl oleate was measured (Figure 2-4). Both control and NPC$^{nih/nih}$ mouse fibroblasts showed a 20-40% increase in the percent esterification of [^{3}H]cholesterol when treated with 25-HC. Suggesting that the transport of newly synthesized cholesterol to ER is independent of NPC1.

Analysis of Cholesterol Content of Purified ER Membranes from Control and NPC1 Human Fibroblasts —We wanted to study the changes in the cholesterol content of ER membranes isolated from control and NPC1 human fibroblasts when the cells are treated with LDL or cholesterol/MCD complex. A fractionation scheme to isolate pure ER

membranes from CHO-K1 cells was developed in the lab [13]. We used a similar scheme to isolate pure ER membranes from h-TERT-control and h-TERT-NPC1(P237S/I1061T) human skin fibroblasts as outlined in Figure 2-5*A*. We assessed for the purity of the designated fractions (I-V) by immunoblot analysis for proteins from different organelles in each cell line (Figure 2-4*B*). The plasma membrane protein (transferrin receptor) is found in the light membrane Fraction V and is almost completely absent from the heavy membrane Fraction IV in h-TERT-control and h-TERT-NPC1(P237S/I1061T) human skin fibroblasts. The lysosomal membrane proteins (LAMP1 and NPC1) are present in both Fractions II and III collected from the sucrose gradient, but are almost exclusively present in the light membrane fraction V after the iodixanol gradient in h-TERT-control cells. In h-TERT-NPC1(P237S/I1061T) human skin fibroblasts, most of the LAMP1 signal was in the light membrane fraction II from the sucrose gradient because the lysosomes in NPC1 cells are rich in cholesterol which makes them float. Also, LAMP1 signal was observed in the light membrane Fraction V after the iodixanol gradient in h-TERT-NPC1(P237S/I1061T) cells. NPC1 expression could not be detected in h-TERT-NPC1(P237S/I1061T) cells due to the mutation that these cells have in NPC1. ER-resident membrane protein (Sec61α) is localized almost completely to the heavy membrane Fractions III after the sucrose gradient and is found in both the heavy and light membrane fractions IV and V, respectively collected from the iodixanol gradient. We further characterized the iodixanol gradient fractions with enzyme assays as shown in Figure 2-4*C*. Consistent with the immunoblot results of Figure 2-4*B*, the activities of the lysosomal enzyme, acid phosphatase, was localized exclusively to Fraction V in both h-TERT-control and h-TERT-NPC1(P237S/I1061T) human skin fibroblasts, whereas

the activity of the ER enzyme glucose-6-phosphatase was present in Fraction IV. Based on the immunoblot and enzymatic analysis, and consistent with the data obtained from the CHOK1 cells [13] we conclude that Fraction IV contains ER membranes and contains less than 10% contamination with lysosomal, plasma, or other membranes. Fraction IV is hereafter designated as "purified ER membranes". Purified ER membranes were isolated form h-TERT-control and h-TERT-NPC1(P237S/I1061T) mutant human fibroblasts that were incubated with no sterols, LDL or cholesterol/MCD complex (Figure 2-4*E*). The ER cholesterol content in h-TERT-control human skin fibroblasts increased from 2% where no sterols were added, to 10% and 8% when the cells were treated with LDL and cholesterol/MCD complex respectively. In h-TERT-NPC1(P237S/I1061T) human skin fibroblasts on the other hand, the ER cholesterol content increased from 3% where no sterols were added, to 8% when the cells were treated with cholesterol/MCD complex but not when treated with LDL. The increase in the ER cholesterol content in h-TERT-control and h-TERT-NPC1(P237S/I1061T) cells was accompanied by a decrease in SREBP-2 processing when the cells were treated with cholesterol/MCD complex (Figure 2-4*D*). h-TERT-NPC1(P237S/I1061T) mutant cells fail to suppress SREBP-2 processing and to increase ER cholesterol content when treated with LDL.

Transport of Cholesterol form the Plasma Membrane to ER is Independent of NPC1 — Previous studies have shown that depletion of sphingomyelin by treatment with neutral sphingomyelinase causes a fraction of cellular cholesterol to translocate from the plasma membrane to the ER where it executes its regulatory functions that leads to down-regulation of cholesterol synthesis by inhibiting SREBP-2 processing and up-regulation of cholesterol

esterification by activating ACAT [62, 70]. We wanted to test the effect of neutral sphingomyelinase when added to h-TERT-NPC1(P237S/I1061T) human skin fibroblasts on SREBP-2 processing, activation of ACAT and ER cholesterol content (Figure 2-5). For SREBP-2 processing experiments the cells were pre-incubated with compound 58-035, an inhibitor of ACAT [71, 72] which prevents esterification, increasing the buildup of free cholesterol. Both neutral sphingomyelinase and 25-HC blocked the generation of nuclear SREBP-2 in h-TERT-control and h-TERT-NPC1(P237S/I1061T) human skin fibroblasts (Figure 2-5A, *lanes 2 and 4 respectively*). As a positive control for NPC1 function, we added β-VLDL, which inhibited cleavage in h-TERT-control, but not in h-TERT-NPC1(P237S/I1061T) cells that fail to transport lipoprotein-derived cholesterol to the ER (Figure 2-4A, *lane 3*). We then measured the ability of h-TERT-control and h-TERT-NPC1(P237S/I1061T) human skin fibroblasts to stimulate the incorporation of [^{14}C]oleate into cellular cholesteryl [^{14}C]oleate when treated with neutral sphingomyelinase. As shown in Figure 2-4*B*, neutral sphingomyelinase increased the amount of cholesteryl [^{14}C]oleate formed in h-TERT-control, but not in h-TERT-NPC1(P237S/I1061T) fibroblasts. Treatment with neutral sphingomyelinase also increased the cholesterol content of the ER purified from h-TERT-control and h-TERT-NPC1(P237S/I1061T) from 2% in the untreated condition up to 7% when neutral sphingomyelinase was added (Figure 2-4*C*).

FIGURE 2-1. Role of NPC1 in sterol-mediated cholesteryl ester formation (*A*-*C*) and in inhibition of SREBP-2 processing (*D, E*) in control and NPC1 fibroblasts.

On day 0, nontransformed control and NPC1(P237S/I106IT) human fibroblasts were set up in medium A with 10% FCS at $2x10^4$ cells/60-mm dish. On day 3, the cells were refed with the same medium, and on day 5 the cells were switched to medium A with 10% human LPDS. *A-C*, cholesterol esterification. On day 7, each dish received medium A containing 5% human LPDS, 50 μM compactin, 50 μM sodium mevalonate, and the indicated concentration of LDL (*A*), 25-HC (*B*), or cholesterol/MCD complex (*C*). After incubation for 5 h at 37°C , each monolayer was pulse-labeled for 2 h with 0.2 mM sodium [^{14}C]oleate-albumin (7966 dpm/pmol). The cells were then harvested for measurement of their content of cholesteryl [^{14}C]oleate and [^{14}C]triglycerides. Each value is the average of duplicate incubations. The rate of synthesis of [^{14}C]triglycerides in control and NPC1(P237S/I106IT) cells incubated with 200 μg protein/ml of LDL was 24 and 114 nmol/h per mg, respectively. *D* and *E*, immunoblot analysis of SREBP-2 processing. On day 7, after incubation for 5 h with the indicted concentration of 25-HC, LDL, or cholesterol/MCD, cells received a direct addition of 25 μg/ml of N-acetyl-leucinal-leucinal norleucinal. After 1 h at 37°C, six dishes were harvested and pooled for preparation of nuclear extract and 100,000*g* membrane fractions, which were analyzed by immunoblotting for the indicated protein as described under "Experimental Procedures." P, precursor form of SREBP-2; N, cleaved form of SREBP-2.

FIGURE 2-1

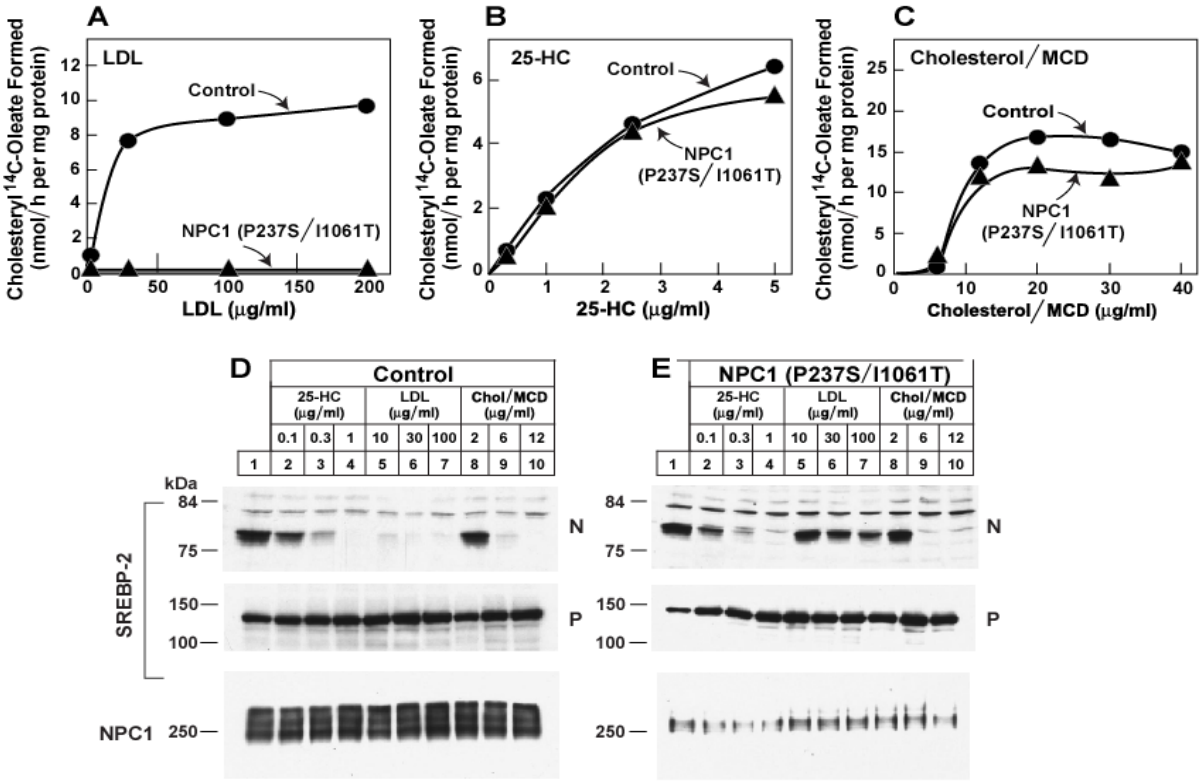
A
LDL
Control
NPC1 (P237S/I1061T)
Cholesteryl 14C-Oleate Formed (nmol/h per mg protein)
LDL (μg/ml)
B
25-HC
Control
NPC1 (P237S/I1061T)
25-HC (μg/ml)
C
Cholesterol/MCD
Control
NPC1 (P237S/I1061T)
Cholesterol/MCD (μg/ml)
D
Control
E
NPC1 (P237S/I1061T)
25-HC (μg/ml)
LDL (μg/ml)
Chol/MCD (μg/ml)
kDa
SREBP-2
N
P
NPC1

FIGURE 2-2. 25-HC stimulated esterification of cholesterol in control and NPC1 macrophages prelabeled with [^{3}H]cholesterol.

On day 0, mouse peritoneal macrophages from control or *npc*$^{nih/nih}$ mice were set up in medium B containing 10% FCS as described under "Experimental Procedures." *A,* esterification of [^{3}H]cholesterol. On day 1, the cells were incubated with medium B containing 10% FCS and 8.3 nM [^{3}H]cholesterol (132 dpm/fmol). After incubation for 24 h at 37°C, each dish was washed with 5 ml PBS containing 0.2% BSA, after which the cells received fresh medium B containing 0.2% BSA. After 12 h at 37°C, each monolayer received medium B with 0.2% BSA in the absence or presence of 5 μg/ml 25-HC. After incubation for the indicated time, the cells were harvested for measurement of their content of [^{3}H]cholesteryl oleate and [^{3}H]cholesterol as described under "Experimental Procedures." Each value is the average of duplicate incubations and represents the percentage of [^{3}H]cholesterol incorporated into [^{3}H]cholesteryl esters relative to the [^{3}H]cholesterol content at zero time. The zero time values for [^{3}H]cholesterol were 10.0 and 14.5 pmol/mg for control and *npc*$^{nih/nih}$ cells, respectively. *B,* cholesterol esterification in mouse peritoneal macrophages using [^{14}C]oleate. On day 1, mouse peritoneal macrophages from control or *npc*$^{nih/nih}$ mice received fresh medium B containing 10% newborn calf LPDS. On day 3, fresh medium B was added supplemented with 10% newborn calf LPDS, 50 μM compactin , 50 μM sodium mevalonate, and either 100 μg of protein/ml acetyl-LDL, 100 μg of protein/ml LDL, 5 μg/ml 25-HC in ethanol. After incubation for 5 h at 37°C, each monolayer was pulse-labeled for 2 h with 0.2mM sodium [^{14}C]oleate-albumin (9395 dpm/pmol). The cells were then harvested for measurement of their content of cholesteryl [^{14}C]oleate and

[^{14}C]triglycerides. Each value is the average of duplicate incubations. The rate of synthesis of [^{14}C]triglycerides in control and NPC1 cells incubated with 100 μg protein/ml of acetyl-LDL was 215 and 231 and 114 nmol/h per mg, respectively.

FIGURE 2-2

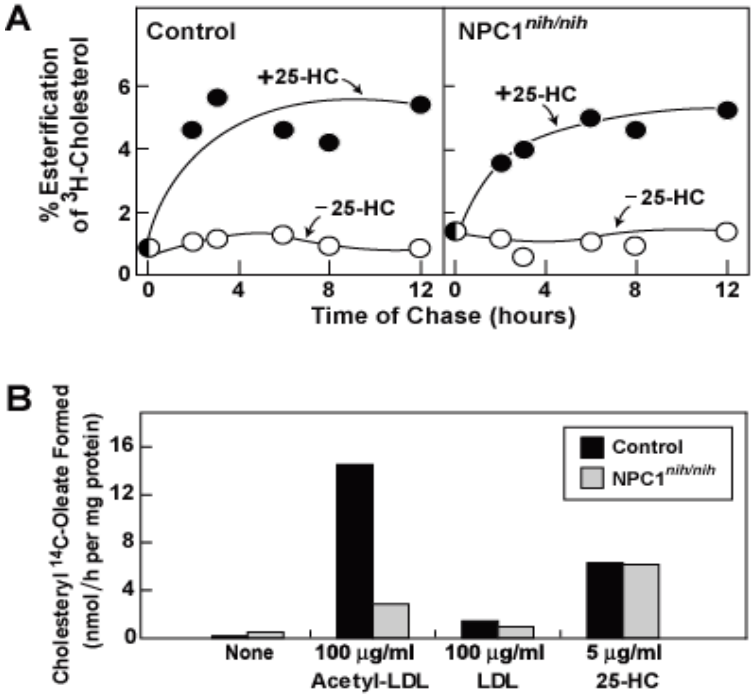

FIGURE 2-3. 25-HC stimulated esterification of newly synthesized cholesterol in control and NPC1 fibroblasts prelabeled with [^{3}H]acetate.

On day 0, control and *npc*$^{nih/nih}$ mouse fibroblasts were set up in medium B with 10% FCS at 4x10^4 cells/60-mm dish. On day 3, the cells were switched to medium B with 5% newborn calf LPDS. On day 4, the cells were pulsed-labeled with 200 μM [^{3}H]acetate (333 dpm/pmol) for 3 h at 14°C in medium C with 5% newborn calf LPDS. After the pulse, each monolayer was washed twice with 3 ml PBS containing 0.2% BSA and then chased at 37°C with medium B containing 5% newborn calf LPDS, 50 μM compactin, 50 μM mevalonate, and the indicated concentration of 25-HC. At the indicated time of chase, the cells were harvested for measurement of their content of [^{3}H]cholesteryl oleate and [^{3}H]cholesterol. Each value is the average of duplicate incubations and represents the percentage of [^{3}H]cholesterol incorporated into [^{3}H]cholesteryl esters relative to the [^{3}H]cholesterol content at zero time. The zero time values for cellular content of [^{3}H]cholesterol ranged from 151 to 162 pmol/mg in control cells and from 149 to 212 pmol/mg in *npc* $^{nih/nih}$ cells.

FIGURE 2-3

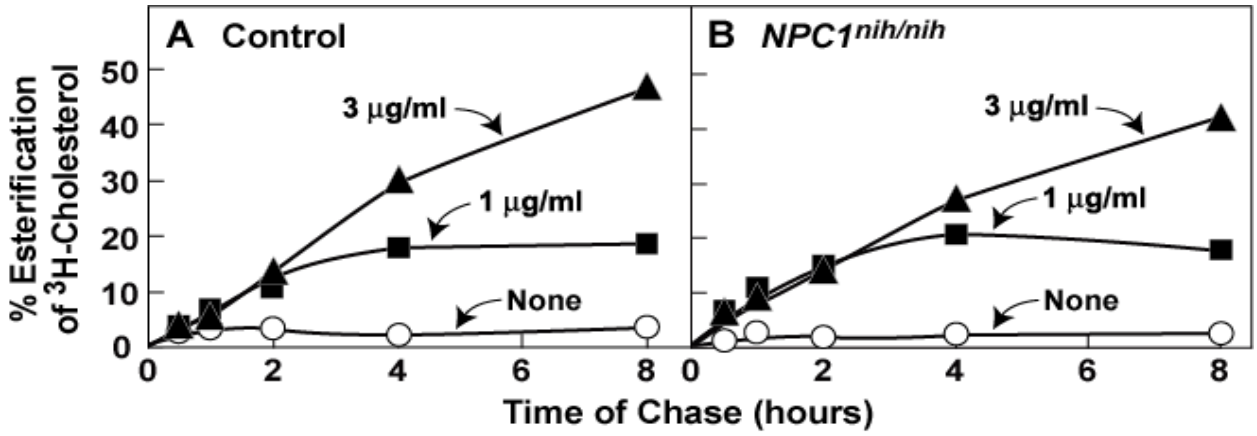

FIGURE 2-4. Analysis of cholesterol content of purified ER membranes from control and NPC1 human fibroblasts.

A, diagram of ER membrane fractionation scheme. I-V denote major fractions recovered and analyzed by immunoblot analysis or the indicated enzyme activity. *B* and *C*, immunoblot analysis and enzyme activity of membrane fractions. On day 0, 13 dishes of h-TERT-control and h-TERT-NPC1(P237/I106IT) fibroblasts were set up in medium A with 10% FCS at $4x10^5$ cells/100-mm dish. On day 3, cells were harvested, and ER membranes were treated according to the fractionation scheme described by Radhakrishnan *et al.* (2008) [13]and shown in A. Cells were disrupted using a ball-bearing homogenizer and centrifuged at 3,000*g*. The supernatant was then loaded at the top of a discontinuous sucrose gradient and centrifuged at 100,000*g* at 4°C for 1 h, yielding two distinct membrane layers. The heavy membrane fraction was loaded below a continuous 19%-25% iodixanol gradient, centrifuged for 2 h at 110,000*g* at 4°C, after which fractions were collected from the bottom. Equal volumes of the indicated membrane fraction were subjected to immunoblot analysis for the indicated organelle markers (*B*) or assayed for the indicated enzyme activity (*C*). *D* and *E*, immunoblot analysis of SREBP-2 cleavage (*D*) and analysis of cholesterol content of purified ER membranes (*E*). h-TERT-control and h-TERT-NPC1(P237/I106IT) fibroblasts (13 dishes for each condition) were set up as described above. On day 2, cells were switched to medium A with 5% human LPDS. On day 3, the cells were switched to medium A containing 5% human LPDS, 5 μM compactin, and 50 μM sodium mevalonate. On day 4, the cells received the same medium with 50 μM rather than 5 μM compactin and supplemented with either 100 μg protein/ml LDL or 20 μg/ml cholesterol/MCD complex as

indicated. After incubation for 6 h at 37°C, cells were harvested, and a portion (5% of total) was fractionated and subjected to immunoblot analysis (*D*) of SREBP-2. P, precursor form of SREBP-2; N, cleaved form of SREBP-2. The remaining 95% of the harvested cells were used to purify ER membranes (*E*) as described above. Lipids were extracted and the amount of cholesterol and phospholipids was quantified as described under "Experimental Procedures." The cholesterol content in *E* is expressed as the mole percentage of total lipids (phospholipids + cholesterol). Each bar represents the means ± SEM from 5 experiments.

FIGURE 2-4

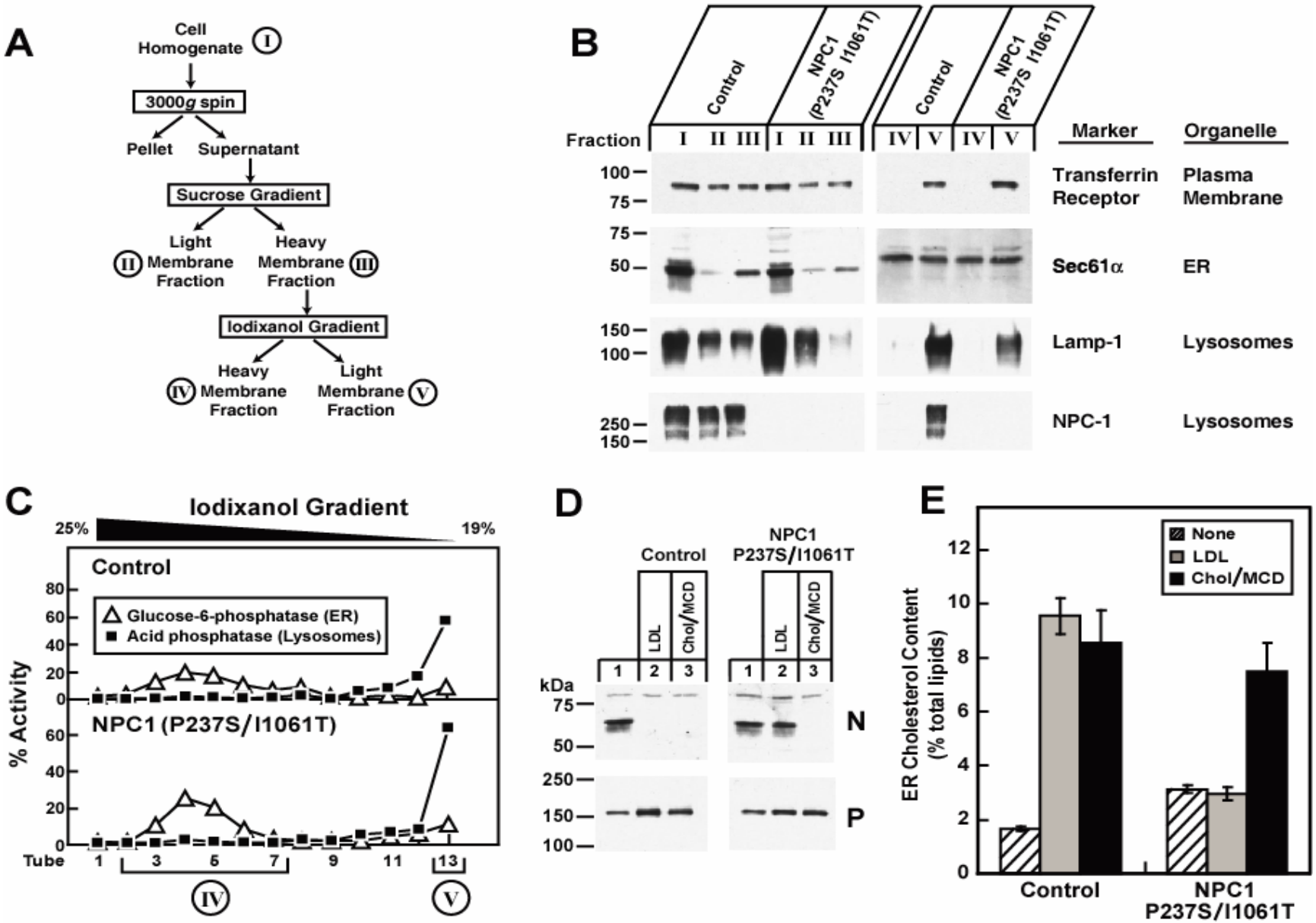
A
Cell Homogenate I
3000g spin
Pellet
Supernatant
Sucrose Gradient
Light Membrane Fraction II
Heavy Membrane Fraction III
Iodixanol Gradient
Heavy Membrane Fraction IV
Light Membrane Fraction V
B
Control
NPC1 (P237S I1061T)
Control
NPC1 (P237S I1061T)
Fraction
I II III I II III IV V IV V
Marker
Organelle
100
75
Transferrin Receptor
Plasma Membrane
75
50
Sec61α
ER
150
100
Lamp-1
Lysosomes
250
150
NPC-1
Lysosomes
C
Iodixanol Gradient
25%
19%
Control
Glucose-6-phosphatase (ER)
Acid phosphatase (Lysosomes)
% Activity
NPC1 (P237S/I1061T)
Tube 1 3 5 7 9 11 13
IV
V
D
Control
NPC1 P237S/I1061T
LDL
Chol/MCD
1 2 3 1 2 3
kDa
75
50
N
250
150
100
P
E
None
LDL
Chol/MCD
ER Cholesterol Content (% total lipids)
Control
NPC1 P237S/I1061T

FIGURE 2-5. Transport of cholesterol from the plasma membrane to ER is independent of NPC1.

On day 0, h-TERT-control and h-TERT-NPC1(P237S/I1061T) human fibroblasts were set up for experiments in medium A with 10% FCS at either $7x10^4$ cells per 60-mm dish (*A* and *B*) or $4x10^5$ cells per 100-mm dish (*C*). On day 2, the cells were switched to medium A with 5% human LPDS. *A*, immunoblot analysis of SREBP-2 cleavage. On day 4, the cells were incubated with medium A containing 5% human LPDS, 50 μM compactin, 50 μM sodium mevalonate, 0.1% DMSO, and 10 μg/ml of the ACAT inhibitor compound 58-035 (dissolved in DMSO). After incubation for 30 min at 37°C, cells received a direct addition of 200 milliunits/ml of sphingomyelinase, 10 μg protein/ml β-VLDL, or 1 μg/ml of 25-HC. After incubation for 2 h at 37°C, triplicate dishes were harvested and pooled for preparation of nuclear extract and 100,000*g* membrane fractions, which were analyzed by immunoblotting for SREBP-2. P, precursor form of SREBP-2; N, cleaved form of SREBP-2. *B*, cholesterol esterification assay. On day 4, each dish received medium A containing 5% human LPDS, 50 μM compactin, 50 μM sodium mevalonate in the presence or absence of 200 milliunits/ml of sphingomyelinase. After incubation for 1 h at 37°C, each monolayer was pulse-labeled for 1 h with 0.2 mM sodium [^{14}C]oleate-albumin (32,433 dpm/pmol). The cells were then harvested for measurement of their content of cholesteryl [^{14}C]oleate and [^{14}C]triglycerides. Each value is the average of duplicate incubations. The rate of synthesis of [^{14}C]triglycerides for control and NPC1 cells was 15 and 34 nmol/h per mg, respectively. *C*, analysis of cholesterol content of purified ER membranes. On day 3, the cells from 13 100-mm dishes for each condition were switched to medium A containing, 5% human LPDS, 5 μM

compactin, and 50 μM sodium mevalonate. On day 4, the cells received the same medium supplemented with 50 μM rather 5 μM compactin and in the absence or presence of 200 mU/ml of sphingomyelinase. After incubation for 2 h at 37°C , the cells were harvested, and ER membranes were purified as described under "Experimental Procedures" and Figure 5. Lipids were extracted and the amount of cholesterol and phospholipids was quantified as described in "Experimental Procedures." The cholesterol content is expressed as the mole percentage of total lipids (phospholipids + cholesterol). Each bar represents the means ± SEM from 3 experiments.

FIGURE 2-5

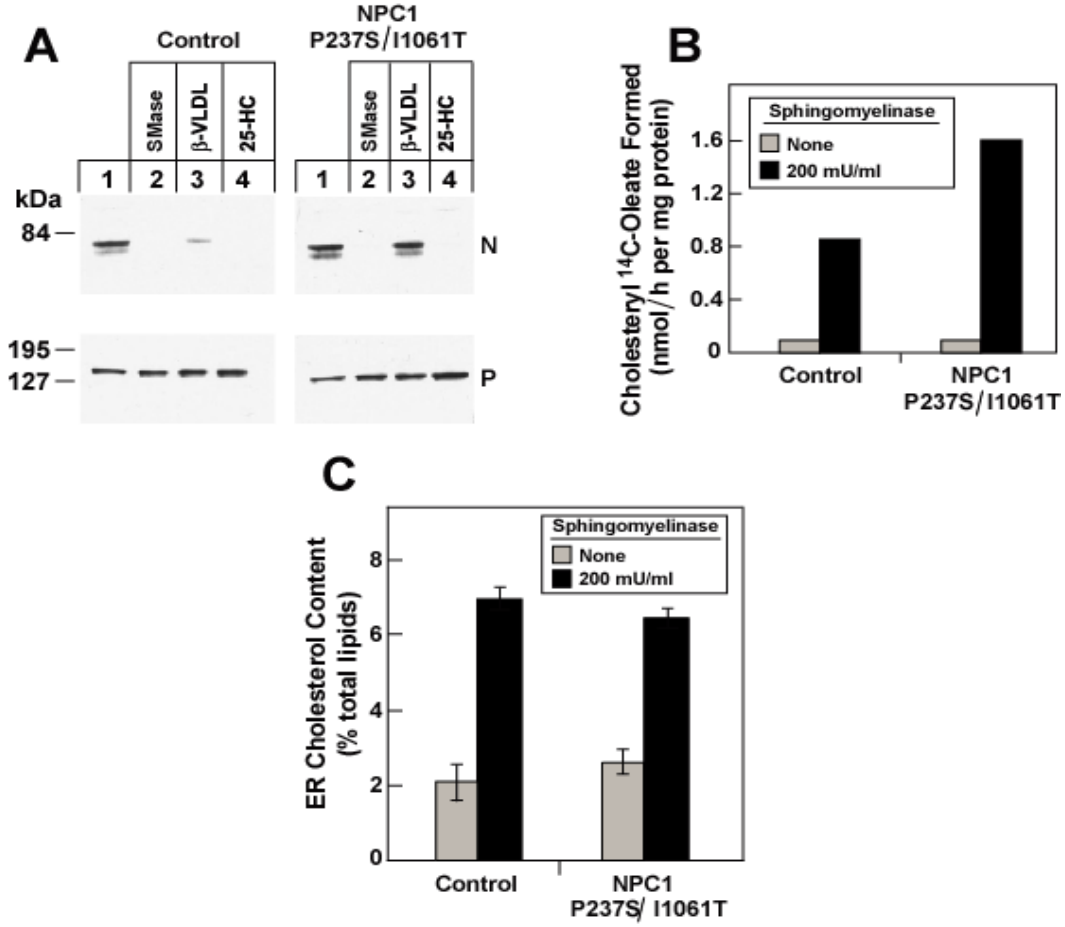
A
Control
NPC1
P237S/I1061T
SMase
β-VLDL
25-HC
1
2
3
4
kDa
84
195
127
N
P
B
Cholesteryl ^{14}C-Oleate Formed
(nmol/h per mg protein)
Sphingomyelinase
None
200 mU/ml
1.6
1.2
0.8
0.4
0
Control
NPC1
P237S/I1061T
C
ER Cholesterol Content
(% total lipids)
Sphingomyelinase
None
200 mU/ml
8
6
4
2
0
Control
NPC1
P237S/ I1061T

DISCUSSION

The present study focuses on understanding the NPC1 dependent and independent cholesterol transport in cells. We have one direct and three indirect methods of measuring the transport of cholesterol to the ER. The indirect measurements are based on the known regulatory actions of cholesterol once it reaches the ER. These regulatory actions are as follows: 1) the cholesterol binds to Scap, causing Scap to bind to Insig, thereby blocking the transport of SREBPs from ER to Golgi and preventing their proteolytic processing to the active nuclear form [65]; 2) the cholesterol serves as a substrate for acyl-CoA:cholesterol acyltransferase, which esterifies the cholesterol with a long chain fatty acid for storage in cholesteryl ester droplets [3]; and 3) the cholesterol causes the ubiquitination and rapid degradation of the ER enzyme HMG CoA reductase. The direct method consists of purifying ER membranes and measuring the ratio of cholesterol to phospholipids [73]. Using this procedure we can measure changes in the cholesterol content of ER membranes when cells are incubated with different sterols. We were able to show that the transport of cholesterol from plasma membrane to ER is independent of NPC1. The first clue came from cholesterol/MCD complex studies that deliver cholesterol to plasma membrane of cells [61]. When complexed to MCD, cholesterol could bypass the lysosomes and reach the ER as assessed by SREBP-2 processing, ACAT activation and direct cholesterol measurement of the purified ER. Similar results were obtained when NPC1 human skin fibroblasts were treated with neutral sphingomyelinase. Interactions between cholesterol and sphingomyelin are important in regulating cholesterol homeostasis in animal cells [74-76] and previous

studies in the lab [70] have shown that the depletion of sphingomyelin in Chinese hamster ovary cells (CHO) by treatment with neutral sphingomyelinase could suppress the proteolytic processing of SREBP-2 due to the mobilization of a fraction of the cholesterol from plasma membrane to ER. We performed similar experiment in the NPC1 human skin fibroblasts and we observed that that neutral sphingomyelinase could suppress SREBP-2 processing, increase the amount of cholesterol esters formed and increase the cholesterol content of the ER similar to the control cells. This finding provides further evidence that the transport of cholesterol from plasma membrane to ER is independent of NPC1.

Previous studies have shown that the effect of NPC1 on trafficking of cholesterol is cell-type dependent: macrophages and glial cells are prominently affected by the NPC1 mutation, whereas embryonic fibroblasts are less affected [27]. Moreover, a study done by Leventhal *et al.* (2001), shows that mouse peritoneal macrophages isolated from acid sphingomyelinase (ASM) knock out mice could not increase the amount of cholesterol esters formed in response to 25-HC treatment when the cells were prelabeled with [^{3}H]cholesterol [77]. ASM gene encodes for lysosomal sphingomyelinase, an enzyme involved in the hydrolysis of sphingomyelin in late endosomes and lysosomes [78]. Because sphingomyelin binds cholesterol [62, 79], its hydrolysis by L-SMase enables cholesterol transport by preventing cholesterol sequestration by sphingomyelin. Their study shows that the defect in cholesterol esterification in ASM knockout macrophages reflects a defect in cholesterol trafficking to ACAT rather than decreased ACAT enzyme activity since lysates from these cells showed an increase in ACAT activity *in vitro* in the presence of exogenous cholesterol [77]. To that end, we performed pulse-chase experiments in mouse peritoneal macrophages

and mouse skin fibroblasts that were isolated from littermate wild-type BALB/c and mutant homozygous BALB/c *npc* $^{nih/nih}$. There was no difference in the percentage of cholesterol esters formed between control and NPC1 mutant cells after long term labeling with [^{3}H]cholesterol in mouse peritoneal macrophages (Figure 2-2*A*) or short term labeling with [^{3}H]acetate in mouse skin fibroblasts (Figure 2-3) in response to 25-HC treatment. Similar experiments were performed in the NPC1 human skin fibroblasts and showed equivalent results to those obtained with mouse peritoneal macrophages (data not shown). We could not detect the differences in the percentage esterification of [^{3}H]cholesterol that were seen in the other studies [27, 77]. The discrepancy observed between our experiments and the others [27, 77] could be attributed to the fact that in our chase experiments we used 25-HC in order to activate ACAT whereas in those studies cells were only pulsed for a period of time and the percentage esterification was calculated thereafter at different time points. There's a possibility that the 25-HC could mobilize the cholesterol and make it available to ACAT enzyme in the ER; however, in this study, when macrophages (Figure 2-2*A*) or mouse skin fibroblasts (Figure 2-3*A and B*) were chased in the absence of 25-HC, they did not show a significant difference in the percentage esterification at the different time points tested between the control and the NPC1 mutant cell lines.

Our data suggests that the transport of endogenously synthesized cholesterol and plasma membrane derived cholesterol to the ER as evaluated indirectly by assaying for SREBP-2 processing or activation of ACAT, or directly by measuring the cholesterol content in purified ER is independent of NPC1 and that only the egress of LDL derived cholesterol from lysosomes to other membrane compartments in cells is dependent on NPC1. The

challenge now is to understand how NPC1 is involved in the transport of cholesterol from lysosomes. A better understanding of cholesterol transport at the cellular level could potentially lead to developing drugs that would reverse the lysosomal transport defect seen in NPC1 disease.

CHAPTER THREE

N-TERMINAL DOMAIN OF NPC1 IS IMPORTANT FOR THE TRANSFER OF LDL-DERIVED CHOLESTEROL FROM LYSOSOMES

SUMMARY

LDL delivers cholesterol to lysosomes by receptor-mediated endocytosis. Exit of cholesterol from lysosomes requires two proteins, membrane-bound Niemann-Pick C1 (NPC1) and soluble NPC2. Here, we describe two distinct point mutations in the first luminal domain of NPC1, designated the NPC1(NTD); a mutant that does not bind cholesterol and another mutant in this subdomain that cannot accept cholesterol from NPC2 but still binds cholesterol with similar affinity and kinetics as the wild-type protein. Both the binding and transfer mutants cannot restore cholesterol exit from lysosomes in NPC1-deficient cells. This defines the absolute requirement of cholesterol binding to NPC1 as a means for lipoprotein-derived cholesterol to exit the lysosomes. It also supports the idea that NPC1 and NPC2 proteins interact and that the transfer of cholesterol between NPC1 and NPC2 is required for exit of lipoprotein-derived cholesterol from lysosomes

INTRODUCTION

Over the last 30 years, much has been learned about the receptor-mediated endocytosis of plasma low-density lipoprotein (LDL) in coated pits and its subsequent delivery to endosomes and lysosomes [3, 80]. Each LDL particle contains ~500 molecules of free cholesterol and ~1,500 molecules of esterified cholesterol that are hydrolyzed by acid lipase in the lumen of the lysosome [81]. The liberated cholesterol must then exit the lysosomal compartment in order to reach the plasma membrane and the endoplasmic reticulum (ER) where it performs structural and regulatory roles, respectively [41, 60, 82]. A major unanswered question is how this exit process is accomplished.

Insight into two proteins required for cholesterol exit from lysosomes comes from Niemann-Pick Type C (NPC) disease [55], a fatal hereditary disorder characterized by the accumulation of cholesterol, sphingomyelin, and other lipids in endosomes and lysosomes. Evidence indicates that the primary cause is a failure of LDL-derived cholesterol to exit the lysosomes, which secondarily causes the buildup of other lipids. Mutations in either of two genes underlie NPC disease. Both genes encode lysosomal cholesterol-binding proteins. One gene encodes NPC1, a large 1278-amino acid polytopic membrane protein that is localized to the membranes of endosomes and lysosomes [16, 21]. The other gene encodes NPC2, a small soluble protein of 132 amino acids that resides in endosomes and lysosomes and is also secreted from the cell [29]. Homozygous mutations in either gene produce the

same pattern of lysosomal lipid accumulation and the same clinical phenotype, providing strong genetic evidence that both proteins are required for cholesterol egress [30].

NPC2 was shown previously to bind with high affinity to cholesterol, but not to cholesterol derivatives with hydrophilic substitutions on the isooctyl side chain, such as 25-hydroxycholesterol (25-HC) and 27-HC [32, 34, 83, 84]. Xu *et al.* (2007) [35] used x-ray crystallography to reveal the structure of bovine NPC2 in complex with cholesterol sulfate, which contains a sulfate in place of the 3β-hydroxyl group. Their data explained why hydrophilic substitutions on the isooctyl side chain prevent binding [34]. When cholesterol binds to NPC2, its isooctyl side chain is buried deep within a hydrophobic pocket. In contrast, the 3β-hydroxyl group is exposed on the surface. This exposure explains why a sulfate substitution (as in cholesterol sulfate) or a reversal of the orientation of the hydroxyl from 3β to 3α (as in epicholesterol) does not prevent binding. On the other hand, hydrophilic additions to the side chain, as in 25-HC, prevent burial of the side chain in the deep hydrophobic pocket.

NPC1 is much more complex than NPC2. NPC1 contains 13 predicted membrane-spanning helices and 3 large luminal domains [21]. The first luminal domain is designated the N-terminal domain (NTD). It consists of ~240 amino acids, which project into the lumen. This domain is hereafter designated NPC1(NTD). The other two large luminal domains are loops that span between transmembrane helices 2/3 and 8/9. We previously showed that full-length NPC1 binds [^{3}H]cholesterol with nanomolar affinity [31]. Surprisingly, the binding site is localized to the soluble NTD [34]. In sharp contrast to NPC2, NPC1(NTD) binds not only cholesterol, but also its oxygenated derivatives, 25-HC and 27-HC. On the other hand,

NPC1(NTD) does not bind sterols with modifications at the 3β-hydroxyl position such as cholesterol sulfate or epicholesterol. These data led to the suggestion that NPC1(NTD) binds cholesterol in an orientation opposite to that of NPC2 with the 3β-hydroxyl of cholesterol facing the interior of NPC1(NTD) and the isooctyl side chain exposed [34].

In a subsequent study, we provided evidence that cholesterol could transfer between purified NPC1(NTD) and NPC2 in a bidirectional fashion [36]. When [^{3}H]cholesterol was bound to NPC1 at 4°C, the dissociation rate into detergents was extremely slow, but the [^{3}H]cholesterol transferred rapidly to NPC2. The transfer could also proceed in the opposite direction: NPC2 transferred its bound [^{3}H]cholesterol to NPC1(NTD) two orders of magnitude faster than when [^{3}H]cholesterol was delivered to NPC1(NTD) in detergent solution [36]. NPC2 can deliver bound cholesterol directly to liposomes even in the absence of NPC1 [36, 85-87]. However, NPC1(NTD) could not deliver its bound cholesterol to liposomes unless NPC2 was present as an intermediate carrier. Although these studies showed a unique ability of NPC2 to facilitate entry and exit of cholesterol from NPC1(NTD), they did not indicate which direction this transfer took within lysosomes, i.e., LDL to NPC2 to NPC1 vs. LDL to NPC1 to NPC2. Although the NPC2-to-NPC1 model seems more logical [36, 88, 89], direct data in support of this model are lacking.

In a recent study, we used x-ray crystallography to determine a high resolution structure of NPC1(NTD) in the apoprotein (apo) form and in complex with cholesterol or 25-HC [90]. The protein contains a deep pocket that surrounds the sterol, burying the 3ß-hydroxyl group and the tetracyclic ring, but leaving the isooctyl side chain partially exposed. This orientation is opposite to the orientation of cholesterol bound to NPC2 in which the side

chain is buried and the 3ß-hydroxyl exposed [90]. In the current study, through mutational analysis, we identified two functional subdomains of NPC1(NTD) – one for sterol binding and the other for NPC2-mediated transfer. The crystal structure of NPC1(NTD) [90] reveals that mutations that inhibit binding to cholesterol (P202A/F203A), are located deep in the binding pocket; whereas the mutations in NPC1(NTD) that disrupt the transfer of cholesterol between NPC1 and NPC2, are on the surface of the opening where the sterol is inserted in NPC1(NTD). When these mutations were made in the full-length protein and transfected into mutant CHO cells that lack a functional NPC1 protein, they could not rescue the NPC1 phenotype. This study highlights the importance of cholesterol binding to NPC1 as a means for cholesterol to exit the lysosomes and provides the first evidence that NPC1 and NPC2 interact in order to transport cholesterol from lysosomes.

EXPERIMENTAL PROCEDURES

Materials - We obtained [1,2,6,7-^{3}H]cholesterol (60 Ci/mmol) and [26,27-^{3}H]25-HC (75 Ci/mmol) from American Radiolabeled Chemicals; all other sterols from Steraloids; anti-FLAG M2-Agarose affinity beads, FLAG peptide, and anti-FLAG M2 antibody from Sigma; FuGENE6 and NP-40 from Roche Applied Sciences; Ni-NTA agarose from Qiagen; egg yolk L-α-phosphatidylcholine (PC) and bis(monooleoylglycero)phosphate (BMP) from Avanti Polar Lipids; Hybond C Extra nitrocellulose filters and all chromatography products (unless otherwise stated) from GE Healthcare Biosciences. Reagents and lipoproteins for assays of cholesterol esterification and SREBP-2 processing were previously described in Chapter 1.

Buffers and Medium - Buffer A contained 25 mM Tris-chloride (pH 7.5), 150 mM NaCl, and 0.01% (w/v) NaN_3. Buffer B contained 25 mM Tris-chloride (pH 7.5), 50 mM NaCl, 0.01% NaN_3. Buffer C contained 50 mM Tris-chloride (pH 7.4) and 150 mM NaCl. Buffer D contained 50 mM MES-chloride (pH 5.5) and 150 mM NaCl. Medium A contained a 1:1 mixture of Ham's F12 medium and Dulbecco's modified Eagle's medium, 100 units/ml penicillin, and 100 μg/ml streptomycin sulfate.

Plasmid Constructions - Under control of the cytomegalovirus (CMV) promoter, pCMV-NPC1-His_8-FLAG encodes WT human NPC1 followed sequentially by 8 histidines and a FLAG tag was constructed as described in Chapter 1. pCMV-NPC1(1-264)-His8-FLAG encodes (after signal peptide cleavage) the N-terminal domain of WT human NPC1 (amino acids 25-264) followed sequentially by 8 histidines and a FLAG tag (Chapter 1).

pCMV-NPC1(1-264)-LVPRGS-His_8-FLAG encodes the same protein except that a thrombin cleavage site (LVPRGS) is inserted between the C-terminus of NPC1(NTD) and the His8 epitope tag [36]. pCMV-NPC2-His_{10} encodes (after signal peptide cleavage) WT human NPC2 (amino acids 1-132) followed sequentially by 10 histidines under the control of the CMV promoter [36]. pTK-HSV-BP2 encodes WT herpes simplex virus (HSV)-tagged human SREBP-2 under control of the thymidine kinase promoter [50].

Under control of the Herpes Simplex virus thymidine kinase promoter, pTK-NPC1-His_8-$FLAG_3$ encodes WT human NPC1 followed sequentially by 8 histidines and 3 FLAG tags was constructed as described in Chapter 1. The coding regions of all plasmids were sequenced to ensure the integrity of each construct.

Alanine Scan Mutagenesis of NPC1(NTD) - A panel of 84 mutant plasmids in which 1, 2, or 3 contiguous amino acids in NPC1(NTD) were changed to alanines was constructed by site-directed mutagenesis (Stratagene). To evaluate these NPC1(NTD) proteins encoded by these plasmids, we transfected the plasmids into CHO-K1 cells, after which assays for ^{3}H-sterol binding and transfer were performed on the secreted proteins.

CHO-K1 cells were grown in monolayer at 37°C in 8-9% CO_2. On day 0, cells were plated at a density of 6 x 10^6 cells per 100-mm dish in medium A containing 5% (v/v) fetal calf serum. On day 2, each dish was transfected with 5 μg pcDNA3.1 or pCMV-NPC1(1-264)-His_8-FLAG (WT or mutant versions) using FuGENE 6 as previously described [52]. On day 3, each dish was washed twice with 5 ml of Dulbecco's Phosphate-Buffered Saline and then switched to 7 ml of medium A containing 1% (v/v) Cellgro ITS (Fisher Scientific). On day 6, the medium from each dish (7 ml) was collected and concentrated to 1 ml using a

30-kDa Amicon Ultracel filter module (Millipore). Aliquots of the concentrated media were used for the three assays described below. The amount of secreted NPC1(NTD) was estimated by SDS/PAGE (8%) and immunoblot analysis with monoclonal FLAG antibody as described (Infante et al., 2008c), followed by densitometric scanning of the immunoblots.

For the ^{3}H-sterol binding assays, each reaction contained, in a final volume of 160 μl, 76 μl buffer C, 80 μl of concentrated media (representing the media from 0.04-0.08 dish of transfected cells, 1.92 μg of BSA, 0.004% NP-40, and 200 nM [^{3}H]cholesterol (132 dpm/fmol) or 40 nM [^{3}H]25-HC (165 dpm/fmol). After incubation for 24 h at 4°C, the amount of bound ^{3}H-sterol was measured with the ^{3}H-sterol binding assays (see Experimental Procedures). An aliquot of the eluate was also subjected to SDS/PAGE followed by immunoblot analysis with monoclonal FLAG antibody (see above).

For the [^{3}H]cholesterol transfer assay, aliquots of concentrated media from each transfected dish of cells were first incubated with [^{3}H]cholesterol to form a [^{3}H]cholesterol:NPC1(NTD) complex that was isolated by FLAG chromatography. Each reaction, in a final volume of 200 μl, contained 44 μl of buffer C, 150 μl of concentrated media (representing 0.15 dish of cells and containing WT or mutant NPC1(NTD)-His8-FLAG), 2.4 μg BSA, 0.004% NP-40, and 300 nM [^{3}H]cholesterol (132 dpm/fmol). After incubation for 24 h at 4°C, the mixture was passed through a 2-ml gravity column containing 200 μl of anti-FLAG M2-agarose beads preequilibrated with buffer C. Each column was washed first with 4 ml of buffer C containing 0.004% NP-40, then with 2 ml of buffer D, and eluted with 750 μl of buffer D containing 0.1 mg/ml of FLAG peptide. An aliquot of the

eluate (0.1 ml) was subjected to scintillation counting to determine the amount of [^{3}H]cholesterol bound to each mutant protein.

The eluate from each column was then subjected to the [^{3}H]cholesterol:NPC1(NTD)-to-liposome transfer assay. Each reaction, in a final volume of 207 μl, contained 200 μl of the FLAG column eluate (in buffer D) containing the indicated version of NPC1(NTD) complexed to [^{3}H]cholesterol (264 fmol, average for WT in 3 experiments; 214 fmol, average for 71 mutants in 3 experiments; specific activity, 132 dpm/fmol) and 20 μg liposomes containing PC and BMP (9:1) in the absence or presence of 0.8 μg NPC2-His8. After incubation for 15 min at 4°C, the reaction was diluted with 800 μl of buffer C and loaded onto a Ni-NTA-agarose column as previously described [36]. The flow-through fraction, representing the amount of [^{3}H]cholesterol transferred to liposomes, was quantified by scintillation counting. Liposomes were prepared as previously described (Infante et al., 2008c) except for the addition of BMP to the PC mixture.

Purification of Epitope-Tagged NPC1(NTD) and NPC2 from Medium of Transfected CHO Cells - WT NPC1(NTD) was purified by Ni-NTA-agarose and gel filtration chromatography of the media from CHO-K1 cells stably transfected with pCMV-NPC1(1-264)-LVPRGS-His8-FLAG as previously described [36]. NPC2 and mutant versions of NPC1(NTD) were purified by Ni-NTA-agarose and gel filtration chromatography of the media from CHO-K1 cells that had been transiently transfected with pCMV-NPC2-His_{10} or pCMV-NPC1(1-264)-LVPRGS-His_8-FLAG as previously described for NPC1(NTD) in Chapter 1.

^{3}H-Sterol Binding Assays for Purified NPC1(NTD) - The assays for binding of [^{3}H]cholesterol and [^{3}H]25-HC to purified NPC1(NTD) were previously described in Chapter 1. In brief, each reaction contained, in a final volume of 80 μl of the indicated buffer, varying concentrations of [^{3}H]cholesterol or [^{3}H]25-HC (132 and 165 dpm/fmol, respectively; delivered in ethanol), 1 μg bovine serum albumin (BSA), and varying amounts of NPC1(NTD). After incubation for 24 h at 4°C, each assay mixture was loaded onto a 2-ml column packed with 0.3 ml of Ni-NTA-agarose beads that had been preequilibrated with buffer C containing 0.004% (w/v) Nonidet P-40 (NP-40) and then washed with 5 ml of buffer C with 1% NP-40. Protein-bound [^{3}H]cholesterol was eluted with 1 ml of buffer C containing 250 mM imidazole and 1% NP-40 and quantified by scintillation counting.

[^{3}H]Cholesterol Transfer Assays for Purified NPC Proteins - The transfer assays, including methods for isolation of complexes of [^{3}H]cholesterol bound to NPC1(NTD) or NPC2 and for preparation of liposomes, have been described [36]. For transfer assays of NPC1(NTD) to liposomes, incubation conditions are described in Figure 5E. After incubation, the 200-μl mixture was diluted with 750 μl of buffer C and loaded onto a 2-ml column packed with 0.3 ml of Ni-NTA-agarose beads preequilibrated with buffer C. Each column was washed with 1 ml of buffer C. The amount of [^{3}H]cholesterol transferred to liposomes was quantified by scintillation counting of the combined flow-through and wash fractions. For transfer assays of NPC2 to NPC1(NTD), incubation conditions are described in Figure 5D. After incubation, each mixture was processed as above except that the column was washed with 3 ml of buffer C and eluted with 250 mM imidazole, after which the eluate was subjected to scintillation counting.

Assays for Cholesterol Esterification and SREBP-2 Processing in Cultured Cells - Mutant CHO 4-4-19 cells, defective in NPC1 function [48], were transfected and tested for incorporation of [^{14}C]oleate into cholesteryl [^{14}C]oleate and proteolytic processing of SREBP-2 as described in Chapter 1. For assays of cholesterol esterification, cells were transfected with 2 μg pcDNA3.1 or pCMV-NPC1-His_8-FLAG (wild-type or mutant versions). For assays of SREBP-2 processing, cells were co-transfected with 0.5 μg pcDNA3.1 or pTK-NPC1-His_8-$FLAG_3$ (wild-type or mutant versions) plus 3 μg pTK-HSV-BP2. Incubation conditions are described in the legend to Figure 3-5.

RESULTS

Alanine Scan Mutagenesis to Identify Residues of NPC1(NTD) Required for Sterol Binding - To determine key residues in NPC1(NTD) that are important for sterol binding, we performed an alanine scan mutagenesis across the protein (amino acids 23-264) and assayed each mutant for binding to [^{3}H]cholesterol and [^{3}H]25-HC (Figure 3-1). We generated a panel of 84 mutant plasmids in which 1, 2, or 3 contiguous amino acids were changed to alanines. This panel included all 242 residues in NPC1(NTD) except for the following: 4 conserved residues previously shown (Chapter 1) to have normal binding activity when replaced with alanine (Asn103, Gln117, Phe120, Tyr157) [34]; 1 conserved residue that when mutated to alanine (Gln79) showed reduced cholesterol binding (60% of normal) and virtually no 25-HC binding [34]; 6 naturally-occurring mutations that were shown previously to have normal binding activity (Gln92, Thr137, Pro166, Asn222, Asp242, Gly248) [34]; 18 cysteines; and the C-terminal 32 residues (amino acids 233-264), which when deleted do not decrease binding of [^{3}H]cholesterol or [^{3}H]25-HC (data not shown).

As described in Experimental Procedures, we developed a rapid assay that allowed measurement of ^{3}H-sterol binding to aliquots of concentrated media from CHO-K1 cells that had been transfected with plasmids encoding epitope-tagged WT or mutant versions of NPC1(NTD). The amount of secreted protein was determined by immunoblotting with an antibody directed against the FLAG epitope tag. Of the 84 mutants, 5 did not produce secreted protein (Y28-E30, L80/Q81, W189/I190, M193/F194, and V208/F209). Binding assays were performed by trapping the His-tagged proteins with bound ^{3}H-sterol on nickel

columns as described in "Experimental Procedures". Media from cells transfected with mock vector showed no binding of [^{3}H]cholesterol or [^{3}H]25-HC (<20 fmol/tube), whereas media from cells transfected with WT NPC1(NTD) showed 860-1500 fmol/tube and 780-1000 fmol/tube for [^{3}H]cholesterol and [^{3}H]25-HC, respectively (Figure 3-1*B*). Six of the 84 NPC1(NTD) mutant proteins showed binding that was less than 25% of WT (Figure 3-1*B*, blue). All of these mutations (R39-N41, T82/L83, N106-F108, D197/N198, P202/F203, and T204/I205) replace residues that map to the binding pocket (Figure 3-3*B and C*, blue). These residues include the majority of the hydrophobic amino acids that line the binding pocket around the tetracyclic ring except for Trp27, whose replacement reduced [^{3}H]cholesterol binding to a level slightly above the 25% threshold (Figure 3-1*B*). Of the two hydrophilic residues that form direct hydrogen bonds with the 3β-hydroxy group, the replacement of Asn41 with alanine disrupted [^{3}H]cholesterol binding by 90% (Figure 3-1*B*). The other hydrophilic residue (Gln79) was previously shown in Chapter 1 to produce a 40% reduction in cholesterol binding when replaced with alanine [34]. The only amino acid in the sterol binding domain that could not be evaluated in the alanine scan was Glu30; which forms a water-mediated bond with the 3ß-hydroxyl. This mutant protein was not secreted into the media. We identified 7 mutant NPC1(NTD) proteins that exhibited a preferential reduction of binding of [^{3}H]25-HC as compared with [^{3}H]cholesterol (Figure 3-1*B*, pink). All 7 of these mutations replaced amino acids that mapped either to the binding pocket (V26/W27 and G199/Q200) or to adjacent amino acids (F101/Y102, L144/Q145, Y146/Y147, T187/N188, and N195/K196).

To validate the major findings from the assays with unfractionated culture media, we purified the mutant protein with the least amount of cholesterol binding (P202A/F203A) and analyzed it in detail. As shown in Figures 3-4*A* and 3-4*B*, the purified protein showed no detectable binding of either [^{3}H]cholesterol or [^{3}H]25-HC.

Alanine Scan Mutagenesis to Identify Residues Required for NPC2-mediated Transfer - Previously, we showed that NPC2 catalyzes the bidirectional transfer of cholesterol between NPC1(NTD) and liposomes *in vitro* [36]. To test the amino acids in NPC1(NTD) that are important for this action, we performed a transfer assay with all of the alanine scan mutants except for the 8 mutants whose [^{3}H]cholesterol binding activity was less than 50% of the WT. For this assay, we prepared stable complexes of [^{3}H]cholesterol:NPC1(NTD) and purified them by immunoaffinity chromatography as described in "Experimental Procedures". We then measured the transfer of the bound [^{3}H]cholesterol to liposomes in the presence and absence of purified NPC2. In the absence of NPC2, less than 8% of bound [^{3}H]cholesterol from WT NPC1(NTD) was transferred to liposomes. In the presence of NPC2, WT NPC1(NTD) transferred an additional 54-90% of bound [^{3}H]cholesterol in 3 experiments (Figure 3-2*B*, shaded region) with an average of 80%. Six mutant NPC1(NTD) proteins transferred less than 25% of their bound [^{3}H]cholesterol to liposomes in an NPC2-dependent manner (Figures 3-2*B*, red). These mutations replaced residues L175/L176, D180/D182, N185, T187/N188, E191/Y192, and G199/Q200, all of which map to a surface of a subdomain of NPC1(NTD) spanning amino acids 162-200. This region includes helices 7 and 8 and the intervening loop (Figure 3-3*B and C*, red). Of the 6 mutants in this region, the two most deficient in transfer are L175A/L176A and E191A/Y192A. Two of these 4 WT

residues (L176 and Y192) are identical in 12 out of 12 mammalian species, and the other two (L175 and E191) are identical in 11 of the 12 species [34].

To validate the findings from the above transfer assays done with culture media, we purified one of the mutants, L175A/L176A, that showed a marked decrease in the amount of NPC2-dependent [^{3}H]cholesterol transfer from NPC1(NTD) to liposomes. When incubated with [^{3}H]cholesterol for 24 h at 4°C, a time necessary to achieve equilibrium binding in the absence of NPC2 [36], the mutant protein bound cholesterol with similar affinity to that of the WT protein (Figure 3-4*C*). Moreover, its rates of association and dissociation of [^{3}H]cholesterol at 4°C and 37°C were virtually identical to those of WT NPC1(NTD) (data not shown). Equilibrium binding for both WT and mutant proteins was achieved within 30 min at 37°C, and dissociation of previously bound [^{3}H]cholesterol for both proteins occurred rapidly at 37°C and extremely slowly at 4°C (data not shown).

Despite its normal binding kinetics, the mutant protein showed a marked defect in NPC2-stimulated transfer of cholesterol to liposomes (Figure 3-4*E*). As compared to WT NPC1(NTD), the mutant protein required 5 times more NPC2 to transfer an equivalent amount of [^{3}H]cholesterol to liposomes. To show that this transfer defect is the result of defective interaction with NPC2 and not with liposomes, we tested the ability of NPC2 to transfer its cholesterol to WT NPC1(NTD) and to this mutant. Within 15 min, NPC2 transferred 4-fold more [^{3}H]cholesterol to WT NPC1(NTD) as compared to the L175A/L176A mutant (Figure 3-4*D*).

Cholesterol Binding and Transfer Mutants Fail to Restore Function to NPC1-deficient Cells - To assay the function of mutant NPC1 proteins, we measured the two

reactions that occur when cholesterol or oxysterols reach the ER: 1) activation of acyl-CoA:cholesterol acyltransferase (ACAT), thereby increasing incorporation of radiolabeled fatty acids into cholesteryl esters [54]; and 2) inhibition of the proteolytic processing of sterol regulatory element-binding proteins (SREBPs), thereby inactivating transcription of genes for cholesterol synthesis and uptake [7, 31]. Figures 3-5*A and B* show an experiment in which we transfected plasmids encoding full-length WT and mutant NPC1 into CHO 4-4-19 cells. These cells lack NPC1 function as a result of a point mutation (G660R) in transmembrane helix 3 [34, 48]. 48 h after transfection, the cells were incubated for 5 h with varying concentrations of β-VLDL, a cholesterol-rich lipoprotein that binds LDL receptors and delivers cholesterol to lysosomes. (Because of its high affinity for the LDL receptor, β-VLDL is frequently used as a ligand in cell culture studies [56]). After incubation with β-VLDL, the cells then received [^{14}C]oleate and the incorporation into cholesteryl [^{14}C]oleate was measured. When transfected with a control (mock) plasmid, the CHO 4-4-19 cells showed little cholesteryl [^{14}C]oleate formation. Expression of WT NPC1 allowed β-VLDL to stimulate cholesteryl oleate formation by 20-fold (Figure 3-5*A*). Full-length NPC1 harboring the P202A/F203A mutation in the NTD was markedly defective in restoring sensitivity to β-VLDL (Figure 3-5*A*, red triangles). Similar defects were seen when full-length NPC1 contained the L175A/L176A mutation (blue triangles). None of the mutant proteins interfered with the ability of 25-HC to stimulate cholesteryl ester formation, a response that is normal in the NPC1 mutant cells (Figure 3-5*B*).

Immunoblotting revealed that the mutant proteins were expressed at the same level as WT (Figure 3-5*A*, inset). Both mutant and WT proteins showed a diffuse band characteristic

of fully glycosylated lysosomal proteins that have left the ER [57]. Moreover, treatment of the mutant proteins with the glycosidase Endo H (which removes only high mannose chains) did not alter their migration pattern on SDS-PAGE, providing further evidence that the mutant proteins had folded properly and left the ER (data not shown). In the same experiment, Endo H treatment of a control protein containing a high mannose chain (Site-1 protease) [91] showed the expected increase in electrophoretic mobility.

To study the inhibition of SREBP processing, we employed similar experiments as Chapter 1 in which CHO 4-4-19 cells that are deficient in NPC1 function were deprived of sterols and then incubated with β-VLDL for 5 h after which membrane and nuclear extracts were subjected to immunoblotting to detect the full-length precursor and the processed nuclear form of SREBP-2. Mock-transfected CHO 4-4-19 cells failed to suppress SREBP-2 cleavage when incubated with β-VLDL (Figure 3-5*C*; lanes 2,3). Suppression was restored by transfection with a plasmid encoding WT NPC1 (lanes 4-7), but not with plasmids encoding the binding-defective mutant (lanes 8-11) or transfer-defective mutant (lanes 12-15). None of these plasmids affected suppression by 25-HC, which is normal in NPC1 deficient cells (Figure 3-5*D*).

FIGURE 3-1. Alanine scan of NPC1(NTD): ^{3}H-Sterol binding activity

(A) Sequence of human NPC1(NTD), amino acids 22-264. Black boxes denote residues invariant in 12 vertebrate species[34]. Blue ovals denote residues that when mutated to alanine decrease binding of both [^{3}H]cholesterol and [^{3}H]25-HC by > 75%. Pink ovals denote residues that when mutated to alanine preferentially decrease by >2.5-fold the binding of [^{3}H]25-HC relative to [^{3}H]cholesterol, as determined in 2 independent experiments. (B) Alanine scan for binding activity of [^{3}H]cholesterol (top panel) and [^{3}H]25-HC (bottom panel). Each reaction, in a final volume of 160 μl, contained 76 μl buffer C, 80 μl of concentrated media (representing 0.04-0.08 dish of cells and containing the indicated WT or mutant version of NPC1(NTD)-His_8-FLAG), 1.92 μg of BSA, 0.004% NP-40, and either 200 nM [^{3}H]cholesterol (132 dpm/fmol; top panel) or 40 nM [^{3}H]25-HC (165 dpm/fmol; bottom panel). After incubation for 24 h at 4°C, the amount of bound ^{3}H-sterol was measured as described in "Experimental Procedures". Each bar is the average of duplicate assays and represents the amount of binding relative to that of WT NPC1(NTD) studied in the same experiment. All data were adjusted for variations (typically <2-fold) in the amount of secreted NPC1(NTD) protein as determined by densitometric scanning of immunoblots of the assayed protein. The data in the graph were obtained in three separate experiments. The "100% of control" values for WT NPC1(NTD) in the three experiments ranged from 0.86-1.5 pmol for [^{3}H]cholesterol and 0.78-1.0 pmol for [^{3}H]25-HC. All mutants giving transfer values of <50% were repeated with similar results. Color coding is same as in A.

FIGURE 3-1

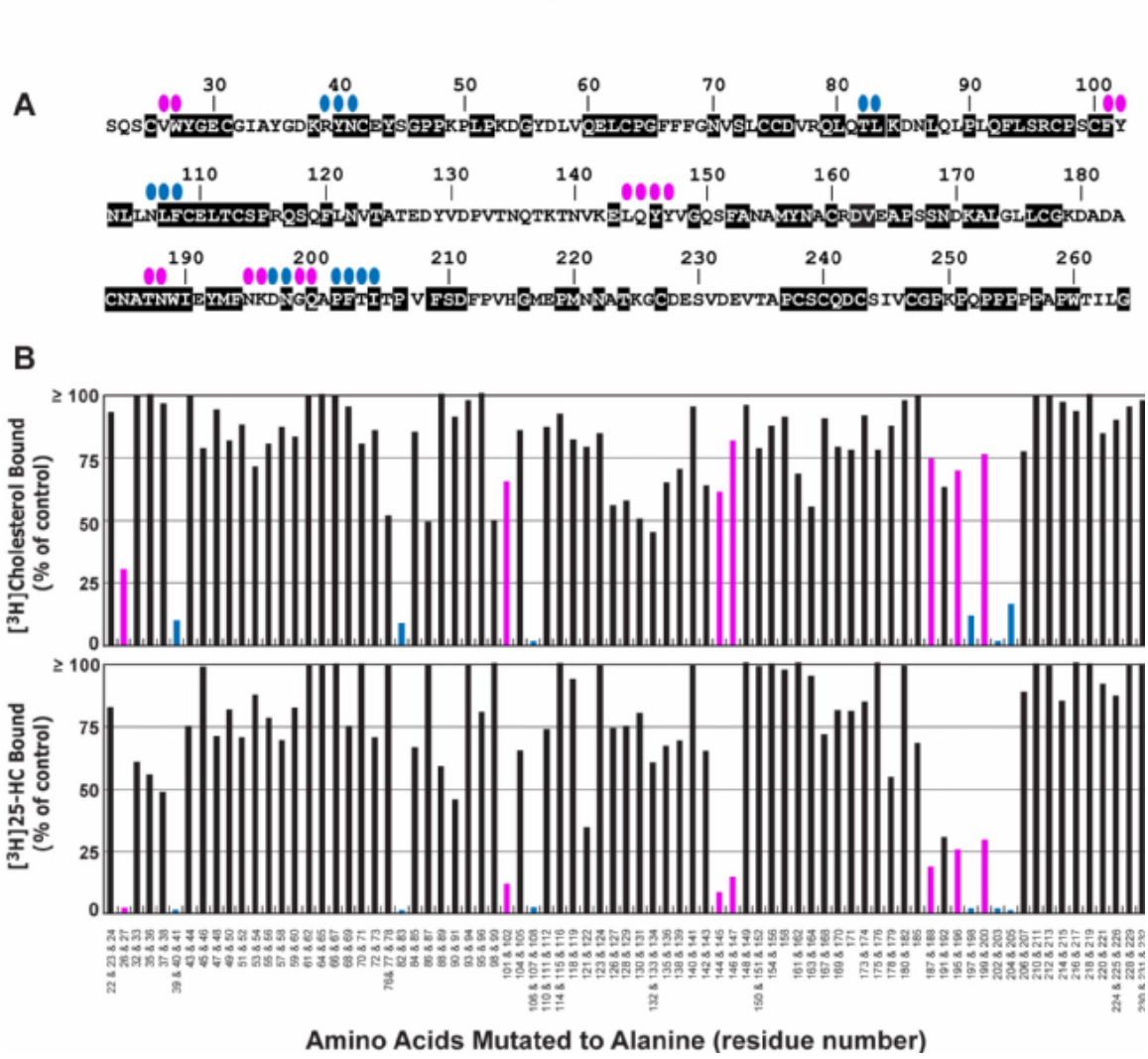

(This data reproduced with permission by Rodney Infante and Michael Wang)

FIGURE 3-2. Alanine scan of NPC1(NTD): [^{3}H]Cholesterol transfer activity

(A) Sequence of human NPC1(NTD), amino acids 22-264. Black boxes denote residues invariant in 12 vertebrate species [34]. Red ovals denote residues that when mutated to alanine decrease the amount of [^{3}H]cholesterol transferred from NPC1(NTD) to liposomes by > 70%.

(B) Alanine scan for [^{3}H]cholesterol transfer from NPC1(NTD) to liposomes. WT and mutant [^{3}H]cholesterol:NPC1(NTD) complexes were isolated by FLAG chromatography as described in "Experimental Procedures". Each reaction, in a final volume of 207 μl, contained 200 μl of the indicated [^{3}H]cholesterol:NPC1(NTD)-His_8-FLAG complex and 20 μg PC:BMP (9:1) liposomes in the presence or absence of 0.8 μg NPC2-His_{10}. After incubation for 15 min at 4°C, the amount of [^{3}H]cholesterol transferred to liposomes was measured as described in "Experimental Procedures". Each value represents the percentage of [^{3}H]cholesterol transferred to liposomes in the presence of NPC2 after subtraction of the percentage in the absence of NPC2. The data in the graph were obtained in 3 separate experiments. The shaded region denotes the range of WT values obtained in the 3 experiments. The entire experiment was repeated with similar results. Color coding is the same as in A.

FIGURE 3-2

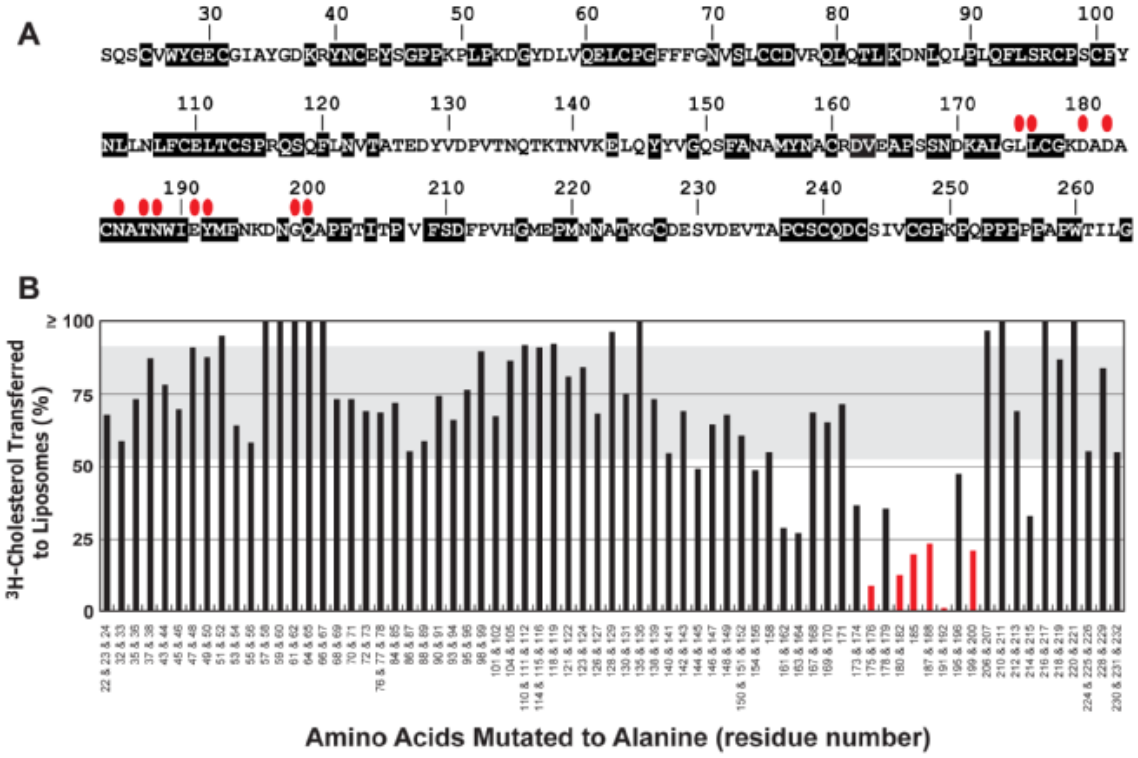

(This data reproduced with permission by Rodney Infante and Michael Wang)

FIGURE 3-3. Location of functionally important residues in NPC1(NTD)

(A) Amino acid sequence of NPC1(NTD) with functionally important residues highlighted. Blue ovals denote residues that exhibit decreased binding of cholesterol and 25-HC by >75% when mutated to alanine. Red ovals denote residues that exhibit decreased transfer of cholesterol to liposomes by >70% when mutated to alanine. Cyan ovals denote naturally-occurring mutations in patients with NPC1 disease. Residues that line the binding pocket are shaded yellow. N-linked glycosylation sites that were eliminated are shaded green. The secondary structure of NPC1(NTD) is indicated below the sequence.

(B and C) Ribbon diagram (B) and surface representation (C) of NPC1(NTD), showing the positions of functionally important residues. Bound 25-HC is shown as a stick model in green. Color coding is the same as in (A). The location of the L175, L176, P202, and F203 residues are denoted by arrows.

FIGURE 3-3

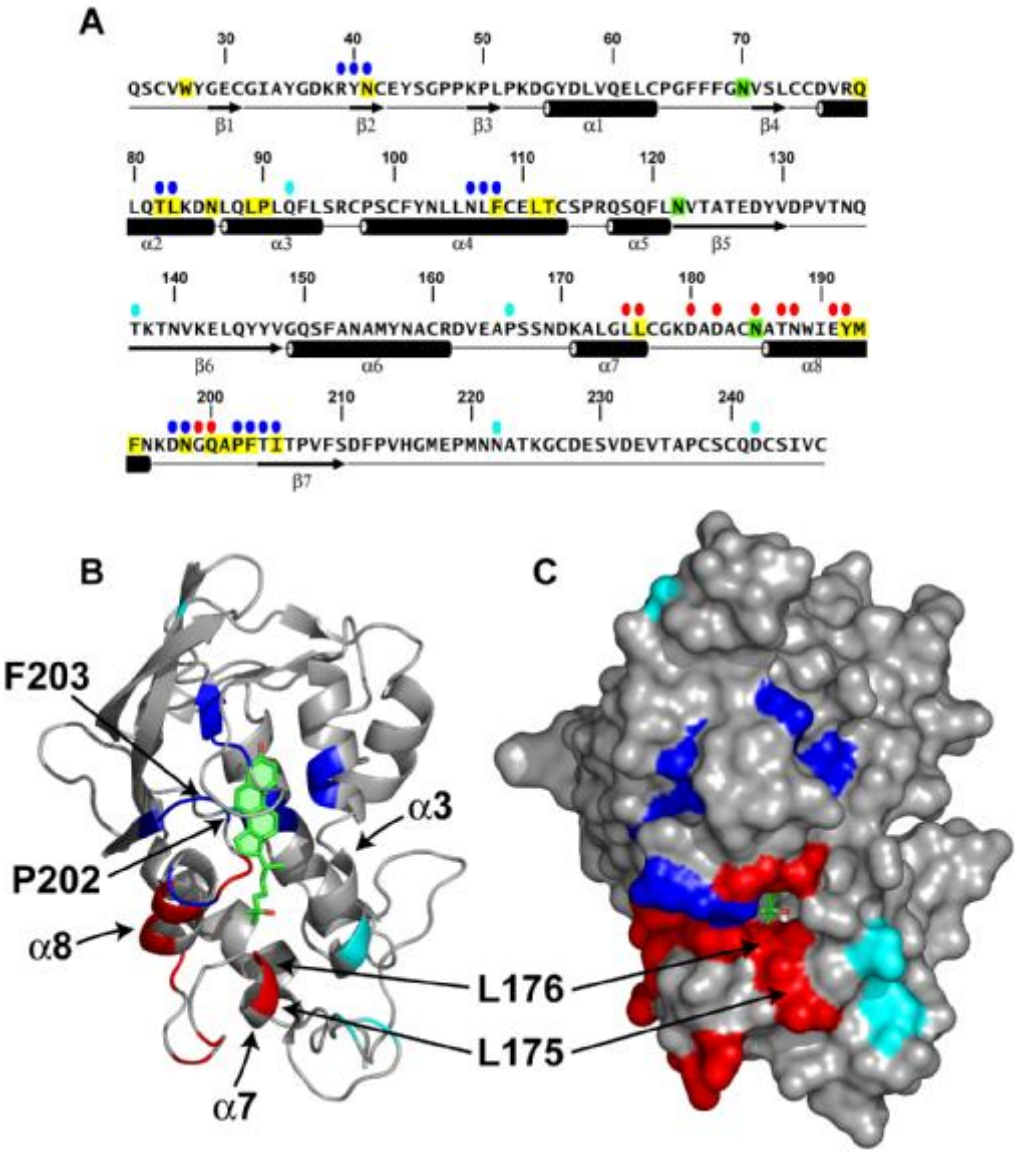

(This data reproduced with permission by Rodney Infante , Michael Wang and Hyock Joo Kwon)

FIGURE 3-4. Biochemical analysis of sterol binding and transfer mutants

(A-C**)** ^{3}H-Sterol binding. Each reaction, in a final volume of 80 μl buffer C with 0.004% NP-40, contained 220 ng purified WT or mutant NPC1(NTD)-LVPRGS-His_8-FLAG, 1 μg BSA, and indicated concentration of [^{3}H]cholesterol (132 dpm/fmol) (A,C) or [^{3}H]25-HC (165 dpm/fmol) (B). After incubation for 24 h at 4°C, the amount of bound ^{3}H-sterol was measured as described in "Experimental Procedures". Each value is the average of duplicate assays and represents total binding after subtraction of a blank value (10-70 fmol/tube). Mean variation for each of the duplicate assays in A, B, and C were 6.1%, 5.0%, and 5.0%, respectively.

(D) [^{3}H]Cholesterol transfer from NPC2 to NPC1(NTD). Each reaction, in a final volume of 200 μl buffer D (pH 5.5) without detergent, contained ~40 pmol of donor protein NPC2-FLAG complexed to [^{3}H]cholesterol (830 fmol, 132 dpm/fmol) and increasing concentrations of purified WT or mutant NPC1(NTD)-LVPRGS-His_8-FLAG acceptor protein. After incubation for 15 min at 4°C, the amount of [^{3}H]cholesterol transferred to NPC1(NTD) was measured by Ni-NTA-agarose chromatography as described in the [^{3}H]cholesterol transfer assay in "Experimental Procedures". Each value is the average of duplicate assays and represents percentage of [^{3}H]cholesterol transferred to NPC1(NTD). The 100% value for transfer from NPC2 was 830 fmol/tube. Mean variation for each of the duplicate assays for WT and mutant were 7.9% and 8.2%, respectively

(E) [^{3}H]Cholesterol transfer from NPC1(NTD) to liposomes as a function of NPC2. Each reaction, in final a volume of 200 μl buffer D (pH 5.5) without detergent, contained ~50

pmol of WT or L175A/L176A versions of NPC1(NTD)-LVPRGS-His_8-FLAG, each complexed to [^{3}H]cholesterol (950 and 660 fmol, respectively; 132 dpm/fmol); 20 μg PC liposomes labeled with Texas red dye; and increasing concentrations of NPC2-His_{10}. After incubation for 10 min at 4°C, the amount of [^{3}H]cholesterol transferred to liposomes was measured in the flow-through of the nickel column as described for the [^{3}H]cholesterol transfer assay in "Experimental Procedures". Each value is the average of duplicate assays and represents the percentage of [^{3}H]cholesterol transferred to liposomes. Blank values in the absence of NPC2 (5-6% transfer) were subtracted. The 100% values for transfer from WT and L175A/176A versions of NPC1(NTD) were 950 and 660 fmol/tube, respectively. Mean variation for each of the duplicate assays for WT and mutant were 8.8% and 9.3%, respectively.

FIGURE 3-4

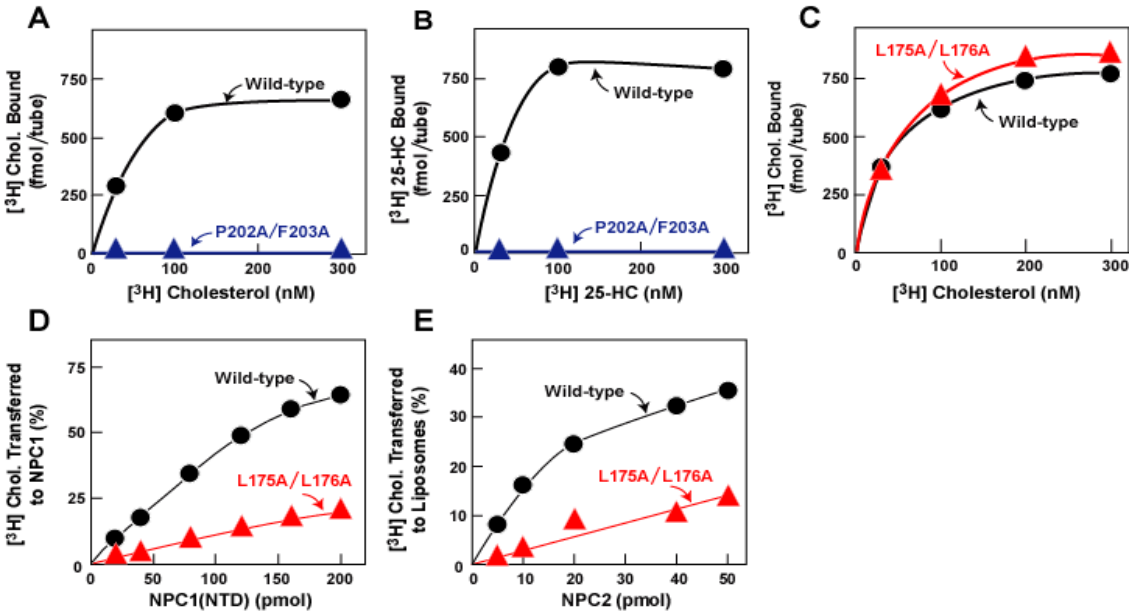

(This data reproduced with permission by Rodney Infante and Michael Wang)

FIGURE 3-5. Functional analysis of sterol binding and transfer mutants

(A-D**)** Cholesterol esterification and SREBP-2 processing in mutant CHO cells lacking NPC1 function transfected with NPC1 cDNAs. Mutant CHO 4-4-19 cells were set up for experiments and transfected with 2 μg pcDNA3.1 or with WT or mutant versions of pCMV-NPC1-His_8-FLAG (A and B); or co-transfected with 0.4 μg pcDNA3.1 or with WT or mutant versions of pTK-NPC1-His_8-$FLAG_3$ plus 3 μg pTK-HSV-BP2 (C and D) as described in "Experimental Procedures". 24 h after transfection, the medium was switched to medium A containing 5% newborn calf lipoprotein-deficient serum, 5 μM compactin, and 50 μM sodium mevalonate. After incubation for 24 h, the medium was switched to the same medium containing 50 μM compactin and various concentrations of ß-VLDL (A and C) or 25-HC (B and D) as indicated.

(A and B) Cholesterol esterification. After incubation for 5 h at 37°C, each cell monolayer was pulse-labeled for 1 h with 0.2 mM sodium [^{14}C]oleate (6301 dpm/pmol). The cells were then harvested for measurement of their content of cholesteryl [^{14}C] oleate and [^{14}C] triglycerides. Each value is the average of duplicate incubations. Mean variation for each of the duplicate incubations for WT, P202A/F203A, and L175A/L176A were 9.6%, 14.5%, and 4.3%, respectively. The rate of synthesis of [^{14}C]triglycerides for mock, NPC1 WT, NPC1(P202A/F203A), and NPC1(L175A/L176A) transfected cells incubated with 5 μg/ml ß-VLDL was 340, 396, 352, and 365 nmol/h per mg protein, respectively. The rate of synthesis of [^{14}C]triglycerides incubated with 25-HC was 347, 496, 304, and 434 nmol/h per mg protein, respectively.

(C and D) SREBP-2 processing. After incubation for 4 h at 37°C, cells received a direct addition of 25 μg/ml of N-acetyl-leucinal-leucinal norleucinal. After 1 h, triplicate dishes were harvested and pooled for preparation of nuclear extracts and 100,000 *g* membrane fractions, which were analyzed by immunoblotting for the indicated protein. The concentrations of antibodies were 0.2 and 4 μg/ml for SREBP-2 (anti-HSV) and NPC1 (anti-FLAG), respectively. All filters were exposed on x-ray film for 2-10 s.

FIGURE 3-5

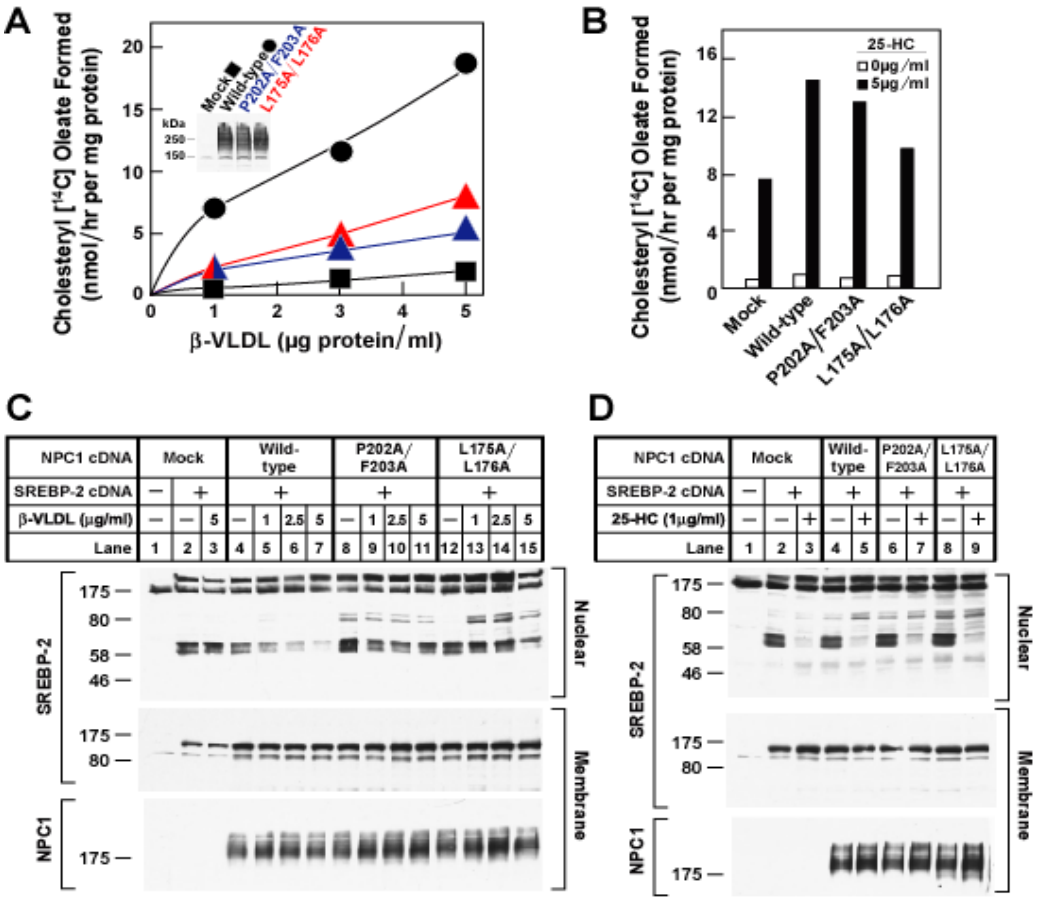

DISCUSSION

Egress of lipoprotein-derived cholesterol from lysosomes requires two lysosomal proteins, polytopic membrane-bound Niemann–Pick C1 (NPC1) and soluble Niemann–Pick C2 (NPC2). The reason for this dual requirement is unknown. In Chapter 1, we showed that the soluble luminal N-terminal domain (NTD) of NPC1 (amino acids 25–264) binds cholesterol. We and others showed that soluble NPC2 also binds cholesterol [34-36]. Infante *et al.* (2008) established an *in vitro* assay to measure transfer of [^{3}H]cholesterol between these two proteins and phosphatidylcholine liposomes [36]. In that study they show that NPC1(NTD) act slowly in terms of donating or accepting cholesterol from liposomes whereas NPC2 acts rapidly. Bidirectional transfer of cholesterol between NPC1(NTD) and liposomes is accelerated >100-fold by NPC2 suggesting that NPC2 may be essential to deliver or remove cholesterol from NPC1. This is the first study that suggests that an interaction between both proteins is linked to the cholesterol egress process from lysosomes. In order to prove that such an interaction exists, in the current study we carried out mutational analysis on NPC1(NTD) to identify amino acid residues that would disrupt the transfer of cholesterol between NPC1(NTD) and liposomes in the presence of NPC2. Mutational analysis allowed us to identify two functional subdomains in NPC1(NTD), L175A/L176A for NPC2-mediated transfer and P202A/F203A for sterol binding. While these studies were in progress, using x-ray crystallography, Kwon *et al.* (2009, *Cell in press*) determined a high resolution structure of NPC1(NTD) in the apoprotein (apo) form and in complex with cholesterol or 25-HC. The ribbon diagram and surface representation of

NPC1(NTD) show that L175A/L176A amino acid residues reside on the surface of the protein (Figure 3-3*B*, red) whereas the P202A/F203A amino acid residue are embedded deep in the pocket of NPC1(NTD) that surrounds the sterol (Figure 3-3*B*, blue). When both of these mutations were made in the full length protein and transfected into CHO 4-4-19 cells, they expressed similar to wild-type NPC1, displaying a heavy glycosylation pattern that was Endo H resistant (data not shown) which suggests that both mutants and the wild-type protein exit the ER. However, further experiments using immunostaining with antibodies against the mutant versions of NPC1 and a lysosomal marker such as LAMP1 are necessary in order to show co-localization of both mutant proteins to the lysosomes. These mutants could not suppress SREBP-2 processing when transfected into mutant CHO cells that lack a functional NPC1 protein in response to β-VLDL treatment. They also showed a decreased ability to activate ACAT enzyme, suggesting that lipoprotein-derived cholesterol is stuck in the lysosomes and could not reach the ER. This study provides the fist evidence that cholesterol binding to NPC1 protein is important for the transport of the lipoprotein-derived cholesterol from the lysosomes to the plasma membrane and the ER and that the dual interaction between NPC1 and NPC2 is necessary in order for the cholesterol to be able to exit the lysosomes.

CONCLUSION AND PERSEPECTIVE

Maintenance of cellular cholesterol homeostasis necessitates the transport of cholesterol between subcellular membranes and its exchange with lipoproteins. Much of our knowledge of intracellular cholesterol trafficking comes from studies on inherited metabolic diseases [4]. Insight into the export of LDL-derived cholesterol comes from studies on cells from patients with Niemann-Pick Type C Disease (NPC) disease whish is caused by mutations in either one of two proteins, a membrane protein NPC1 and a soluble protein NPC2 [55]. Although both proteins have been cloned for over 10 years, not much is known about their involvement in cholesterol trafficking within cells. Experiments presented in this study tackle the NPC1 dependent and independent cholesterol transport pathways within cells and the requirement of cholesterol binding to NPC1 protein in the trafficking of cholesterol out of lysosomes. They also highlights the importance of the interaction between NPC1 and NPC2 proteins for the egress of LDL-derived cholesterol from lysosomes.

Our initial aim was to identify a membrane protein that could bind oxysterols and block the proteolytic cleavage of SREBPs. We were surprised when we purified NPC1, a previously described protein with a known role in intracellular transport of cholesterol, as an integral membrane protein that binds [^{3}H]25-HC [31]. Using recombinant DNA technology, full-length human NPC1 was expressed and purified from CHO cells and we confirmed it's binding to oxysterols [31]. Full-length NPC1 also bound [^{3}H]cholesterol when the detergent

concentrations were slightly above their CMC [31]. In Chapter 1, the functional significance of oxysterol binding to NPC1 was addressed. Using cultured cells with mutations in NPC1, we looked at the effect of 25-HC treatment on SREBP-2 cleavage, HMG CoA reductase degradation and activation of ACAT. 25-HC was delivered to cells in ethanol as well as in an LDL particle in order to ensure that 25-HC is reaching the lysosomes where NPC1 is located. In both cases, 25-HC could suppress the proteolytic processing of SREBP-2, induce the degradation of HMG CoA reductase and activate ACAT. During these studies, Radhakrishnan, et al. (2007) demonstrated that the ER membrane protein Insig was the high affinity receptor responsible for the oxysterol effect on SREBP activation [58]. This coupled with the fact that oxysterols continue to block SREBP cleavage in NPC deficient cells suggested that NPC1's oxysterol binding does not directly affect the regulatory effects we observe due to oxysterols.

We localized the binding of oxysterols to the N-terminal domain of NPC1 (NPC1(NTD)) and specifically to the glutamine at position 79. The Q79A mutant of NPC1, which does not bind [^{3}H]-oxysterols *in vitro*, restored the ability of cholesterol-carrying β-VLDL to activate ACAT and block SREBP-2 processing in mutant CHO cells that lack NPC1 function (Figure 1-6). Furthermore, the Q79A version of NPC1(NTD) showed a 40% reduction in its binding to [^{3}H]cholesterol relative to wild-type (Figure 1-5*B*). If this is physiological, it is understandable that the overexpressed Q79A mutant NPC1 protein restores the ability of β-VLDL to activate ACAT and block SREBP-2 processing in NPC1 deficient cells. It is interesting to note that most of the clinical mutants with mutations in

NPC1(NTD) when overexpressed in mutant CHO cells, they too could restore the ability of β-VLDL to suppress SREBP-2 processing.

Meanwhile, studies by Infante *et al.* (2008) established that NPC1(NTD) and NPC2 bind cholesterol with similar affinities but only NPC1 bound 25-HC [36]. Cross-competition studies suggested that NPC1(NTD) binds the cholesterol molecule on its steroid nucleus side, whereas NPC2 binds towards the isooctyl side chain of cholesterol. This explains why a hydroxyl group addition to the isooctyl side chain, such as 25-HC, disrupts the ability of this molecule to bind to NPC2 but not NPC1 and suggests that the binding of NPC1 to 25-HC was rather nonspecific.

Since the oxysterol binding to NPC1 did not seem to have a functional significance and because NPC1's known function is in the transport of cholesterol in cells, we focused in Chapter 2 on understanding which cholesterol transport pathways were dependent on NPC1 protein. To monitor the transport of cholesterol to the ER within cells, we assayed for SREBP-2 processing and activation of ACAT enzyme, which are the two indirect commonly used methods. We also made direct cholesterol measurements of purified ER fractions using mass spectroscopy. In order to deliver cholesterol to the plasma membrane of cells, we added the cholesterol as a complex with β-methyl cyclodextrin (MCD) [61]. We also induced the mobilization of endogenous plasma membrane cholesterol within cells by treatment with neutral sphingomyelinase [62, 70]. In both cases, the plasma membrane cholesterol could reach the ER as assayed by SREBP-2 processing, activation of ACAT, and the direct cholesterol measurement from pure ER fractions. The NPC1 mutant cells could neither increase the cholesterol content nor execute the regulatory functions in the ER when the cells

were supplemented with LDL. Furthermore, using two different cell types, we performed pulse-chase experiments with [^{3}H]cholesterol or [^{3}H]acetate [27, 77]. Those studies revealed that NPC1 mutant cells could activate ACAT enzyme and increase the percentage of [^{3}H]cholesteryl oleate when treated with 25-HC. All data suggest that the transport of cholesterol from the plasma membrane of cells to the ER is independent of NPC1 and that only the transport of LDL-derived cholesterol is dependent on NPC1 protein.

After establishing that the only NPC1 dependent pathway of cholesterol transport is through lysosomes, in Chapter 3 we focused on understanding how this process occurs. As mentioned earlier, both NPC1 and NPC2 bind cholesterol and mutations in either NPC1 or NPC2 are known to cause the accumulation of cholesterol in the lysosomes of cells. Infante *et al.* (2008) established an *in vitro* assay to measure transfer of [^{3}H]cholesterol between these two proteins and phosphatidylcholine liposomes [36]. We were able to recognize two important domains in NPC1(NTD), one for cholesterol binding and the other for cholesterol transport. Mutants that diminished NPC1's ability to bind cholesterol or interact with NPC2 could not activate ACAT enzyme or rescue the proteolytic processing of SREBP-2 in response to β-VLDL treatment when overexpressed in mutant CHO cells.

Meanwhile, Kwon *et al.* (2009) determined a high resolution structure of NPC1(NTD) in the apoprotein form and in complex with cholesterol or 25-HC [90]. The ribbon diagram and surface representation of NPC1(NTD) show that the amino acid residues of the transfer mutant (L175A/L176A) reside on the surface of the protein (Figure 3-3*B*, red) whereas the amino acid residues of the cholesterol binding mutant (P202A/F203A) are embedded deep in the pocket of NPC1(NTD) that surrounds the sterol (Figure 3-3*B*, blue).

Considered together with previous studies of NPC1 and NPC2 [31, 34-36, 90], the current studies permit us to formulate a hypothetical working model to explain the requirement for these two proteins in the egress of lipoprotein-derived cholesterol from lysosomes (see Figure 2). The major consideration in formulating this model is the striking reversal in the orientation of cholesterol when it transfers between NPC2 and NPC1.

As described previously by Xu et al. (2007), cholesterol binds to NPC2 with its 3β-hydroxyl group exposed to solvent (Figure 2*A*) [35]. The exposure of the 3ß-hydroxyl allows NPC2 to bind lipoprotein-derived cholesterol either before or immediately after the fatty acid on the hydroxyl group is removed by acid lipase. Even though NPC2 can deliver cholesterol directly to liposomes *in vitro* as mentioned in the Introduction, genetics reveals that NPC2 alone is not sufficient for cholesterol egress from lysosomes, and hence the requirement for NPC1 [30, 55]. We hypothesize that the NPC1 requirement may be imposed to overcome either of two impediments: 1) cholesterol should enter the hydrophobic lysosomal membrane most readily when its hydrophobic isooctyl side chain leads the way. When cholesterol is bound to NPC2, the hydrophobic side chain is deeply buried in the protein and it cannot lead the way into the lysosomal membrane bilayer; and/or 2) the carbohydrate glycocalyx that lines the interior of the lysosomal membrane [92] creates a diffusion barrier that would prevent NPC2 from interacting directly with the membrane [88, 93]. Both of these impediments could be overcome if NPC2 transferred its cholesterol to NPC1(NTD). This would reverse the orientation of cholesterol so that its hydrophobic side chain could lead the way into the membrane, and it likely provides a mechanism for cholesterol to transit the glycocalyx.

The model of Figure 2*C* is supported by our previously published *in vitro* data showing that [^{3}H]cholesterol binds to and dissociates from NPC1(NTD) extremely slowly and that both processes are accelerated in the presence of NPC2 [36]. As is apparent from the NPC1(NTD) crystal structure, entry or exit of cholesterol from NPC1(NTD) requires enlargement of the opening, which could be accomplished by displacement of the loop between helix8/strand7 and/or a shift in the position of helix3, helix7, or helix8 (Figure 3-3*B and C*). This is supported by mutagenesis studies. Alanine substitutions at multiple sites in helix7, helix8, and the helix8/strand7 loop decreased the ability of NPC2 to open the NPC1(NTD) binding site as indicated by a reduced ability of NPC2 to facilitate the transfer of NPC1(NTD)-bound [^{3}H]cholesterol to liposomes (Figure 3-1*B* and Figure 3-2*B*). This phenotype was not observed with mutations in helix3 or any other site in the protein. These data suggest that NPC2 interacts with NPC1(NTD) to elicit a rearrangement in helix7, helix8, and the intervening loop between helix8/strand7, thereby expanding the opening and allowing cholesterol to enter or exit from the binding pocket of NPC1(NTD). Helix3 may also contribute to the expansion of the opening. Exit through that side of the protein is consistent with the idea that the hydrophobic side chain of cholesterol is the first part of the sterol to leave NPC1(NTD), thereby allowing it to insert into the lysosomal membrane.

The cell culture data in Figure 3-5 support the notion that transfer of cholesterol between NPC1 and NPC2 is required for exit of lipoprotein-derived cholesterol from lysosomes. When the L175A/L176A mutation was introduced into full-length NPC1, the protein could not restore egress of cholesterol from lysosomes to a normal degree as judged by a failure of normal cholesterol esterification (Figure 3-5*A*) and suppression of SREBP-2

cleavage (Figure 3-5*C*) in the presence of β-VLDL. These data provide strong support for the notion that cholesterol must be transferred between NPC2 and NPC1(NTD) in order to exit the lysosome. However, the result does not in itself determine that the transfer goes in the direction of NPC2-to-NPC1. In our model, this directionality is hypothesized in order to overcome the two impediments discussed above, i.e., the directionality of cholesterol insertion into the bilayer and the necessity to transit the glycocalyx.

The NTD is separated from the membrane domain of NPC1 by a linker composed of ~20 amino acids, 8 of which are prolines (Figure 2*D*). It is likely that this sequence extends in such a way that the NTD domain can project through the glycocalyx, which has been measured at ~8 nm [92]. This glycocalyx is shown as stipples in Figure 2*C*. In order to deliver cholesterol to the membrane, the NTD would have to move toward the membrane. Moreover, another protein would have to enlarge the opening on NPC1(NTD) in order for cholesterol to leave the NTD and enter the membrane. It is likely that these processes are mediated by the membrane domain of NPC1 which contains 13 transmembrane helices and two large loops that project into the lysosomal lumen. Five of the 13 transmembrane helices (no. 3-7) bear sequence homology to the sterol-sensing domains of Scap, a polytopic membrane protein in the SREBP pathway that has been shown to bind cholesterol with high affinity [53]. It seems likely that the sterol-sensing domain of NPC1 participates in cholesterol transfer. In Figure 2*C*, we show the NPC1(NTD) domain interacting with the membrane domain of the same protein. However, we have not ruled out the possibility that the NPC1(NTD) transfers the cholesterol directly to the membrane.

In transferring its bound cholesterol to the lysosomal membrane, the NTD of NPC1 could interact either with its own membrane domain (as shown in Figure 2*C*) in which case it might transfer the cholesterol to the putative sterol-sensing domain in transmembrane helices 3-7, or it could interact with the membrane domain of a neighboring NPC1 molecule. In this regard, Ohgami *et al.* (2004) reported that they could crosslink photoactivated cholesterol to NPC1 when the photoactivated cholesterol was added to the culture medium of wild-type CHO cells [33]. The reaction was reduced when the cells harbored mutant NPC1 with a point mutation in transmembrane helix3, which is part of the sterol-sensing domain. Once cholesterol is transferred to the membrane domain of NPC1, it could be flipped to the cytosolic leaflet from which it could then be picked up by cytosolic cholesterol-binding proteins. It seems likely that additional proteins would be required for the export process. Clues may come from study of patients with the NPC disease phenotype who do not have mutations in *NPC1* or *NPC2*.

One caveat to the model of Figure 2*C* arises because we have thus far been unable to demonstrate a stable complex between NPC1(NTD) and NPC2. Therefore, the postulated interaction between these two proteins might be transient. We are currently exploring methods to capture such transient interactions using NMR, chemical crosslinkers, and fluorescence energy transfer methods.

Although the model of Figure 2 still remains to be proven, it offers a scheme that can be tested by further experiments using *in vitro* biochemistry and cell culture methodologies. It is hoped that testing of this model may lead to new insights into a fundamental biologic process - namely, how lipoprotein-derived cholesterol is transported out of the lysosomal

compartment so that it can exert its structural and regulatory functions within the cell. Understanding this process hopefully will shed new light on a devastating disease.

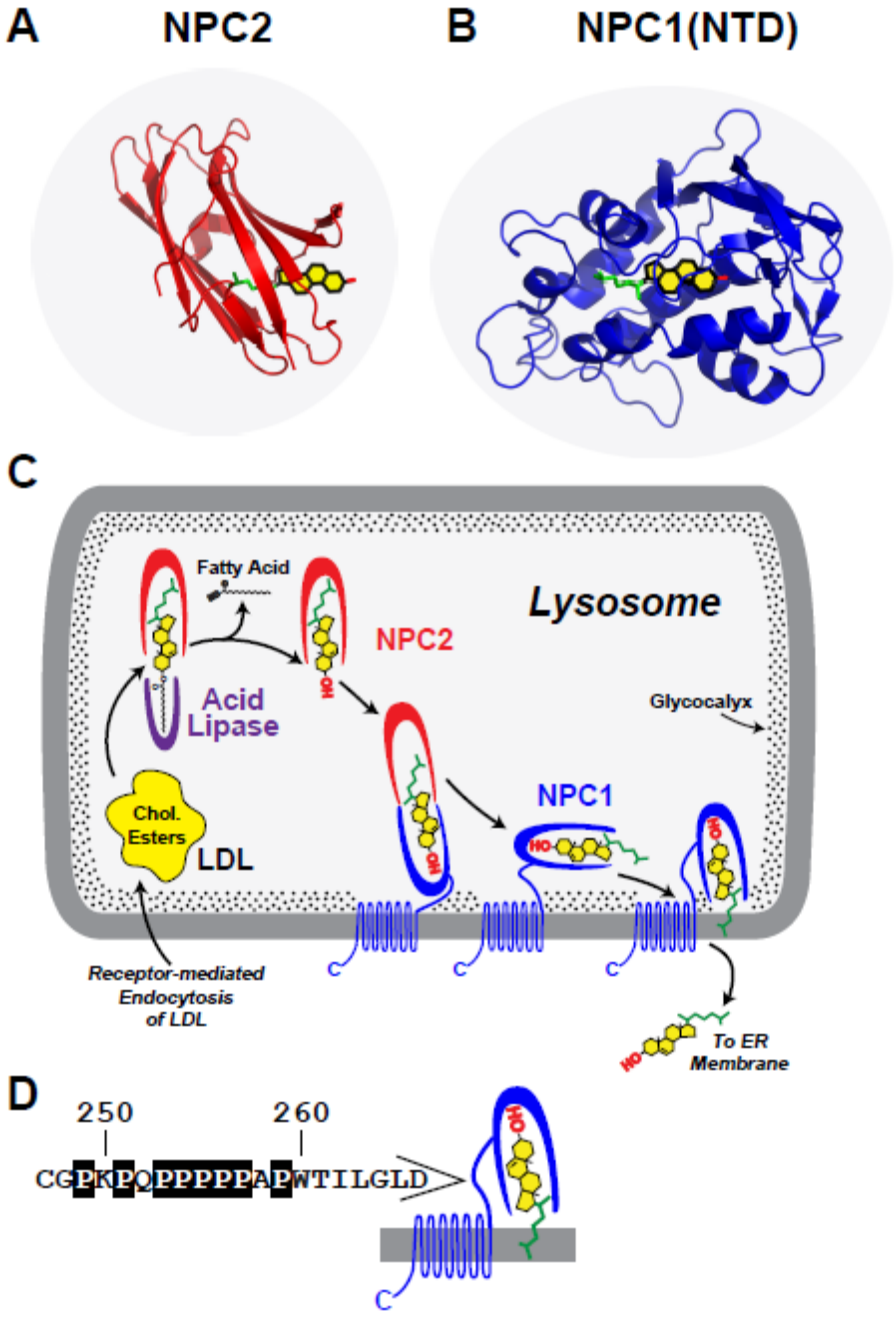

Figure 2. Model for egress of lipoprotein-derived cholesterol from lysosomes

(A) Structure of NPC2 bound to cholesterol. Redrawn from Xu, et al. (2007) [35].

(B) Structure of NPC1(NTD) bound to cholesterol [90].

(C) Proposed pathway for transfer of cholesterol from LDL or ß-VLDL to NPC2 to NPC1 to membranes. See "Conclusion and Perspective" for explanation of this working model.

(D) Sequence of amino acids 247-266 that link the NTD to the first transmembrane domain in NPC1 [21]. Prolines in this sequence are boxed. These prolines are invariant in 12 vertebrate species [34] except for P256, which is conserved in 8 of the 12 species.

BIBLIOGRAPHY

1. Kosters, A., M. Jirsa, and A.K. Groen, *Genetic background of cholesterol gallstone disease.* Biochim Biophys Acta, 2003. **1637**(1): p. 1-19.
2. Miller, M., *New developments in the treatment of low high-density lipoprotein cholesterol.* Curr Atheroscler Rep, 1999. **1**(1): p. 24-30.
3. Brown, M.S. and J.L. Goldstein, *A receptor-mediated pathway for cholesterol homeostasis.* Science, 1986. **232**(4746): p. 34-47.
4. Ikonen, E., *Mechanisms for cellular cholesterol transport: defects and human disease.* Physiol Rev, 2006. **86**(4): p. 1237-61.
5. Pentchev, P.G., et al., *Group C Niemann-Pick disease: faulty regulation of low-density lipoprotein uptake and cholesterol storage in cultured fibroblasts.* FASEB J, 1987. **1**(1): p. 40-5.
6. Blanchette-Mackie, E.J., et al., *Type-C Niemann-Pick disease: low density lipoprotein uptake is associated with premature cholesterol accumulation in the Golgi complex and excessive cholesterol storage in lysosomes.* Proc Natl Acad Sci U S A, 1988. **85**(21): p. 8022-6.
7. Brown, M.S. and J.L. Goldstein, *The SREBP pathway: regulation of cholesterol metabolism by proteolysis of a membrane-bound transcription factor.* Cell, 1997. **89**(3): p. 331-40.
8. Kumagai, H., K.T. Chun, and R.D. Simoni, *Molecular dissection of the role of the membrane domain in the regulated degradation of 3-hydroxy-3-methylglutaryl coenzyme A reductase.* J Biol Chem, 1995. **270**(32): p. 19107-13.

9. Roitelman, J., et al., *Immunological evidence for eight spans in the membrane domain of 3-hydroxy-3-methylglutaryl coenzyme A reductase: implications for enzyme degradation in the endoplasmic reticulum.* J Cell Biol, 1992. **117**(5): p. 959-73.

10. Sakai, J., et al., *Identification of complexes between the COOH-terminal domains of sterol regulatory element-binding proteins (SREBPs) and SREBP cleavage-activating protein.* J Biol Chem, 1997. **272**(32): p. 20213-21.

11. Chang, T.Y., C.C. Chang, and D. Cheng, *Acyl-coenzyme A:cholesterol acyltransferase.* Annu Rev Biochem, 1997. **66**: p. 613-38.

12. Bergstrand, A. and G. Dallner, *Isolation of rough and smooth microsomes from rat liver by means of a commerically available centrifuge.* Anal Biochem, 1969. **29**(3): p. 351-6.

13. Radhakrishnan, A., et al., *Switch-like control of SREBP-2 transport triggered by small changes in ER cholesterol: a delicate balance.* Cell Metab, 2008. **8**(6): p. 512-21.

14. Zambrano, F., S. Fleischer, and B. Fleischer, *Lipid composition of the Golgi apparatus of rat kidney and liver in comparison with other subcellular organelles.* Biochim Biophys Acta, 1975. **380**(3): p. 357-69.

15. Chang, T.Y., et al., *Cholesterol sensing, trafficking, and esterification.* Annu Rev Cell Dev Biol, 2006. **22**: p. 129-57.

16. Carstea, E.D., et al., *Niemann-Pick C1 disease gene: homology to mediators of cholesterol homeostasis.* Science, 1997. **277**(5323): p. 228-31.

17. Neufeld, E.B., et al., *The Niemann-Pick C1 protein resides in a vesicular compartment linked to retrograde transport of multiple lysosomal cargo.* J Biol Chem, 1999. **274**(14): p. 9627-35.

18. Vanier, M.T. and G. Millat, *Niemann-Pick disease type C.* Clin Genet, 2003. **64**(4): p. 269-81.

19. Pentchev, P.G., et al., *A defect in cholesterol esterification in Niemann-Pick disease (type C) patients.* Proc Natl Acad Sci U S A, 1985. **82**(23): p. 8247-51.

20. Brady, R.O., *Sphingolipidoses.* Annu Rev Biochem, 1978. **47**: p. 687-713.

21. Davies, J.P. and Y.A. Ioannou, *Topological analysis of Niemann-Pick C1 protein reveals that the membrane orientation of the putative sterol-sensing domain is identical to those of 3-hydroxy-3-methylglutaryl-CoA reductase and sterol regulatory element binding protein cleavage-activating protein.* J Biol Chem, 2000. **275**(32): p. 24367-74.

22. Hua, X., et al., *Regulated cleavage of sterol regulatory element binding proteins requires sequences on both sides of the endoplasmic reticulum membrane.* J Biol Chem, 1996. **271**(17): p. 10379-84.

23. Millard, E.E., et al., *The sterol-sensing domain of the Niemann-Pick C1 (NPC1) protein regulates trafficking of low density lipoprotein cholesterol.* J Biol Chem, 2005. **280**(31): p. 28581-90.

24. Nohturfft, A., M.S. Brown, and J.L. Goldstein, *Sterols regulate processing of carbohydrate chains of wild-type SREBP cleavage-activating protein (SCAP), but not sterol-resistant mutants Y298C or D443N.* Proc Natl Acad Sci U S A, 1998. **95**(22): p. 12848-53.

25. Scott, C. and Y.A. Ioannou, *The NPC1 protein: structure implies function.* Biochim Biophys Acta, 2004. **1685**(1-3): p. 8-13.

26. Pentchev, P.G., et al., *Type C Niemann-Pick disease. A parallel loss of regulatory responses in both the uptake and esterification of low density lipoprotein-derived cholesterol in cultured fibroblasts.* J Biol Chem, 1986. **261**(35): p. 16775-80.

27. Reid, P.C., S. Sugii, and T.Y. Chang, *Trafficking defects in endogenously synthesized cholesterol in fibroblasts, macrophages, hepatocytes, and glial cells from Niemann-Pick type C1 mice.* J Lipid Res, 2003. **44**(5): p. 1010-9.

28. Turley, S.D., D.K. Burns, and J.M. Dietschy, *Preferential utilization of newly synthesized cholesterol for brain growth in neonatal lambs.* Am J Physiol, 1998. **274**(6 Pt 1): p. E1099-105.

29. Naureckiene, S., et al., *Identification of HE1 as the second gene of Niemann-Pick C disease.* Science, 2000. **290**(5500): p. 2298-301.

30. Sleat, D.E., et al., *Genetic evidence for nonredundant functional cooperativity between NPC1 and NPC2 in lipid transport.* Proc Natl Acad Sci U S A, 2004. **101**(16): p. 5886-91.

31. Infante, R.E., et al., *Purified NPC1 protein. I. Binding of cholesterol and oxysterols to a 1278-amino acid membrane protein.* J Biol Chem, 2008. **283**(2): p. 1052-63.

32. Ko, D.C., et al., *The integrity of a cholesterol-binding pocket in Niemann-Pick C2 protein is necessary to control lysosome cholesterol levels.* Proc Natl Acad Sci U S A, 2003. **100**(5): p. 2518-25.

33. Ohgami, N., et al., *Binding between the Niemann-Pick C1 protein and a photoactivatable cholesterol analog requires a functional sterol-sensing domain.* Proc Natl Acad Sci U S A, 2004. **101**(34): p. 12473-8.

34. Infante, R.E., et al., *Purified NPC1 protein: II. Localization of sterol binding to a 240-amino acid soluble luminal loop.* J Biol Chem, 2008. **283**(2): p. 1064-75.

35. Xu, S., et al., *Structural basis of sterol binding by NPC2, a lysosomal protein deficient in Niemann-Pick type C2 disease.* J Biol Chem, 2007. **282**(32): p. 23525-31.

36. Infante, R.E., et al., *NPC2 facilitates bidirectional transfer of cholesterol between NPC1 and lipid bilayers, a step in cholesterol egress from lysosomes.* Proc Natl Acad Sci U S A, 2008. **105**(40): p. 15287-92.

37. Verot, L., et al., *Niemann-Pick C disease: functional characterization of three NPC2 mutations and clinical and molecular update on patients with NPC2.* Clin Genet, 2007. **71**(4): p. 320-30.

38. Adams, C.M., et al., *Cholesterol and 25-hydroxycholesterol inhibit activation of SREBPs by different mechanisms, both involving SCAP and Insigs.* J Biol Chem, 2004. **279**(50): p. 52772-80.

39. Gil, G., et al., *Membrane-bound domain of HMG CoA reductase is required for sterol-enhanced degradation of the enzyme.* Cell, 1985. **41**(1): p. 249-58.

40. Brown, M.S., S.E. Dana, and J.L. Goldstein, *Cholesterol ester formation in cultured human fibroblasts. Stimulation by oxygenated sterols.* J Biol Chem, 1975. **250**(10): p. 4025-7.

41. Goldstein, J.L., R.A. DeBose-Boyd, and M.S. Brown, *Protein sensors for membrane sterols.* Cell, 2006. **124**(1): p. 35-46.

42. Kovanen, P.T., et al., *Saturation and suppression of hepatic lipoprotein receptors: a mechanism for the hypercholesterolemia of cholesterol-fed rabbits.* Proc Natl Acad Sci U S A, 1981. **78**(3): p. 1396-400.

43. Kita, T., M.S. Brown, and J.L. Goldstein, *Feedback regulation of 3-hydroxy-3-methylglutaryl coenzyme A reductase in livers of mice treated with mevinolin, a competitive inhibitor of the reductase.* J Clin Invest, 1980. **66**(5): p. 1094-100.

44. Ouellette, M.M., et al., *Telomerase activity does not always imply telomere maintenance.* Biochem Biophys Res Commun, 1999. **254**(3): p. 795-803.

45. Wood, L.D., et al., *Characterization of ataxia telangiectasia fibroblasts with extended life-span through telomerase expression.* Oncogene, 2001. **20**(3): p. 278-88.

46. Loftus, S.K., et al., *Murine model of Niemann-Pick C disease: mutation in a cholesterol homeostasis gene.* Science, 1997. **277**(5323): p. 232-5.

47. Willnow, T.E. and J. Herz, *Genetic deficiency in low density lipoprotein receptor-related protein confers cellular resistance to Pseudomonas exotoxin A. Evidence that this protein is required for uptake and degradation of multiple ligands.* J Cell Sci, 1994. **107 (Pt 3)**: p. 719-26.

48. Dahl, N.K., et al., *Isolation and characterization of Chinese hamster ovary cells defective in the intracellular metabolism of low density lipoprotein-derived cholesterol.* J Biol Chem, 1992. **267**(7): p. 4889-96.

49. Krieger, M., J.L. Goldstein, and M.S. Brown, *Receptor-mediated uptake of low density lipoprotein reconstituted with 25-hydroxycholesteryl oleate suppresses 3-hydroxy-3-methylglutaryl-coenzyme A reductase and inhibits growth of human fibroblasts.* Proc Natl Acad Sci U S A, 1978. **75**(10): p. 5052-6.

50. Hua, X., et al., *Sterol resistance in CHO cells traced to point mutation in SREBP cleavage-activating protein.* Cell, 1996. **87**(3): p. 415-26.

51. Goldstein, J.L., S.K. Basu, and M.S. Brown, *Receptor-mediated endocytosis of low-density lipoprotein in cultured cells.* Methods Enzymol, 1983. **98**: p. 241-60.

52. Rawson, R.B., et al., *Failure to cleave sterol regulatory element-binding proteins (SREBPs) causes cholesterol auxotrophy in Chinese hamster ovary cells with genetic absence of SREBP cleavage-activating protein.* J Biol Chem, 1999. **274**(40): p. 28549-56.

53. Radhakrishnan, A., et al., *Direct binding of cholesterol to the purified membrane region of SCAP: mechanism for a sterol-sensing domain.* Mol Cell, 2004. **15**(2): p. 259-68.

54. Liscum, L. and J.R. Faust, *Low density lipoprotein (LDL)-mediated suppression of cholesterol synthesis and LDL uptake is defective in Niemann-Pick type C fibroblasts.* J Biol Chem, 1987. **262**(35): p. 17002-8.

55. Pentchev, P.G., *Niemann-Pick C research from mouse to gene.* Biochim Biophys Acta, 2004. **1685**(1-3): p. 3-7.

56. van Driel, I.R., et al., *First cysteine-rich repeat in ligand-binding domain of low density lipoprotein receptor binds Ca2+ and monoclonal antibodies, but not lipoproteins.* J Biol Chem, 1987. **262**(36): p. 17443-9.

57. Watari, H., et al., *Mutations in the leucine zipper motif and sterol-sensing domain inactivate the Niemann-Pick C1 glycoprotein.* J Biol Chem, 1999. **274**(31): p. 21861-6.

58. Radhakrishnan, A., et al., *Sterol-regulated transport of SREBPs from endoplasmic reticulum to Golgi: oxysterols block transport by binding to Insig.* Proc Natl Acad Sci U S A, 2007. **104**(16): p. 6511-8.

59. Chalvardjian, A. and E. Rudnicki, *Determination of lipid phosphorus in the nanomolar range.* Anal Biochem, 1970. **36**(1): p. 225-6.

60. Simons, K. and E. Ikonen, *How cells handle cholesterol.* Science, 2000. **290**(5497): p. 1721-6.

61. Kilsdonk, E.P., et al., *Cellular cholesterol efflux mediated by cyclodextrins.* J Biol Chem, 1995. **270**(29): p. 17250-6.

62. Slotte, J.P. and E.L. Bierman, *Depletion of plasma-membrane sphingomyelin rapidly alters the distribution of cholesterol between plasma membranes and intracellular cholesterol pools in cultured fibroblasts.* Biochem J, 1988. **250**(3): p. 653-8.

63. Kovanen, P.T., J.L. Goldstein, and M.S. Brown, *High levels of 3-hydroxy-3-methylglutaryl coenzyme A reductase activity and cholesterol synthesis in the ovary of the pregnant rabbit.* J Biol Chem, 1978. **253**(14): p. 5126-32.

64. Basu, S.K., et al., *Degradation of cationized low density lipoprotein and regulation of cholesterol metabolism in homozygous familial hypercholesterolemia fibroblasts.* Proc Natl Acad Sci U S A, 1976. **73**(9): p. 3178-82.

65. Brown, A.J., et al., *Cholesterol addition to ER membranes alters conformation of SCAP, the SREBP escort protein that regulates cholesterol metabolism.* Mol Cell, 2002. **10**(2): p. 237-45.

66. Brown, M.S., et al., *Induction of 3-hydroxy-3-methylglutaryl coenzyme A reductase activity in human fibroblasts incubated with compactin (ML-236B), a competitive inhibitor of the reductase.* J Biol Chem, 1978. **253**(4): p. 1121-8.

67. Basu, S.K., et al., *Biochemical and genetic studies of the apoprotein E secreted by mouse macrophages and human monocytes.* J Biol Chem, 1982. **257**(16): p. 9788-95.

68. Arion, W.J. and R.C. Nordlie, *Liver glucose-6-phosphatase and pyrophosphate-glucose phosphotransferase: effects of fasting.* Biochem Biophys Res Commun, 1965. **20**(5): p. 606-10.

69. Lowry, O.H., et al., *Protein measurement with the Folin phenol reagent.* J Biol Chem, 1951. **193**(1): p. 265-75.

70. Scheek, S., M.S. Brown, and J.L. Goldstein, *Sphingomyelin depletion in cultured cells blocks proteolysis of sterol regulatory element binding proteins at site 1.* Proc Natl Acad Sci U S A, 1997. **94**(21): p. 11179-83.

71. Metherall, J.E., et al., *A 25-hydroxycholesterol-resistant cell line deficient in acyl-CoA: cholesterol acyltransferase.* J Biol Chem, 1991. **266**(19): p. 12734-40.

72. Ross, A.C., et al., *Selective inhibition of acyl coenzyme A:cholesterol acyltransferase by compound 58-035.* J Biol Chem, 1984. **259**(2): p. 815-9.

73. Sever, N., et al., *Accelerated degradation of HMG CoA reductase mediated by binding of insig-1 to its sterol-sensing domain.* Mol Cell, 2003. **11**(1): p. 25-33.

74. Brown, D.A. and J.K. Rose, *Sorting of GPI-anchored proteins to glycolipid-enriched membrane subdomains during transport to the apical cell surface.* Cell, 1992. **68**(3): p. 533-44.

75. Murata, M., et al., *VIP21/caveolin is a cholesterol-binding protein.* Proc Natl Acad Sci U S A, 1995. **92**(22): p. 10339-43.

76. Smart, E.J., et al., *Caveolin moves from caveolae to the Golgi apparatus in response to cholesterol oxidation.* J Cell Biol, 1994. **127**(5): p. 1185-97.

77. Leventhal, A.R., et al., *Acid sphingomyelinase-deficient macrophages have defective cholesterol trafficking and efflux.* J Biol Chem, 2001. **276**(48): p. 44976-83.

78. Wan, Q. and E.H. Schuchman, *A novel polymorphism in the human acid sphingomyelinase gene due to size variation of the signal peptide region.* Biochim Biophys Acta, 1995. **1270**(2-3): p. 207-10.

79. Ridgway, N.D., *Interactions between metabolism and intracellular distribution of cholesterol and sphingomyelin.* Biochim Biophys Acta, 2000. **1484**(2-3): p. 129-41.

80. Roth, M.G., *Clathrin-mediated endocytosis before fluorescent proteins.* Nat Rev Mol Cell Biol, 2006. **7**(1): p. 63-8.

81. Goldstein, J.L., et al., *Role of lysosomal acid lipase in the metabolism of plasma low density lipoprotein. Observations in cultured fibroblasts from a patient with cholesteryl ester storage disease.* J Biol Chem, 1975. **250**(21): p. 8487-95.

82. Demel, R.A. and B. De Kruyff, *The function of sterols in membranes.* Biochim Biophys Acta, 1976. **457**(2): p. 109-32.

83. Friedland, N., et al., *Structure of a cholesterol-binding protein deficient in Niemann-Pick type C2 disease.* Proc Natl Acad Sci U S A, 2003. **100**(5): p. 2512-7.

84. Okamura, N., et al., *A porcine homolog of the major secretory protein of human epididymis, HE1, specifically binds cholesterol.* Biochim Biophys Acta, 1999. **1438**(3): p. 377-87.

85. Babalola, J.O., et al., *Development of an assay for the intermembrane transfer of cholesterol by Niemann-Pick C2 protein.* Biol Chem, 2007. **388**(6): p. 617-26.

86. Cheruku, S.R., et al., *Mechanism of cholesterol transfer from the Niemann-Pick type C2 protein to model membranes supports a role in lysosomal cholesterol transport.* J Biol Chem, 2006. **281**(42): p. 31594-604.

87. Xu, Z., et al., *Regulation of sterol transport between membranes and NPC2.* Biochemistry, 2008. **47**(42): p. 11134-43.

88. Schulze, H., T. Kolter, and K. Sandhoff, *Principles of lysosomal membrane degradation Cellular topology and biochemistry of lysosomal lipid degradation.* Biochim Biophys Acta, 2008.

89. Subramanian, K. and W.E. Balch, *NPC1/NPC2 function as a tag team duo to mobilize cholesterol.* Proc Natl Acad Sci U S A, 2008. **105**(40): p. 15223-4.

90. Kwon, H.J., et al., *Structure of the N-terminal Domain of NPC1 Suggests Transfer Mechanism for Exit of LDL-Cholesterol from Lysosomes.* Cell, 2009.

91. DeBose-Boyd, R.A., et al., *Transport-dependent proteolysis of SREBP: relocation of site-1 protease from Golgi to ER obviates the need for SREBP transport to Golgi.* Cell, 1999. **99**(7): p. 703-12.

92. Neiss, W.F., *A coat of glycoconjugates on the inner surface of the lysosomal membrane in the rat kidney.* Histochemistry, 1984. **80**(6): p. 603-8.

93. Kolter, T. and K. Sandhoff, *Principles of lysosomal membrane digestion: stimulation of sphingolipid degradation by sphingolipid activator proteins and anionic lysosomal lipids.* Annu Rev Cell Dev Biol, 2005. **21**: p. 81-103.